Institut für Geodäsie und Geoinformation der Universität Bonn

Efficient calibration strategies for panoramic terrestrial laser scanners

Dissertation

Zur

Erlangung des akademischen Grades

Doktor der Ingenieurwissenschaften (Dr.–Ing.)

der

Landwirtschaftlichen Fakultät

der

Rheinischen Friedrich–Wilhelms–Universität Bonn

vorgelegt von

M.Sc. Tomislav Medić

aus Zagreb, Croatia

Bonn 2021

Referent: Univ.–Prof. Dr.–Ing. Heiner Kuhlmann

Korreferenten: Univ.–Prof. Dr.–Ing. Andreas Wieser

Univ.–Prof. Dr.–Ing. Hans Neuner

Tag der mündlichen Prüfung: 28. September 2020

Angefertigt mit Genehmigung der Landwirtschaftlichen Fakultät der Universität Bonn

Efficient calibration strategies for panoramic terrestrial laser scanners

Abstract

Terrestrial laser scanner (TLS) measurements are unavoidably affected by systematic errors due to internal mechanical misalignments, while the calibration is the fundamental procedure for mitigating these effects and assuring the high measurement accuracy. Despite different existing calibration solutions, the practice of calibrating TLSs for the sake of quality assurance is rarely exercised from the majority of end-users in the commercial sector. The main reason is the inefficiency of the existing solutions requiring considerable investments of time, funding and effort.

Therefore, this work is dedicated to increasing the efficiency of the existing calibration approaches, development of further efficient calibration approaches that overcome some shortcomings of the existing ones, and aiding the selection of the appropriate calibration strategy based on the analysis of pros and cons. Generally, the calibration approaches can be divided on the a priori calibration, before the measurement campaign, and the in-situ calibration, during the measurement campaign, each having certain advantages and disadvantages. Hence, this work incorporates the investigation of both strategies, as well as their analysis and comparison, and, therefore, it can be separated into three main aspects:

- For pursuing the efficient a priori TLS calibration, this works relies on the well-established target-based self-calibration approach, which suffers from inefficiency, as it requires numerous manually installed targets and multiple scans to assure accurate calibration results. Therefore, herein, based on the detailed analysis of the functional and stochastic model of the calibration adjustment, as well as the sensitivity analysis of different measurement configurations, an optimized calibration field design is derived. The results led to the implementation of the first non-commercial facility for the comprehensive calibration of high-end panoramic TLSs in Europe. It comprises only a handful of targets and requires typically one hour for the calibration procedure, while at the same time assures trustworthy calibration results. However, the main contribution lies in the simple designing workflow, which can be easily reproduced by qualified engineers for establishing new efficient calibration fields.

- As the stability of the calibration parameters is found to be one of the limiting factors of the a priori calibration, further development of the in-situ calibration approaches was pursued. Different calibration strategies are analyzed on the concrete case of deformation monitoring of VLBI telescope's main reflector, pointing out the requirements of the successful calibration: bundled calibration adjustment with sufficient variations in the measurement configuration and the explicit inclusion of two-face measurements. Additionally, the first fully automatic in-situ calibration approach was introduced in the response to the efficiency related shortages of the existing in-situ calibration strategies identified in the latter investigation.

- The advantages and disadvantages of the latter a priori and in-situ calibration approaches were analyzed in detail to aid the decision-making process of the end-users and to help their integration in the usual workflows in the commercial sector. Within the analysis, it was proven that the user-calibration of instruments can indeed improve the point cloud accuracy beyond the manufacturer's initial factory calibration. Moreover, it is proven that, if necessary, user-calibration can even substitute the manufacturer's calibration entirely. However, the highest measurement accuracy is assured when the manufacturer's calibration, a priori calibration and in-situ calibration are adequately combined.

In the overall view, the findings and methods developed in this thesis contribute to the integration of the TLS calibration practices in the commercial applications and aids their wider acceptance. Therefore, this work represents a relevant contribution to the superordinate goal of quality assurance of TLS measurements.

Strategien zur effizienten Kalibrierung von terrestrischen Panoramalaserscannern

Zusammenfassung

Messungen eines terrestrischen Laserscanners (TLS) sind unvermeidlich durch systematische Abweichungen beeinflusst, welche aus inneren Konstruktionsabweichungen im Scanner resultieren. Die Kalibrierung leistet den Beitrag diese Effekte zu reduzieren und eine hohe Messgenauigkeit zu erzielen. Trotz unterschiedlicher existierender Kalibrierlösungen wird die Kalibrierung von TLS zur Qualitätssicherung von der Mehrheit der Endnutzer im kommerziellen Bereich nur selten ausgeübt. Der Hauptgrund dafür ist die Ineffizienz der bestehenden Lösungen, die einen erheblichen Aufwand an Zeit, Geld und Mühe erfordern.

Aus diesem Grund widmet sich diese Arbeit der Effizienzsteigerung der bestehenden Kalibrieransätze, der Entwicklung weiterer effizienter Kalibrieransätze, die einige Mängel der bestehenden Lösungen überwinden, und der Unterstützung bei der Auswahl der geeigneten Kalibrierstrategie auf der Grundlage der Analyse der Vor- und Nachteile. Im Allgemeinen lassen sich die Kalibrieransätze in die a-priori Kalibrierung vor der Messkampagne und die in-situ Kalibrierung während der Messkampagne unterteilen, wobei jeder Ansatz bestimmte Vor- und Nachteile hat. Daher umfasst diese Arbeit die Untersuchung beider Strategien sowie deren Analyse und Vergleich und kann daher in drei Hauptaspekte unterteilt werden:

- Zur Entwicklung einer effizienten a-priori TLS-Kalibrierung, stützt sich diese Arbeit auf den bereits etablierten zielzeichenbasierten Selbstkalibrierungsansatz. Dieser ist in seiner bisherigen Form ineffizient, da er zahlreiche manuell installierte Zielzeichen und mehrere Scans erfordert, um genaue Kalibrierungsergebnisse zu gewährleisten. Daher wird hier, basierend auf der detaillierten Analyse des funktionalen und stochastischen Modells der Ausgleichung sowie der Sensitivitätsanalyse verschiedener Messkonfigurationen, ein optimiertes Design eines Kalibrierfelds abgeleitet. Die Ergebnisse führen zur Realisierung der ersten nicht-kommerziellen Einrichtung für die umfassende Kalibrierung von High-End-Panoramalaserscannern in Europa. Sie umfasst nur eine Handvoll Zielzeichen und benötigt typischerweise eine Stunde für die Kalibrierung und generiert dennoch gleichzeitig zuverlässige Kalibrierergebnisse. Der Hauptbeitrag liegt jedoch in dem einfachen Designworkflow, der von qualifizierten Ingenieuren leicht reproduziert werden kann, um neue effiziente Kalibrierfelder zu etablieren.

- Da sich die Stabilität der Kalibrierparameter als einer der limitierenden Faktoren der a-priori Kalibrierung herausgestellt hat, wurde die Weiterentwicklung der in-situ Kalibrierungsansätze verfolgt. Am konkreten Fall der Deformationsanalyse des Hauptreflektors eines VLBI-Teleskops werden verschiedene Kalibrierstrategien analysiert und die Anforderungen an eine erfolgreiche Kalibrierung aufgezeigt: gebündelte Ausgleichung mit ausreichenden Variationen in der Messkonfiguration und die explizite Einbeziehung von Zwei-Lagen-Messungen. Zusätzlich wurde der erste vollautomatische In-situ Kalibrierungsansatz als Reaktion auf die in der letztgenannten Untersuchung identifizierten effizienzbedingten Mängel der bestehenden in-situ Kalibrierungsstrategien eingeführt.

- Die Vor- und Nachteile der letzteren a-priori und in-situ Kalibrierungsansätze wurden im Detail analysiert, um den Entscheidungsprozess der Endnutzer zu unterstützen und ihre Integration in die üblichen Arbeitsabläufe im kommerziellen Sektor zu erleichtern. Im Rahmen der Analyse wurde nachgewiesen, dass die Anwenderkalibrierung von Instrumenten tatsächlich die Genauigkeit der Punktwolke über die anfängliche Werkskalibrierung des Herstellers hinaus verbessern kann. Darüber hinaus wurde nachgewiesen, dass die Anwenderkalibrierung die Kalibrierung des Herstellers bei Bedarf sogar vollständig ersetzen kann. Die höchste Messgenauigkeit ist jedoch gewährleistet, wenn die Kalibrierung des Herstellers, die a-priori Kalibrierung und die in-situ Kalibrierung angemessen kombiniert werden.

In der Gesamtbetrachtung tragen die in dieser Arbeit entwickelten Erkenntnisse und Methoden zur Integration der TLS-Kalibrierpraktiken in die kommerziellen Anwendungen bei und fördern deren breitere Akzeptanz. Damit stellt diese Arbeit einen relevanten Beitrag zum übergeordneten Ziel der Qualitätssicherung von TLS-Messungen dar.

Contents

Preface

This cumulative dissertation presents the investigations and results aiming at further improvements in the efficiency of calibration approaches for panoramic terrestrial laser scanners. The thesis is based on the following eight publications that were all subject to a peer-review process and five of them are listed as category 1 publications in the Agricultural Faculty of the University of Bonn:

- Publication A1:
  Medić, T., Holst, C., & Kuhlmann, H. (2017) Towards System Calibration of Panoramic Laser Scanners from a Single Station. *Sensors*, 2017, 17, 1145, https://doi.org/10.3390/s17051145.

- Publication A2:
  Medić, T., Holst, C., Janßen, J., Kuhlmann, H. (2019b) Empirical stochastic model of detected target centroids: Influence on registration and calibration of terrestrial laser scanners, *J. Appl. Geodesy*, 13 (3), 179-197, https://doi.org/10.1515/jag-2018-0032.

- Publication A3:
  Medić, T., Kuhlmann, H., Holst, C. (2019d) Sensitivity Analysis and Minimal Measurement Geometry for the Target-Based Calibration of High-End Panoramic Terrestrial Laser Scanners, *Remote Sens.*, 11 (13), 1519, https://doi.org/10.3390/rs11131519.

- Publication A4:
  Medić, T., Kuhlmann, H., & Holst, C**.** (2020b) Designing and Evaluating a User-Oriented Calibration Field for the Target-Based Self-Calibration of Panoramic Terrestrial Laser Scanners, *Remote Sens.*, 12 (1), 15, https://doi.org/10.3390/rs12010015.

- Publication B1:
  Holst, C., Medić, T., & Kuhlmann, H. (2018a) Dealing with systematic laser scanner errors due to misalignment at area-based deformation analyses, *J. Appl. Geodesy*, 12 (2), 169-185, https://doi.org/10.1515/jag-2017-0044.

- Publication B2:
  Medić, T., Kuhlmann, H., & Holst, C. (2019a) Automatic in-situ self-calibration of a panoramic TLS from a single station using 2D keypoints, *ISPRS Ann. Photogramm. Remote Sens. Spatial Inf. Sci*., IV-2/W5, 413-420, https://doi.org/10.5194/isprs-annals-IV-2-W5-413-2019 .

- Publication C1:
  Medić, T., Kuhlmann, H., & Holst, C. (2020c) Empirical evaluation of terrestrial laser scanner calibration strategies: manufacturer-based, target-based and keypoint-based, *Contributions to International Conferences on Engineering Surveying*, INGEO & SIG 2020, Springer, https://doi.org/10.1007/978-3-030-51953-7_4.

- Publication C2:
  Medić, T., Kuhlmann, H., & Holst, C**.** (2020a) A priori versus in-situ terrestrial laser scanner calibration in the context of the instability of calibration parameters, *Contributions to International Conferences on Engineering Surveying*, INGEO & SIG 2020, Springer, https://doi.org/10.1007/978-3-030-51953-7_11.

The publications are summarized in Chapter 4, while in Chapter 5 the most important aspects and results are highlighted. The author of this dissertation has made the main contribution to all publications and in particular, introduced the methodological advances. The only exception is publication C1, where the author of this thesis is responsible for the methodological enhancements regarding the calibration of terrestrial laser scanners, while the analysis and the interpretation of the results were done in collaboration with the coauthors.

1 Motivation and Objective

Terrestrial laser scanners (TLSs) are instruments with the ability to rapidly acquire dense high-quality 3D geometrical data of the environment, usually supplemented with semantic information such as the intensity of reflected laser beams and color. As such, they established themselves as a standard tool in numerous applications, e.g. cultural heritage documentation, as-built modeling, environmental- and geo- sciences, forensics and engineering (Vosselman & Maas, 2010). From the latter applications, photogrammetry and surveying are the engineering fields with the highest accuracy requirements that continuously lead to essential enhancements in this measurement technology, making it competitive even in the most challenging measurement tasks. Although the TLSs emerged two decades ago with the first commercial instruments (Cyrax 2200 and Riegl LMS Z210), their assimilation in demanding engineering tasks within the commercial applications is an ongoing process. This thesis contributes to further integration of terrestrial laser scanners in such applications. The main motivation and objectives are described in Sections 1.1 and 1.2.

1.1 Motivation

TLS in demanding engineering tasks

A subset of TLSs, the high-end panoramic TLSs, are slowly emerging in the high-accuracy demanding engineering applications that are still dominated by traditionally utilized total stations (TSs) and laser trackers (LTs) - (Ogundare, 2015). The panoramic TLSs are distinguishable from the other models by the field-of-view (FoV) that covers the nearly complete 3D surroundings of the instrument (Vosselman & Maas, 2010). Due to their wide FoV, long working range, millimeter level accuracy and fast measurements, they can bring further automation, time savings and comprehensiveness in the existing practices. Typical examples of such applications are deformation monitoring in the field of surveying/geodetic engineering, as well as reverse engineering and quality assurance in the field of industrial large scale metrology (Mukupa et al., 2017). There are many documented use cases of successful TLS utilization in such applications, e.g. the quality assurance of cruise ships assembly (Ford et al., 2016) and nuclear reactor water tank (Zheng et al., 2018), as well as deformation monitoring of water dams (Eling, 2009), tunnels (Nuttens et al., 2010), landslides (Telling et al., 2017), and radio telescopes (Holst et al., 2015). Although highly present in the research community, TLSs are still not an industry-standard in such applications and there are several reasons for this:

- a lack of universally applicable computational methods for processing large-scale irregularly sampled areal data (Neuner et al., 2016; Wunderlich et al., 2016),
- the deficient stochastic models due to insufficient knowledge of the measurement uncertainty and corresponding correlations, leading to incorrect statistical testing results (Holst & Kuhlmann, 2016; Kauker et al., 2016),
- the measurement accuracy that is still lagging behind the established measurement technologies and sensors due to deficient deterministic models of systematic effects on observations (Holst et al., 2016; Holst & Kuhlmann, 2016).

Researches are actively addressing all the above-mentioned topics, e.g. (Gojcic et al., 2019a; Harmening & Neuner, 2020; Kauker & Schwieger, 2017; Lichti, 2019), while in the focus of this thesis is the problem of the achievable measurement accuracy. The factors influencing TLS measurement accuracy can be subdivided in: instrument related errors, external (atmospheric) influences, measurement configuration/geometry, and properties of the measured object (Soudarissanane, 2016). The atmospheric effects influencing the beam propagation are well studied and accounted for with the deterministic models inherited from TSs and LTs (Ogundare, 2015). For the majority of the TLS applications, the remaining residue can be safely neglected in deterministic models and accounted for stochastically. However, the significant impact on the measurement accuracy occurs on larger distances due to the refraction (Friedli et al., 2019). The current research efforts are focusing on overcoming this problem by computing the differential corrections from two or more simultaneous laser pulses with different wavelengths (Salido-Monzú & Wieser, 2019).

The effects of measurement geometry and object properties are interrelated as they jointly influence the laser beam interaction with the measured object. The latter interaction has a strong impact on the measurement accuracy, which

is, up until now, rarely considered in the commercial applications. However, strong research efforts are placed on the stochastic (Soudarissanane, 2016; Wujanz et al., 2017) and the deterministic modeling of these effects (Chaudhry et al., 2019; Zámecnikova et al., 2014, 2015; Zámecnikova & Neuner, 2017).

Finally, the instrument related errors have arguably the most prominent impact on the achievable measurement accuracy, which became evident on several occasions documented in the literature. For example, in Holst & Kuhlmann (2014a), the systematic measurement errors notably surpassed the magnitudes of the measurement noise resulting in biased results of the deformation analysis. The strategy of averaging measurements obtained in two opposite instrument positions, used in the case of TSs and LTs to remove the majority of the instrumental errors (Schofield & Breach, 2007), is not directly transferable to TLSs. Namely, TLSs are incapable of sampling the identical points in space twice, leading to a lack of measurement correspondences between two instrument positions. Some attempts are documented in the literature (Holst et al., 2017), however, they are computationally demanding, time-consuming and not universally applicable. Additionally, the TLS observations typically span through a wide field-of-view. This eliminates the possibility of considering some systematic errors as constant and disregarding them, as it is often the case with the LTs. Hence, to account for the instrument-related systematic errors in TLSs, proper instrument calibration is of high relevance.

Calibration of TLS in the commercial sector

To assure the high measurement accuracy for demanding engineering applications, manufacturers put a large effort into the production and assembly of all instrument components. However, the fabrication procedures are not flawless, and the remaining small mechanical misalignments of the TLS components can cause systematic errors, reducing the measurement accuracy. Hence, they need to be modeled mathematically with the calibration parameters (CPs). The CPs are estimated by a comprehensive factory calibration within specialized facilities upon the instrument assembly, see e.g. (Holst et al., 2016; Mettenleiter et al., 2015; Walsh, 2015). In the case of the high-end instruments, the calibration is a laborious process and it has a large influence on the final price.

Moreover, the geometrical relations between the mechanical components can vary over time due to wear and tear, suffered stress and other influences (Garcia-San-Miguel & Lerma, 2013; Lichti, 2007; Reshetyuk, 2009). Hence, a regular re-calibration of the instrument is necessary to account for these changes and for the sake of the continuous measurement quality assurance (Neuner, 2019; Wunderlich et al., 2013). The re-calibration occurs either in regular time intervals (once every 1 or 2 years, dependent on the manufacturer's recommendation) or when the instrument fails the testing procedure. The testing procedures serve as a control to ensure that the TLS measurement uncertainty is within the values given in the manufacturer's specifications. Typically, the test procedures are realized according to recommendations in DIN or ISO norms (Holst et al., 2018b; International Organization for Standardization 2018; Neitzel et al., 2014) or according to the manufacturer's defined workflows.

In each case, the repeated factory calibration is a costly event for the end-users, typically requiring several weeks at manufacturers and several thousands of euros (from personal correspondence with one of the manufacturers). Some manufacturers like Leica Geosystems and FARO Inc. provide user calibration approaches which can reduce systematic errors in the measurements to some extent (e.g. Leica`s "Check and Adjust" and Faro's "On-site compensation"). However, both factory-based and user-based calibration approaches offered by manufacturers suffer from certain drawbacks:

- **Not standardized**: The joint drawback is that these approaches are manufacturer dependent and not universally applicable or directly comparable. Namely, different manufacturers use different calibration procedures with different outcomes. Also, they calculate the measurement uncertainty values provided in the instrument specifications in different ways. Hence, a fair comparison of the calibration results and achieved measurement quality for different instruments is difficult. For demanding engineering applications, these proprietary accuracy estimates do not necessarily meet the job specifications and requirements. Additionally, the user-based calibration is limited to only a few instruments on the market.

- **Black box:** Moreover, the manufacturers provide information about their calibration procedures only selectively. Generally, the manufacturers do not provide the information about the exact mathematical relations between the mechanical misalignments and the observations, the number of relevant misalignments, as well as the quality indicators of the calibration parameters (uncertainty, correlations, reliability, and stability). This data is treated as a company secret, which makes the correct estimation of the measurement accuracy, e.g. through the variance propagation, difficult to the end-users.

- **Costly or no guarantee:** As mentioned, the repeated factory calibration is a time- and money-wise burdening event for the end-users. However, it results in the calibration certificate and the guaranteed measurement accuracy. On the contrary, the user-based calibration provided by some manufacturers is fast and inexpensive, but there are no means of assuring the quality of the calibration procedure.

Calibration of TLS in the scientific community

To address these drawbacks, in the last two decades, scientists have invested substantial efforts in the establishment, analysis and enhancement of different TLS calibration approaches (Holst et al., 2016; Lichti, 2019). The mentioned approaches can be subdivided into two categories: the ones aiming at the a priori calibration, before the measurements, and the ones aiming at the in-situ calibration, during the measurements (Vosselman & Maas, 2010). Both categories have certain advantages and disadvantages making their co-existence mandatory (see Chapter 2).

Generally, the majority of the documented and openly accessible research efforts focused on the user-oriented system self-calibration (Lichti, 2010a). The "user-oriented" denotes that in principle every qualified engineer should be able to independently use these calibration methods. The self-calibration denotes the calibration approach that uses only the observations of the instrument under investigation, avoiding the expensive and laborious establishment of the reference values with the instruments of higher accuracy. It should be noted that the official term for the self-calibration is "adjustment of a measuring system" (BiPM et al., 2012). However, within this work, the term self-calibration is used due to its wide acceptance in the related literature. The term system calibration denotes that all calibration parameters that are deemed as relevant (concerning all TLS components) are estimated simultaneously, within one calibration approach. These calibration approaches are typically used in the normal working environment deprived of laboratory conditions.

In contrast, in the case of the manufacturer-based calibration, the component-wise laboratory calibration with the controlled ambient conditions and the accurate reference values for additional control is preferred over the self-calibration approaches (Mettenleiter et al., 2015; Walsh, 2015). In the laboratory, the external influences like the ambient temperature and vibrations can be monitored and controlled. Additionally, the reference values can help to expose the unexpected errors in the instrument's measurements. Hence, the impact of these influences causing the bias of the estimated calibration parameters can be reduced or even functionally modeled. For example, Leica GmbH uses climate chambers in the calibration process to functionally model the temperature influence on the calibration parameters (Walsh, 2015). Likewise, there are a few documented studies conducted in earlier years aiming at the component-wise laboratory calibration, with the main intention of examining the general behavior of this recently emerged measurement technology (Schulz, 2007; Zogg, 2008). However, they were never furtherly built-upon.

It is hard to imagine that the manufacturer's factory calibration upon the instrument assembly will ever become redundant. However, for an average end-user setting up, maintaining or getting access to such laboratory conditions is not a feasible option. As it is expected that the instruments are rigorously calibrated after the factory assembly, the requirements for the user-oriented calibration can be relaxed, aiming at only updating the calibration parameter values to account for eventual changes over time. Hence, the TLS self-calibration profiled itself in the literature as a superior alternative due to strong potential in the efficiency and user-friendly character.

To summarize, the efforts of the scientific community aim at the user-oriented re-calibration of the TLSs, either a priori, before the measurements or in-situ, during the measurements. The main aim is to assure standardized, reproducible and efficient calibration routines providing detailed information about the quality of the calibration parameters to the end-users. However, the existing approaches have certain drawbacks limiting them to narrow scientific circles and hindering them in becoming well accepted in the commercial sector. Therefore, this is an active topic of research and this thesis is a part of the ongoing research efforts.

1.2 Objectives

The general goal of this thesis is devoted to further advances in the user-oriented calibration of terrestrial laser scanners by addressing the drawbacks of the existing calibration approaches (see Chapter 2). Currently, the necessary knowledge and the ability to accomplish a successful TLS calibration are primarily limited to the instrument manufacturers and a small circle of scientists. As it is not possible to force the manufacturers to share

their company secrets or force the quicker and cheaper factory calibration, the main missing elements are well-accepted user-oriented calibration approaches, similar to the existing ones for total stations. Therefore, it is necessary to transfer the knowledge of scientific circles to the increasing community of end-users. This can only be achieved by enhancing the efficiency and, therefore, the user-friendly character of the existing calibration approaches and by widening the understanding of achievable calibration results.

Therefore, the main objective of this thesis is to increase the efficiency of the user-oriented calibration to support the transfer to the broad community of the end-users in the commercial sector. As mentioned, the existing user-oriented calibration approaches are segregated in a priori and in-situ calibration approaches, each having certain advantages and disadvantages (more in Chapter 2). Hence, the main objective of this thesis can be separated into three smaller objectives:

- **A:** improving the efficiency of existing a priori calibration approaches (publications A1-A4),
- **B:** improving and developing further efficient in-situ calibration approaches that address the drawbacks of the existing ones (publications B1-B2, partially A1 and C1) and
- **C:** investigating advantages, disadvantages of the a priori and in-situ calibration approaches to support the decision making of the end-users (publications C1-C2).

A: A priori calibration

The a priori calibration is conducted before the measurement campaign in the controlled environment. Hence, it allows imposing strict goals that need to be achieved. Therefore, we aim at establishing a generally accepted a priori calibration approach with the following characteristics. It should be:

- user-friendly and efficient – i.e. it should be easily reproducible by qualified engineers,
- comprehensive – i.e. sensitive to detect and model all relevant systematic errors based on the genuine instrument geometry to assure successful posterior use of the calibration parameters, as well as
- trustworthy and informative – i.e. providing the calibration parameters with pre-defined and complete quality criteria (precision, correlations, reliability and temporal stability).

Each of the state-of-the-art calibration approaches is missing some of the above-mentioned criteria and one of the aims of this thesis is to establish one approach that would fulfill all of them.

B: In-situ calibration

One of the abovementioned requirements, the comprehensiveness, can only be guaranteed for a priori calibration approaches, with well-defined measurement configurations. However, the a priori calibration suffers from the reported partial instability of the instrument's mechanical components, i.e. the calibration parameters. Hence, it is necessary to support the comprehensive a priori calibration, with an up-to-date in-situ calibration. As the existing in-situ calibration strategies also suffer from some limitations, this thesis aims at improving the existing and developing further efficient in-situ calibration approaches that tackle the disadvantages of the existing ones (detailed in Chapter 2).

C: Investigating the advantages and disadvantages

Finally, it is necessary to improve the understanding of the achievable measurement accuracy with the a priori and in-situ calibrations and their limitations. Only with the latter knowledge, the end-users can make informed decisions if the TLS can substitute the industry standards (TSs and LTs) in demanding engineering tasks. Therefore, within this objective, this thesis aims at investigating and indicating the advantages and shortcomings of these calibration approaches. Moreover, to tackle the identified shortcomings, it discusses the optimal, i.e. the most efficient, implementation of the user-oriented calibration in the workflows of different measurement tasks and it discusses the eventual combination of the existing calibration strategies.

The following chapter (Chapter 2) presents an overview of the state-of-the-art, highlighting the main drawbacks and pointing out the particular advances made within this thesis to overcome them. Chapter 3 presents a summary of the main aspects of TLS measurement technology and the theoretical basics of the relevant TLS calibration strategies. The publications presented in the thesis preface, founding the core of this work, are briefly summarized in Chapter 4. Chapter 5 highlights the most important aspects and results of the publications, specifically regarding the previously defined objectives of this thesis. Chapter 6 gives an overview of further considerations, which have arisen in the course of the work but have not been considered in detail so far. The dissertation ends with a conclusion and outlook (Chapter 7). Finally, a list of other publications not directly in the focus of this dissertation is given in Chapter 8.

2 Scientific Context

Shortly after the emergence of the first commercial TLSs in the early 2000s, scientists started working on the means of the measurement quality assessment and assurance (Clark & Robson, 2004; Gordon et al., 2000; Kersten et al., 2005; Lichti et al., 2005), as well as the different calibration strategies (Gielsdorf et al., 2004; Gordon et al., 2005; Lichti & Franke, 2005; Neitzel, 2006; Parian et al., 2005). This thesis focuses on the latter objective.

The existing calibration approaches, primarily user-oriented self-calibration approaches, can be separated by different objects in the instrument's surroundings used to aid the estimation of calibration parameters, such as cylinders (Chan et al., 2015), planes (Bae & Lichti, 2007; Gielsdorf et al., 2004), paraboloids (Holst & Kuhlmann, 2014a), or specialized targets, either intensity-based black and white planar targets (Chow et al., 2010a; Lichti, 2007; Reshetyuk, 2007), monochrome planar targets (Li et al., 2018) or spherical targets (Neitzel, 2006). All the above-mentioned approaches successfully reduced the measurement uncertainty to some degree. However, the improvement in the measurement uncertainty strongly differs in the literature due to the large variety of calibration approaches and investigated instruments. Typically, the calibration introduces significant improvements of 30% to 80% for the accuracy of range, and horizontal and vertical angular measurements (Garcia-San-Miguel & Lerma, 2013).

Additionally, as previously mentioned, the calibration approaches can be separated into the ones aiming at the a priori calibration (Section 2.1), before the measurement task, and the ones aiming at the in-situ calibration (Section 2.2), during the measurement task (Vosselman & Maas, 2010). As both the in-situ and the a priori calibration strategies have individual advantages and shortcomings, they will be separately discussed in the following sections.

2.1 A-priori calibration of TLSs

The most established user-oriented calibration approach of all is the target-based self-calibration (Lichti, 2007). It is the only calibration approach that primarily aims at the a priori calibration in dedicated calibration fields, before the measurement task. The approach was derived from the photogrammetric camera calibration (Förstner & Wrobel, 2016) and introduced in the TLS calibration in Parian et al. (2005). Since then it was used in numerous experiments, successfully reducing the measurement uncertainty of the calibrated instruments (Abbas et al., 2014a; Chow et al., 2010b; Lerma & García-San-Miguel, 2014; Lichti, 2007; Reshetyuk, 2007; Wang et al., 2017).

In the target-based self-calibration, the specialized targets are well distributed in the TLS surroundings, typically smaller indoor facilities like offices, forming so-called target-fields or calibration-fields (Figure 2.1). Scanning these targets from multiple positions allows accurate and comprehensive calibration of the instrument (detailed in Section 3.2). In the following text, the state-of-the-art is discussed, focusing on the main advantages (Section 2.1.1) and disadvantages (Section 2.1.2), as well as the role of this thesis in overcoming some of the highlighted disadvantages.

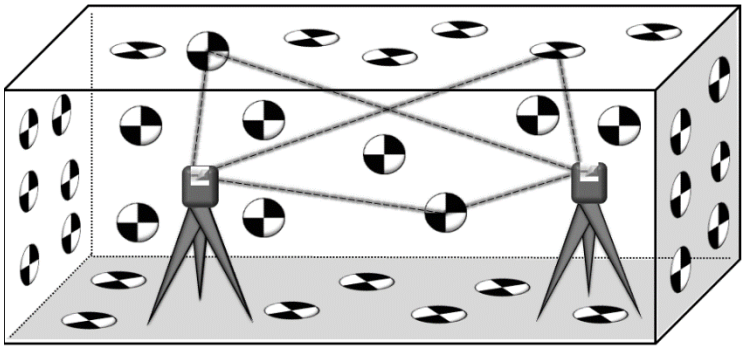

Figure 2.1: A sketch of the calibration field for the target-based self-calibration of terrestrial laser scanners.

2.1.1 Target-based self-calibration: advantages

This calibration approach has several important advantages in comparison to the rest of the existing calibration approaches. First, rather than relying on relatively noisy raw single point measurements, this approach uses centers of the specialized targets estimated using different processing algorithms. The target centers are derived from hundreds or thousands of measurements and, therefore, they are much more precise (Chow et al., 2010a; Janßen et al., 2019; Rachakonda et al., 2018).

Second, dense, nearly continuous TLS areal measurements are reduced to single-point measurements of the defined aims. This means that instead of using highly dense and highly correlated raw TLS observations, we use sparse well-defined pointwise observations. That brings three important advantages:

- The possibility of easily building point-to-point correspondences between consecutive scans, which is a necessary prerequisite for every self-calibration approach. Namely, as there are no reference values for the measured quantities, the calibration parameters are estimated based on differences in the measured quantities observed from different scanner positions or orientations.
- Justified disregarding of the mentioned high, but unknown correlations between observations.
- Possibility to use statistical tools that have been developing for decades for pointwise measurements of instruments such as total stations or GNSS receivers, see e.g. (Mikhail, 1976).

Third, this transformation also means a conversion of a very general task of *improving the efficiency of TLS calibration* into a very specific task of optimization of geodetic networks, aiming at the optimal distribution of pointwise measurements. Again, this task is well studied in the literature and the mathematical and statistical means have been developing for decades (Grafarend & Sanso, 1985; Schmitt, 1982). Hence, if all prerequisites are met, it is possible to estimate the calibration parameters with a guaranteed and predefined quality in a sense of strictly defined limits for the precision, correlations and reliability.

Fourth, it is easy to manipulate the position of targets, i.e. measurement configuration, in the way that we can achieve high sensitivity to detect all relevant mechanical misalignments and to estimate all relevant calibration parameters. Hence, it is possible to guarantee the comprehensiveness of the calibration approach.

Finally, targets are inexpensive to produce and easy to handle. Hence, all of the abovementioned characteristics make a strong case that this approach is the best candidate for becoming a generally accepted user-oriented calibration approach. Therefore, within the first objective of this thesis, i.e. improving the efficiency of the existing calibration approaches, this work builds-upon the target-based self-calibration approach (see Section 5.1). As mentioned, the current implementations of this calibration approach have several shortcomings that are preventing it to become a well-accepted in the broader community of end-users. These shortcomings are in detail presented in the following section and addressed within this thesis.

2.1.2 Target-based self-calibration: disadvantages

Efficiency

One of the main shortcomings of the current implementations is that they lack in efficiency (Abbas et al., 2017; Abbas et al., 2014a; Bae & Lichti, 2007; Chan et al., 2015; Chan & Lichti, 2012; Chow et al., 2013; Chow et al., 2011a; Chow et al., 2011b; Lichti & Chow, 2013). Namely, the majority of the experiments described in literature relies on target-fields with heavily redundant networks of observations, comprising dozens or hundreds of targets and multiple scans from multiple positions (Chow et al., 2013). Although this heavy redundancy assures the high quality of the estimated calibration parameters, it also requires laborious calibration field assembly, measurement acquisition, and processing. Therefore, to achieve wide acceptance, this calibration approach requires the optimization with the accent on the efficiency.

Solution

The efficiency can be realized by solving the task of optimization and design of geodetic networks or in this concrete case the design of the efficient target-field for TLS calibration (in the following text denoted as calibration-field). It is an optimization problem that searches for a cost-efficient solution that fulfills imposed quality criteria, and is solved analytically, only partially, (Grafarend & Sanso, 1985; Kuang, 1996) or heuristically (Baselga, 2011;

Saleh & Chelouah, 2004). The network design is divided into four interrelated sub-problems, known as orders of the design (Grafarend & Sanso, 1985): the zero-order design (ZOD), or the problem of optimal datum; first-order design (FOD), or the problem of optimal network (measurement) configuration; second-order design (SOD), or the problem of optimal observation weights; and the third-order design (TOD), or the problem of densification of existing networks. Niemeier (2008) states that there is no analytical solution for the complete design of geodetic networks.

For the target-based calibration, the datum choice has a negligible effect on the calibration results (Abbas et al., 2014c). Hence, the ZOD can be neglected and the datum can be arbitrarily chosen. Regarding the SOD, the observation weights are typically chosen to reflect the uncertainty of the measurement procedures and the equipment. In the case of the TLS self-calibration, the SOD is given for a particular scanner, scanner settings, the target design and the target center estimation algorithm (Sections 3.2 and 5.1). As the aim is generally to support the efficient realizations of future TLS calibration-fields, the problem of TOD is not relevant.

Hence, in order to assure efficient TLS calibration, it is necessary to solve the FOD problem or the design of the optimal, i.e. efficient, measurement configuration of the calibration fields. In other words, the required number of targets and scans needs to be reduced to a necessary minimum, while at the same time guaranteeing a comprehensive calibration with a predefined calibration parameter quality. There were several published studies with a similar aim. They focused on manually reducing the number of targets within empirical experiments (Abbas et al., 2014a) or simulation experiments (Ge, 2016). However, they did not achieve the latter aim, as they failed to assure comprehensiveness, guaranteed parameter quality, or both (see the quality criteria given in Section 1.2 for the objective A). Therefore, achieving the efficient target-based calibration with predefined quality of the calibration parameters is one of the main concerns of this thesis (publications A1-A4).

Remark: At the moment, the problem of optimizing the calibration field design (FOD problem) is not solvable by using the automatic data-driven optimization algorithms due to the high numerical complexity. To compare it with similar problems, multiple studies were published focusing on the optimal viewpoint planning, i.e. optimal TLS positioning concerning the subject of measurements. In these studies, different heuristic algorithms were utilized to find near-optimal solutions, such as simulated annealing, greedy search, genetic algorithm, particle swarm optimization, and ant colony optimization methods (Díaz-Vilariño et al., 2018; Jia & Lichti, 2017, 2018; Soudarissanane & Lindenbergh, 2012). These studies tend to simplify the problem to reduce its computational complexity, mostly by reducing the whole problem from 3D to 2D. However, such an approach is not suited for TLS calibration since the vertical position of the targets is of high relevance (Lichti, 2007, 2010b). Hence, within this thesis different approach for designing a calibration field was used, which relies on the stepwise workflow (Section 5.1).

Necessary steps

To recapitulate, to solve the problem of the calibration field optimization, several steps need to be resolved. First, the correct functional model describing the genuine and the most relevant mechanical misalignments and TLS measurements must be defined. Namely, the current implementations of the target-based self-calibration rely on different functional models inherited from instruments like total stations and panoramic cameras (see Section 3.1.3), which is justified due to their functional and mechanical similarities. However, they do not necessarily coincide. Omitting the relevant parameters can directly cause the bias in the estimates of the remaining parameters. On the other hand, the over-parameterization makes fulfilling the predefined quality criteria in an efficient manner difficult or even impossible. Hence, there is strong importance in selecting an adequate set of calibration parameters.

Second, the stochastic model describing the true measurement uncertainty needs to be known. The target centers are derived from hundreds of correlated observations using different point cloud processing strategies that influence the final center accuracy. Nevertheless, the current implementations of the target-based self-calibration rely on simple stochastic models (see Section 3.2.1). If the relative uncertainties of different observation groups are wrongly defined, the covariance matrix of the estimated parameters, estimates of their precision, correlations and reliability, as well as the statistical tests, i.e. of the calibration parameter significance, will be biased. Additionally, without an adequate functional and stochastic model, the solutions of the optimization tasks aiming at optimizing the measurement configuration are biased and lead to wrong conclusions (Grafarend & Sanso, 1985). In this thesis, both problems are tackled in publications A1 and A2.

Third, the FOD problem of optimizing the calibration field design needs to be simplified to assure a reduced computational complexity (see above-mentioned remark). Within this thesis, simplifying the FOD optimization

problem is tackled by conducting a sensitivity analysis to find a small subset of well-defined target and TLS locations that are highly sensitive towards estimating relevant calibration parameters (the topic of publication A3). This way, nearly an unlimited number of possible optimization solutions can be reduced to the optimal combination of several pre-selected sensitive measurement configurations. Sensitivity analyses are regularly used to analyze the sensitivity of the measurement geometry with different aims in mind, e.g. (Niemeier, 1985; Schwieger, 2007; Tiede, 2005). Two similar analyses were already published, one aiming at improving the measurement geometry for the plane-based (Gordon, 2008), and one on the target-based TLS calibration (Muralikrishnan et al., 2015b). The latter analysis focused on a reference field of targets with limited dimensions (4 x 4 m), which was realized with an instrument of superior accuracy in laboratory conditions. As the aim of this work is the efficient self-calibration, a new analysis was required. Finally, the last step is the optimization implementation with carefully selected score functions, which are discussed in detail in Section 5.1 (publication A4).

Parameter stability

Another large disadvantage of the target-based self-calibration aiming at a priori calibration is the compulsory presumption that the calibration parameters are stable over time and that they can be reused in the following measurements. Previous studies inspected the stability of the calibration parameters and noticed some significant changes over time (Garcia-San-Miguel & Lerma, 2013; Lichti, 2007; Reshetyuk, 2009). Hence, the presumption about the parameter stability is not entirely fulfilled. Additionally, to the best of the author's knowledge, none of the published studies investigated if applying the calibration parameters estimated on a calibration field improves the point cloud accuracy in latter applications. Hence, some definite proof that the target-based self-calibration fulfills the a priori calibration character is still missing.

Within this study, the stability of the calibration parameters is further investigated, identifying and quantifying some of the influencing factors (publication C1). Additionally, the use of the a priori estimated parameters in the subsequent measurement campaigns is examined. The advantages and the remaining shortcomings of the approach are detected and discussed, with further considerations on how it can be supplemented with an adequate additional in-situ calibration (publication C2).

2.2 In-situ calibration of TLSs

On the contrary to the a priori target-based self-calibration in a dedicated calibration field, the remaining self-calibration approaches aim at the in-situ calibration assuring up-to-date calibration parameters. The most studied and developed is the plane-based self-calibration. It first appeared in Gielsdorf et al. (2004), where multiple wooden boards have been well distributed within a room to assure a sufficient measurement configuration for a successful calibration. Further studies mainly relied on the planes found during a measurement campaign, e.g. the planar walls and surfaces, mostly in indoor facilities (Bae & Lichti, 2007; Chow et al., 2011b). As the sufficient distribution of the planar surfaces was not assured in all cases, new in-situ self-calibration approaches emerged: the cylinder-based and the paraboloid based calibration, again relying on the measurement configuration and elements found at the scene (Chan & Lichti, 2012; Holst & Kuhlmann, 2014a). The latter approaches in the documented studies successfully improved the measurement accuracy to some degree. Their main advantage was that the parameters are directly estimated on-site and, hence, no presumption about the stability of the calibration parameters was necessary. However, these approaches have certain disadvantages, which are detected, discussed (Section 2.2.1) and partially addressed (Sections 5.2 and 5.3) within this thesis.

2.2.1 In-situ calibration: disadvantages

For the successful calibration, all in-situ self-calibration approaches require objects that can be approximated with the geometrical primitives and which are well distributed in the instruments field-of-view. They all have a similar working principle and they are realized as the best-fit algorithms estimating at the same time the parameters of geometrical primitives and the calibration parameters, based on the TLS measurements.

The first disadvantage appears if the objects used for the calibration are at the same time the subjects of the measurement campaign. For example, in the case of the deformation monitoring of the VLBI telescopes (Holst et al., 2015), the rotational paraboloid is at the same time the subject of deformation analysis and the object used for the TLS calibration. If the estimated calibration parameters are strongly correlated with the monitored quantities, e.g. the paraboloid form parameters, the results of the deformation monitoring analysis are likely to be biased. In

such cases, the in-situ calibration can even negatively impact TLS performance. Within this thesis, this disadvantage is tackled and several strategies to efficiently mitigate it are proposed and analyzed (publication B1).

The second disadvantage is that all approaches require geometrically describable man-made objects that are well distributed and a priori identified in the surroundings. Namely, for the plane- and cylinder-based approaches to work, we need at least several planar or cylindrically shaped objects distributed on-site, such as walls, pipes or street lamps. To perform the TLS self-calibration, it is necessary to build the object correspondences between two or more scans. The latter is usually solved by employing some a priori knowledge about the environment. These requirements make the existing calibration approaches less efficient and hardly feasible for the measurement tasks outside the urban areas, such as deformation monitoring of landslides and slopes. To account for this shortcoming, within this work, a new efficient in-situ calibration approach is developed and analyzed in detail (publications B2 and partially C1).

Third, all in-situ approaches use highly correlated TLS measurements. These correlations are disregarded (without exception) due to the lack of sufficient knowledge (Jurek et al., 2017; Kauker et al., 2016). This leads to biased estimates of the calibration parameter precision, correlations and reliability. Therefore, these approaches lack the objective criteria describing the quality of the estimated calibration parameters. This disadvantage was not tackled within this thesis due to the sheer amount of work required for overcoming it. However, some current research efforts are going towards this direction (Kauker & Schwieger, 2017; Kermarrec et al., 2019b; Schmitz et al., 2020a).

Another significant shortcoming is that it is impossible to guarantee that the geometry found on a certain job will provide a sufficient measurement configuration for revealing and estimating all relevant mechanical misalignments. Moreover, in the case that configuration is not sufficient, it is hard to manipulate planar walls and cylindrical pipes to achieve better measurement configuration. Hence, these calibration approaches typically lack comprehensiveness. The latter shortcoming cannot be resolved by further research efforts due to its fortuitous character.

The presented disadvantages were the essential motivation for relying on the target-based self-calibration for fulfilling the first objective of this thesis. However, within this work, a disadvantage of the a priori target-based calibration due to the questionable parameter stability was analyzed and quantified (publication C1). Therefore, to reach the highest achievable measurement accuracy, necessary for stringent engineering tasks, the optimal and efficient combination of the a priori and in-situ calibration approaches was also analyzed (publication C2).

Remark: Some authors considered the target-based self-calibration as an in-situ calibration strategy (Abbas et al., 2014a; Chow et al., 2011a; Garcia-San-Miguel & Lerma, 2013). There, the measurement task is expected to occur within an indoor facility that is previously equipped with a sufficient number of targets for the TLS calibration. This strategy successfully improved the TLS measurement accuracy to some extent in one specific case of the 3D modeling of a ship hull (Abbas et al., 2017). However, the calibration was not comprehensive, targeting only a few most important calibration parameters. Moreover, such a calibration approach is limited to the measurement task that can be carried out indoors. Hence, although feasible for some industrial large-scale metrology applications, it can hardly be applied in the case of the deformation monitoring. Therefore, within this thesis, the target-based self-calibration is primarily considered as the a priori calibration approach.

3 Theoretical Basics

This chapter first gives a short overview of the most relevant theoretical knowledge related to terrestrial laser scanners necessary for understanding the content of the thesis (Section 3.1). Afterward, the main mathematical principles of the target-based, 2D keypoint-based and paraboloid-based self-calibration are explained in Sections 3.2, 3.3 and 3.4, which are the core instruments for the investigations conducted within this work.

3.1 Basics of panoramic TLSs

Terrestrial laser scanners can be separated into three categories according to their field-of-view and underlying mechanism on camera, hybrid and panoramic instruments (Vosselman & Maas, 2010). Due to different mechanisms, they have different measurement characteristics and a different set of relevant misalignments that could significantly influence the measurement accuracy. Consequently, the optimization of the calibration approaches for each of them is different. Therefore, this work focuses only on panoramic TLSs as they are the most often used type in stringent engineering tasks, including the tasks within the field of engineering geodesy.

3.1.1 Main working principle

The panoramic TLS mainly comprises two angular encoders measuring the angular steps, a spinning mirror deflecting the laser beam and an electronic distance measurement (EDM) device, which also records the intensity of the returned signal. The EDM unit measures distances according to one of the following principles: time-of-flight, phase-shift, or Wave Form Digitizer (WFD) by Leica Geosystems AG (Maar & Zogg, 2014; Vosselman & Maas, 2010).

The instrument has three main axes (vertical or standing, horizontal/trunnion or tilt, and the collimation axis or line-of-sight), which are supposed to be orthogonal in the perfect case (Figure 3.1, a). The mirror spins around the horizontal (tilt) axis and deflects the laser beam within one vertical profile making full circles (0°-360°). This mirror is inclined for 45°, and thus, the exiting laser beam closes a right angle with the horizontal axis (Figure 3.1, a).

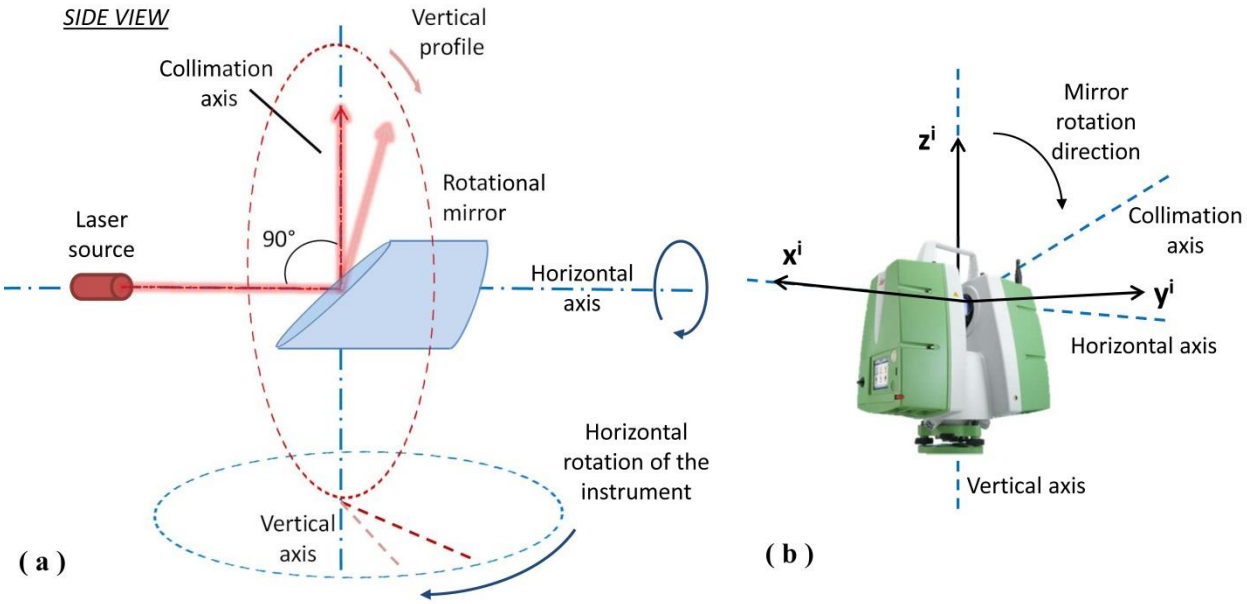

Figure 3.1: (a) Ideal panoramic TLS geometry, (b) Local Cartesian coordinate system of a panoramic TLS

Additionally, the whole system is rotating around the vertical (standing) axis making a half of a circle for one full panoramic 3D scan. This means that by making a full circle around the standing axis, the panoramic TLSs can capture the whole environment twice (two consecutive scans). Therefore, in the 1st scan (0°-180°) a part of the

environment is measured from the front side of the instrument, and part from the back side. In the 2nd scan (180°-360°), the same scenery is measured again. However, the parts of the environment measured from the front and the back are swapped. This measurement concept is called two-face measurements and it can reveal multiple instrument related systematic errors. It is widely used in the geodetic community for the calibration of total stations (Schofield and Breach, 2007), which have a similar construction as TLSs. This property of the panoramic TLSs is heavily exploited for the TLS calibration within this work.

During one full panoramic scan, the whole surrounding is sampled nearly continuously through dense pointwise measurements recording horizontal angles, vertical angles and distances (from further on ranges). These 3D spherical coordinates are internally transformed and stored as Cartesian coordinates of the local scanner coordinate system with the origin in the ideal intersection of the three main axes (Fig. 3.1, b). To imitate genuine TLS observations, which is a prerequisite of the TLS calibration, it is necessary to reverse this transformation.

There are several different ways the angular observations are parameterized in the literature (Amiri Parian & Gruen, 2010; Lichti, 2009; Lichti et al., 2019; Muralikrishnan et al., 2015a; Reshetyuk, 2010), which has an impact on the calibration results. In this thesis, the angular motion, both for the horizontal and vertical angles, is represented with the values from 0° to 360° (typically used in total stations), which makes it simple to explicitly implement the two-face measurements in the calibration adjustment. Hence, the following functions are used:

$$r_j^i = \sqrt{{x_j^i}^2 + {y_j^i}^2 + {z_j^i}^2}, \qquad (3.1) \qquad \varphi_j^i = arctan\left(\frac{x_j^i}{y_j^i}\right), \qquad (3.2) \qquad \theta_j^i = \arccos\left(\frac{z_j^i}{r_j^i}\right). \qquad (3.3)$$

Where r_j^i, φ_j^i, θ_j^i denote the range, horizontal and vertical angle measurements and x_j^i, y_j^i, z_j^i are 3D Cartesian coordinates (axes referring to Fig. 3.1, b) of the i^{th} point measured from the j^{th} scanner station. The horizontal angles are further corrected for each quadrant by adding 180° or 360° where necessary, and the vertical angles are corrected by subtracting the calculated value from 360° where necessary, see e.g. Medić et al. (2019c).

Remark: This part of the functional model did not receive sufficient attention in the literature, making some existing implementations inconsistent with the true instrument's motions, which adversely affect the calibration results. Namely, the Equations (3.1)-(3.3) are valid for the y-headed right-handed clockwise-rotating coordinate system. That means that the 0° direction of horizontal angles is in the direction of the $+y^i$ axis (Fig. 3.1, b). The examples of instruments on the market using this coordinate system are Leica HDS-series, Leica ScanStation P-series and Z+F Imager series. On the contrary, the instruments like Leica BLK360 and Faro Focus^{3D} series use the x-headed coordinate system. Hence, the 0° direction of horizontal angles coincides with the $+x^i$ axis direction, see e.g. Medić et al. (2019c) for more details.

3.1.2 Additional sensors

The high-end panoramic TLSs have typically high measurement accuracy, software that allows two-face measurements and they are equipped with dynamic dual-axis compensators. The examples of high-end instruments equipped with dynamic dual-axis compensators are Leica ScanStation P-series and Z+F Imager-series (Leica Geosystems AG, 2015; Z+F GmbH, 2016). The dynamic compensator measures the instrument's inclination, i.e. standing axis deviation concerning the local gravity direction, in the motion while scanning (Mettenleiter et al., 2015; Walsh, 2015). These values are applied to all angular measurements to compensate for the standing axis inclination mathematically. The two axes of the dual-axis compensators are orthogonal, and they are most often regarded as longitudinal, i.e. in the direction of line-of-sight, and transversal, i.e. in the direction of trunnion axis. The compensator measurements are very often introduced in the TLS calibration and registration as direct pseudo-observations of unknown rotational parameters.

TLSs can have supplementary sensors such as digital and thermal cameras for acquiring additional semantic information about the environment. Additionally, some instruments have Global Navigation Satellite System modules (GNSS), barometers and Inertial Measurement Units (IMUs) to aid the coarse registration of the TLS point clouds (Vosselman & Maas, 2010). However, these sensors are so far not considered in the TLS calibration. Additionally, most of the TLSs on the market have more than one temperature sensor to monitor the internal instrument's temperature. These values are either used to monitor if the instrument works within the temperature tolerances given in the manufacturer's specifications or to adjust the manufacturer's calibration parameters for the temperature (Walsh, 2015).

3.1.3 Relevant mechanical misalignments

The previous works revised in Chapter 2 used different functional models to describe the mechanical misalignments of terrestrial laser scanners. Consequently, no functional model could be considered as a generally accepted one. The latter models were most often based on the model of total station (TS) systematic errors due to the high similarity of these two instruments (Vosselman & Maas, 2010). The TS-based models can be divided on the simple model, e.g. in Abbas et al. (2014a) and Lichti (2010b), that compromises only four main calibration parameters (rangefinder offset, collimation and trunnion axis error, vertical index offset) and complex models, e.g. in Holst & Kuhlmann (2014a) and Lichti (2007), that compromise all known TS systematic errors. Some studies even extended the list of the calibration parameters empirically by observing the behavior of the calibration adjustment residuals, see e.g. Chow et al. (2013). Moreover, some publications used a functional model based on panoramic cameras (Amiri Parian & Gruen, 2010).

Relatively recently, the researchers at the American National Institute of Standards and Technology (NIST) developed a functional model of TLS mechanical misalignments based on genuine instrument geometry. This model consists of 18 parameters and it was derived for and tested only in a laborious component-wise laboratory calibration relying on the expensive laser tracker reference measurements (Muralikrishnan et al., 2015a). Hence, this thesis relies on the latter model, however, with some minor modifications (explanation follows).

According to the latter model, several possible mechanical misalignments can cause systematic errors in measurements of panoramic TLSs and there are two ways to divide them. First, they can be divided into tilts (rotations) and offsets (translations) of the main instrument components. The tilts have a higher impact on the measurement quality because the magnitude of the related systematic errors grows with the distance. On the contrary, the systematic errors of the offsets are constant concerning the distance and usually small in magnitude (after the factory calibration).

A second way to divide the TLS misalignments is by the instrument part which is tilted or offset in the laser source tilts and offsets (Fig. 3.2-a and Fig. 3.2-b), the mirror tilts and offsets (Fig. 3.2-c and Fig. 3.2-d) and the horizontal axis tilt and offset (Fig. 3.2-e and Fig 3.2-f). The remaining systematic errors are equal to the total station errors and those are rangefinder errors, vertical index offset, and angular encoder errors (Schofield & Breach, 2007). The list of all relevant systematic errors (calibration parameters) for panoramic TLSs is given in Table 3.1. The nomenclature (symbols) is adopted from NIST, who originally derived the parametrization and proved it as valid in the run-off experiment, where several leading manufacturers were involved (Muralikrishnan et al., 2016).

Table 3.1 gives an overview of which of the TLS parameters also exist in the same or similar form in total stations, which parameters can be revealed using two-face measurements (two-face sensitive parameters) and which parameters exist in the high-end TLSs. For the high-end instruments, it is expected that they are equipped with angular encoders with multiple reading heads or that the angular encoders are a priori factory calibrated, e.g. on a rotary table (Prieto et al., 2018; Walsh, 2015). This eliminates a considerable amount of the overall possible TLS misalignments, which has a direct impact on the optimization of the calibration approach.

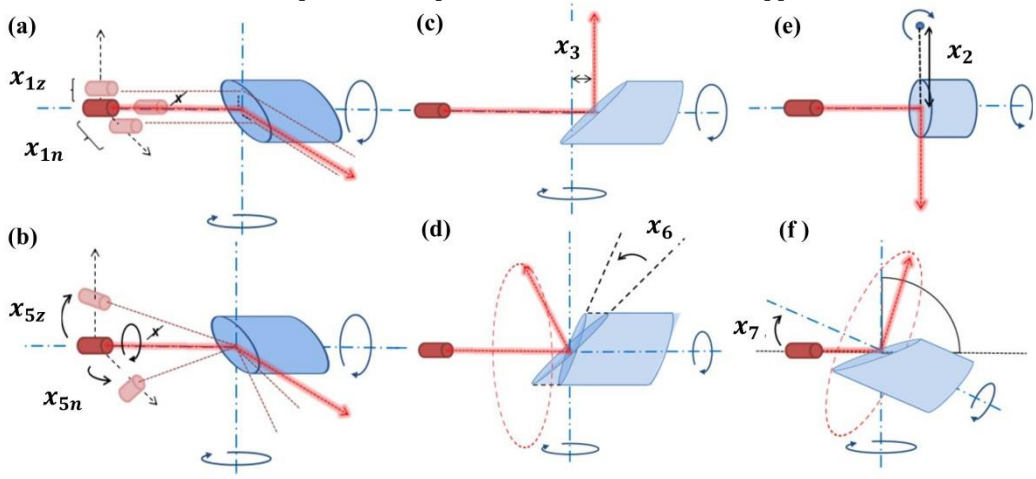

Figure 3.2: Mechanical misalignments of panoramic TLSs, (a), (b) – laser offsets & tilts, (c), (d) – mirror offset & tilt, (e), (f) – horizontal axis offset & tilt.

Within this thesis, the parameters from Table 3.1 are investigated in detail (publication A1) and the functional model comprising the most relevant mechanical misalignments for the high-end panoramic TLSs is derived and given in the following equations:

$$\Delta r_j^i = x_2 \sin\left(\theta_j^i\right) + x_{10} + v_{r_j^i}, \tag{3.4}$$

$$\Delta\varphi_j^i = \frac{x_{1z}}{r_j^i \tan(\theta_j^i)} + \frac{x_3}{r_j^i \sin(\theta_j^i)} + \frac{x_{5z} - x_7}{\tan(\theta_j^i)} + \frac{2x_6}{sin(\theta_j^i)} + \frac{x_{1n}}{r_j^i} + v_{\varphi_j^i}, \tag{3.5}$$

$$\Delta\theta_j^i = \frac{(x_{1n} + x_2)\cos(\theta_j^i)}{r_j^i} + x_4 + x_{5n}\cos\left(\theta_j^i\right) - \frac{x_{1z}\, sin\left(\theta_j^i\right)}{r_j^i} - x_{5z}\, sin\left(\theta_j^i\right) + v_{\theta_j^i}. \tag{3.6}$$

where Δr_j^i, $\Delta\varphi_j^i, \Delta\theta_j^i$ denote the overall sum of the measurements errors for each measurement r_j^i, φ_j^i, θ_j^i, $x_{1n/2/\dots}$ are calibration parameters denoting instrument related systematic errors and $v_{r_j^i}$, $v_{\varphi_j^i}, v_{\theta_j^i}$ are the calibration adjustment residuals describing the random measurement errors.

Table 3.1: The comprehensive list of mechanical misalignments in TLSs: nomenclature by NIST, existence in total stations, the possibility to estimate with two-face measurements, and existence in high-end TLSs.

Description	Parameter	TS	2-faces	high-end
Horizontal beam offset	x_{1n}	similar	no	yes
Vertical beam offset	x_{1z}	no	yes	yes
Horizontal axis offset	x_2	similar	yes	yes
Mirror offset	x_3	no	yes	yes
Vertical index offset	x_4	yes	yes	yes
Horizontal beam tilt	x_{5n}	similar	yes	yes
Vertical beam tilt	x_{5z}	similar	no	yes
Mirror tilt	x_6	similar	yes	yes
Horizontal axis error (tilt)	x_7	yes	yes	yes
Horizontal angle encoder eccentricity	x_{8x}	yes	yes	no
Horizontal angle encoder eccentricity	x_{8y}	yes	yes	no
Vertical angle encoder eccentricity	x_{9n}	yes	yes	no
Vertical angle encoder eccentricity	x_{9z}	yes	no	no
Second-order scale error in the horizontal angle encoder	x_{11a}	yes	no	no
Second-order scale error in the horizontal angle encoder	x_{11b}	yes	no	no
Second-order scale error in the vertical angle encoder	x_{12a}	yes	yes	no
Second-order scale error in the vertical angle encoder	x_{12b}	yes	no	no
Rangefinder offset	x_{10}	yes	no	yes
Rangefinder scale error	/	yes	no	yes
Rangefinder cyclic error	/	yes	no	yes*

* existing only in TLSs using phase-shift distance measuring principle

It should be noted that in this work three errors are disregarded. First, this work does not focus on the comprehensive rangefinder calibration (scale and cyclic errors), only the rangefinder offset is considered. It is important to include the rangefinder offset in the functional model because:

- its value is typically detected as significant in the literature,

- it is known to change over time, see e.g. Reshetyuk (2009) for both points, and
- disregarding it can bias the estimates of other calibration parameters not sensitive to two-face measurements (publication A3).

On the contrary, the scale and cyclic errors are rarely detected as significant in the literature, see e.g. Abbas et al. (2019) and Chow et al. (2012), and they are expected to be negligible after the factory calibration upon the instrument assembly. Hence, it is arguable justified to disregard them for the efficient user-oriented re-calibration of TLSs. This simplification is argued in Section 6.2.

Additionally, this work does not deal with the problem of sensor synchronization. Namely, the angular, EDM and compensator measurements all have different measurement frequency and they work independently. Hence, incorrect sensors synchronization can induce additional systematic errors influencing the point cloud accuracy. The presumption in this work is that after the factory calibration upon the instrument assembly, this influence is insignificant.

Finally, the measurements of the dual-axis compensator can also be influenced by systematic errors. The compensator index error appears when the zero index is out of the alignment with the direction of the local gravity vector. In dual-axis compensators, this error is separated into the longitudinal index error (C_L), along the line-of-sight, and the transversal index error (C_T), along the trunnion axis. If not accurately calibrated, C_L adds up with the vertical index offset (x_4) and C_T adds up with the horizontal axis error (x_7), see e.g. Ogundare (2015). Additionally, an incorrectly calibrated compensator can cause wrong estimates of the TLS orientation during the calibration. This further influences the estimated calibration parameters due to high correlations with the instrument's orientation in the calibration adjustment (Lichti, 2010b). Thus, it is important to assure that the compensator measurements are unbiased as well. In the case of high-end TLSs Leica ScanStation P-series and Z+F Imager-series, the compensator index errors can be self-calibrated in-situ before scanning, and this calibration process lasts several minutes.

3.2 Target-based self-calibration of TLSs

The target-based self-calibration requires that special laser scanning targets are well distributed in the environment and scanned from several stations (Figure 2.1). Afterward, the target centers are estimated using different algorithms and used as point-wise TLS observations in the calibration adjustment (Chow et al., 2010a; Ge & Wunderlich, 2014; Kregar et al., 2013; Rachakonda et al., 2017). There are two common TLS target types, which are presented in Figure 3.3 (Becerik-Gerber et al., 2011):

- Spherical targets - typically made of different nearly-diffuse white-colored plastic materials due to good reflective properties, with a radius of circa 10-20 centimeters. In this case, the target center is the central point of the sphere.
- Planar targets – typically consisting of plastic or metal plates (sometimes just paper) with a printed pattern from one side that signalizes the target center, most often compromising four fields, two black (or gray) and two white fields forming a checkboard pattern. Different colors have an impact on the recorded intensity values making the intersection of the black and white fields (target center) detectable in scans.

In the target-based self-calibration related literature, the planar targets are preferred and strongly dominant due to two main reasons. Firstly, they are easier to produce and handle, which is especially important for the TLS calibration where they are required in high quantities. Secondly, multiple studies are reporting the bias in the target center estimation of the spherical targets that changes with the measurement range and it depends on the EDM type, laser beam properties (primarily spot size), as well as the target properties (Klapa et al., 2017; Lenda et al., 2017; Rachakonda et al., 2017). The bias primarily occurs due to steep angles of incidence between the sphere's surface normals and the upcoming laser beam, which appears on the edges of the visible target's hemisphere. This phenomenon so far cannot be mathematically modeled. Similar problems were never reported for the planar targets.

Therefore, due to the efficiency and the measurement accuracy, the target-based calibration in this thesis relies on the planar targets. At the Institute of Geodesy and Geoinformation (IGG) of the University of Bonn, we conducted a thorough investigation of different target center estimation algorithms and different target designs to assure the highest measurement accuracy (Janßen et al., 2019). From all analyzed algorithms the one based on the template matching between the known target pattern and the image representation of the point cloud was proven to be the most precise. Additionally, the new BOTA8 (BOnn TArget 8) targets were designed with a "cake alike" 8-fold

black and white pattern, matt finish and a size of 30 x 30 centimeters. These targets assured the highest measurement precision in comparison to multiple commercially available target designs (Janßen et al., 2019).

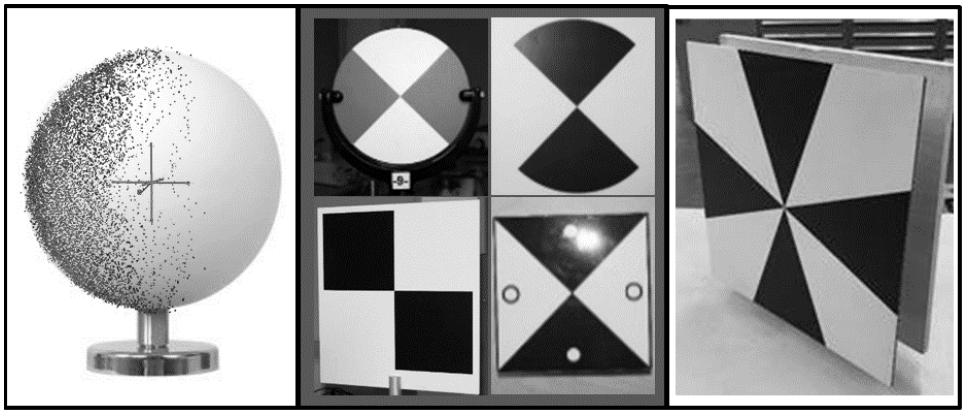

Figure 3.3: TLS targets: spherical (left), usual planar targets with 4-fold checkboard (middle), BOTA8 target (right); authors adaptation from Janßen et al. (2019)

In the case of the target-based calibration (point-wise TLS measurements in general), there are three main information sources for the detection of systematic measurement errors caused by mechanical misalignments:

- An absolute displacement of a single target (a spatial vector in arbitrary direction within a well-defined coordinate system);
- A length consistency of a test-length (change of a distance between two targets observed from different positions);
- A difference of two-face measurements of a single target (a vector in the direction of range, horizontal or vertical angle measurements with a magnitude equaling two-times the systematic error).

From this logic, three different adjustment algorithms for the target-based TLS self-calibration were derived in the literature. Namely, the network-method, the length consistency method, and the two-face method (Wang et al., 2017). Herein, the network-method (Section 3.2.1) and the two-face method (Section 3.2.2) are described, as they are used in the following experiments. The network-method is predominant in the literature revised in Section 2.1, and it is the basis for the development of the cost-efficient calibration field in this thesis (Section 5.1). The two-face method has its origin in Neitzel (2006) where it is used for a simplified TLS calibration experiment. It is introduced in the TLS self-calibration in its current form within this thesis in publication A1 (Medić et al., 2017). An alternative form was developed shortly after in Wang et al. (2017). Although initially developed for the target-based calibration, the two-face method in this work is primarily used as a foundation of the 2D keypoint-based self-calibration introduced in publications B2.

3.2.1 Network method

To sum up, the estimated target centers mimic the raw instrument measurements and they are introduced in the calibration adjustment as observations. The target-based self-calibration was originally derived in Lichti (2007). In short, multiple local coordinate systems associated with each scanner station are simultaneously transformed (registered) in the reference system of choice using a sufficient number of corresponding targets observed from each station:

$$\boldsymbol{f}_j^i = \boldsymbol{R}^i_{(k,\phi,\omega)}\,\boldsymbol{xyz}_j^i + \boldsymbol{T}^i_{(X,Y,Z)} - \boldsymbol{XYZ}_j^{ref.} = \boldsymbol{0}, \tag{3.7}$$

where $i = 1,2\ldots,s$; $j = 1,2\ldots,p$; s and p are total numbers of scanner stations and targets used in the experiment. The estimated (unknown) parameters are separated in the rotation matrix $\boldsymbol{R}^i_{(k,\phi,\omega)}$ defined with Euler angles $(\mathrm{k}, \phi, \omega)$ and the translation vector $\boldsymbol{T}^i_{(X,Y,Z)}$ (jointly called exterior orientation parameters, EOPs), the vector of Cartesian coordinates of targets in the reference system $\boldsymbol{XYZ}_j^{ref.}$ (also called object points, OPs), and the calibration parameters (CPs). The measurement vector from the scanner station i to the target j equals

$$\boldsymbol{xyz_j^i} = \begin{bmatrix} x_j^i \\ y_j^i \\ z_j^i \end{bmatrix} = \begin{bmatrix} (r_j^i + \Delta r_j^i)\, sin(\theta_j^i + \Delta\theta_j^i) sin(\varphi_j^i + \Delta\varphi_j^i) \\ (r_j^i + \Delta r_j^i)\, sin(\theta_j^i + \Delta\theta_j^i) cos(\varphi_j^i + \Delta\varphi_j^i) \\ (r_j^i + \Delta r_j^i)\, cos(\theta_j^i + \Delta\theta_j^i) \end{bmatrix}, \tag{3.8}$$

in the case of the right-handed, y-headed, clockwise-rotating coordinate system. In this study, the initial least-squares adjustment algorithm based on the strict Gauss–Helmert model (GHM) is transformed into the robust parameter estimator based on the Danish method (Krarup et al., 1980). An adequate strategy for the detection and elimination of eventual outliers was necessary, as it is known that the target center estimation process can suffer from gross errors. If no outliers are detected, the Danish method equals to the least-squares solution. This target-based self-calibration algorithm implementation is directly adopted from Reshetyuk (2009).

If the TLS is equipped with a dynamic dual-axis compensator, the direct observations of the rotation angles k and ϕ are additionally included in the calibration adjustment in the form of the constraints (Lichti, 2007):

$$\begin{aligned} \mathrm{k} &= \mathrm{k}_{\mathrm{observed}} \pm \sigma_{\mathrm{k}}, \\ \phi &= \phi_{\mathrm{observed}} \pm \sigma_{\phi}. \end{aligned} \tag{3.9}$$

where σ_k and σ_ϕ denote the uncertainty of the compensator measurements (typically based on the values given in the manufacturer's specifications).

The usual stochastic models for the TLS calibration in the literature are based on the values provided in the manufacturers' specifications given for a single point accuracy (Abbas et al., 2017; Ge, 2016; Lerma & García-San-Miguel, 2014; Lichti, 2010b). Most often, these are single scalar values separately provided for the horizontal angle, vertical angle, and range measurements, see e.g. Leica Geosystems AG (2015) and Z+F GmbH (2016). Such stochastic models are furtherly iteratively refined using the variance component estimation (VCE) based on the estimated measurement residuals of three observation groups ($\sigma_{r[mm]}, \sigma_{\varphi["]}$, and $\sigma_{\theta["]}$) until the global test is accepted (Förstner & Wrobel, 2016). The covariance matrices are without an exception built as the diagonal matrices by disregarding the unknown correlations between the observations. Within this thesis, the stochastic model of the calibration adjustment is analyzed and altered according to the conclusions presented in Section 5.1 (Eq. 5.1) based on publications A2 and A4. As the choice of the geodetic datum has a negligible impact on the calibration results (see Section 2.1.2), the minimally constrained datum by fixing six EOPs (Eq. 3.7) is implemented herein, see e.g. Abbas et al. (2014b).

3.2.2 Two-face method

Within this thesis (publication A1), a simplified algorithm for the calibration of panoramic TLSs from a single scanner station is introduced, exploiting the differences of the two-face measurements (Section 3.1.1). The concept is adopted from the total station component calibration (Schofield & Breach, 2007) and expanded for the case of TLSs. Contrary to the total station case, due to the larger number of relevant calibration parameters, a stepwise parameter estimation, or separate component calibration is not feasible. Hence, all estimable calibration parameters are searched for simultaneously within the least-squares adjustment algorithm (GHM):

$$\boldsymbol{f^i} = \boldsymbol{xyz_2^i} - \boldsymbol{xyz_1^i} = \begin{bmatrix} \boldsymbol{x_2^i} \\ \boldsymbol{y_2^i} \\ \boldsymbol{z_2^i} \end{bmatrix} - \begin{bmatrix} \boldsymbol{x_1^i} \\ \boldsymbol{y_1^i} \\ \boldsymbol{z_1^i} \end{bmatrix} = \boldsymbol{0}, \tag{3.10}$$

where xyz_2^i and xyz_1^i are the vectors of TLS observations in the second (back) and first (front) face of two-face measurements, equivalent to the ones in Equations (3.7) and (3.8). As explained in Section 3.1.3, some calibration parameters are not two-face sensitive (Table 3.1). Hence, for the two-face adjustment algorithm the calibration parameter equations are in the reduced form:

$$\Delta r_j^i = x_2 \sin\left(\theta_j^i\right) + v_{r_j^i}, \tag{3.11}$$

$$\Delta\varphi_j^i = \frac{x_{1z}}{r_j^i \tan(\theta_j^i)} + \frac{x_3}{r_j^i \sin(\theta_j^i)} + \frac{x_{5z-7}}{\tan(\theta_j^i)} + \frac{2x_6}{sin(\theta_j^i)} + v_{\varphi_j^i}, \tag{3.12}$$

$$\Delta\theta_j^i = \frac{x_{1n+2}\cos(\theta_j^i)}{r_j^i} + x_4 + x_{5n}\cos\left(\theta_j^i\right) + v_{\theta_j^i}. \tag{3.13}$$

In latter equations, the rangefinder offset (x_{10}) is completely omitted, while the parameter x_{5z} is omitted from the vertical angles equation and combined with the parameter x_7 in the case of horizontal angles, due to the same functional relation to the later observations. Therefore, the proposed algorithm can be used for almost complete calibration of the panoramic TLSs using only two scans from a single scanner station. The adopted stochastic model for the target-based two-face calibration method equals the one for the network method developed herein (publication A4) and described in Section 5.1 (Eq. 5.1). Again, due to the expected outliers, the algorithm based on the least-squares minimization problem is transformed into a robust estimator, using the modified Danish approach, as introduced in the TLS calibration in Reshetyuk (2009), see Section 3.2.1.

3.3 2D Keypoint-based calibration of TLSs

In response to the disadvantages of the existing in-situ TLS calibration approaches identified in Section 2.2.1, a new efficient approach is developed within this work (publications B2 and C1). Although it is not a part of the existing theoretical background, the concept of the established 2D keypoint-based self-calibration is shortly presented in the following text for the sake of completeness and for a better understanding of the experimental results presented in Sections 5.3 and 5.5. The approach is based on the algorithm of the two-face calibration method described in the previous section (Section 3.2.2). The only difference is that instead of the laser scanning targets, the observations in the calibration adjustments are keypoints that are automatically detected in the point clouds.

Numerous studies introduced and analyzed different algorithms for the detection and description of well-defined unique natural targets that are distinctive in the surroundings (features, keypoints or objects). The algorithms are applied either on the 3D geometrical data, i.e. point clouds (Guo et al., 2014), or 2D semantic data, typically RGB images (Remondino, 2006). Due to the high similarity of panoramic TLSs and panoramic cameras, the TLS measurements can be represented as panoramic or spherical images (Amiri Parian & Gruen, 2010). That makes using both 2D and 3D natural targets possible (from now on referred to as keypoints). Consequently, both keypoint types were used in the tasks related to TLS calibration such as deformation monitoring with TLS point clouds (Gojcic et al., 2019b), deformation monitoring with RGB images of image assisted total stations (Wagner et al., 2016), intrinsic camera calibration (Liu & Hubbold, 2006), camera to TLS calibration (Liang et al., 2016), as well as the registration of TLS point clouds (Böhm & Becker, 2007; Ge, 2017; Gojcic et al., 2020; Kang et al., 2009; Markiewicz et al., 2019; Urban & Weinmann, 2015; Wang & Brenner, 2008).

From all possibilities, herein, the Förstner interest point detector (Förstner & Gülch, 1987) was selected due to its verified high (sub-pixel) localization accuracy (Rodehorst & Koschan, 2006), which is a necessary prerequisite for the task of calibration. This algorithm detects and localizes salient local 2D image keypoints (junctions/corners and circular points), which are distinctive in their neighborhood and are similarly reproduced in corresponding images.

The pipeline of the 2D keypoint-based calibration algorithm is summarized in Figure 3.4. To detect the keypoints, the 3D point cloud is represented as a spherical image based on the polar TLS measurements and intensity values. First, the rasterized grids of the horizontal and vertical angular values are created with the resolution corresponding to the selected scanning resolution. Afterward, the interpolation is used both on the range and intensity values to assign a value for each grid cell based on the recorded data. This interpolation step is necessary because partial measurement gaps are unavoidable in the terrestrial laser scanning. This way, two image representations of the observed environment are created: the range image and the intensity image. The intensity image is used for the detection of the keypoints due to the high amount of details, while the range image is used to calculate back the 3D coordinates of the 2D keypoints found in the intensity image.

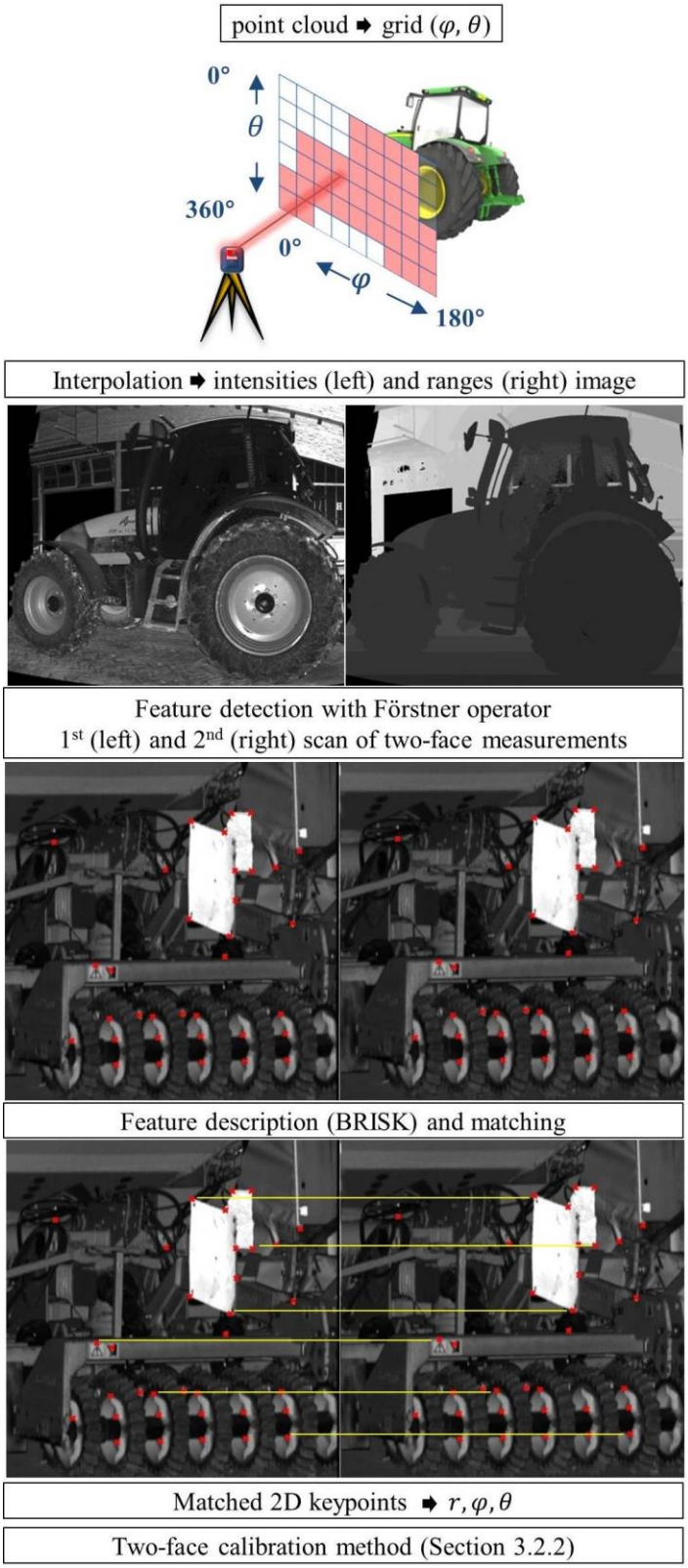

Figure 3.4: Pipeline of the 2D keypoint-based calibration approach

Then, within this intensity image, the well-defined 2D keypoints are automatically detected using the Förstner interest point detector. Consecutively, the keypoints are uniquely described using the BRISK feature description

algorithm (Leutenegger et al., 2011) based on their local neighborhood. Using these descriptions, the corresponding keypoints between the first and the second scan of two-face measurements are searched for and matched together. After the successful matching, each 2D keypoint is assigned range, horizontal and vertical angle measurements by linear interpolation on the horizontal and vertical angular grids, as well as the range image. These observations are introduced in the calibration adjustment based on the two-face method (Section 3.2.2). Overall, 8 out of 10 calibration parameters relevant for high-end panoramic TLSs can be estimated this way (Eq. 3.11-3.13).

To assure a high number of the correct matches and their good distribution in the instrument's field-of-view several additional steps are implemented within the abovementioned workflow (detailed in publications B2 and C1). As a result, the detected and correctly matched keypoints densely cover almost the complete instrument's field-of-view, which assures successful TLS calibration (Figure 3.5) used in Sections 5.3 and 5.5.

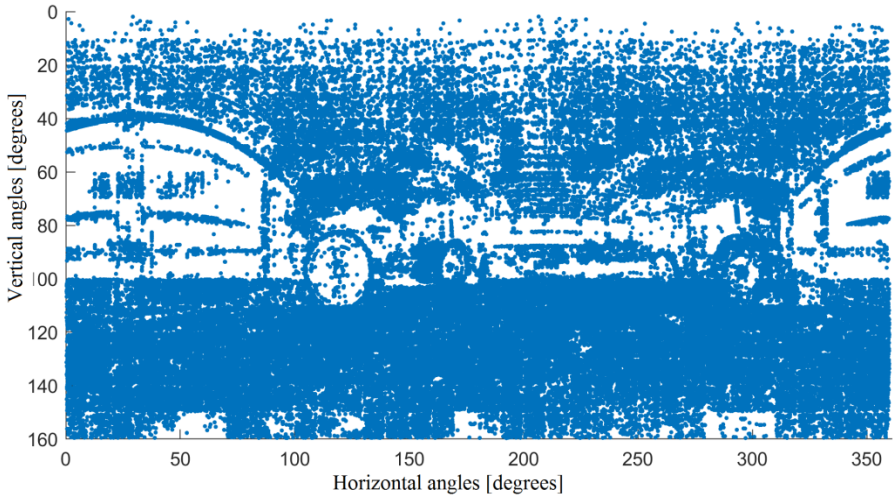

Figure 3.5: Distribution of observations (keypoints) in the scanner's field-of-view

3.4 Paraboloid-based calibration of TLSs

The original implementation of the paraboloid-based calibration is derived in Holst & Kuhlmann (2014a). It is an in-situ self-calibration approach that suffers from some disadvantages identified in Section 2.2.1 and tackled within this work (Section 5.2). It was developed for a special case of the deformation monitoring of the main reflectors of VLBI radio telescopes, which can be geometrically approximated with a rotational paraboloid. A detailed motivation for this deformation analysis, explanations regarding the measurement concept and the data processing can be found for example in Holst & Kuhlmann (2014a) and Holst et al. (2017). The approach is based on the simultaneous estimation of the calibration parameters and the geometrical approximation of the measurement object (disadvantage discussed in Section 2.2.1), where the object needs to fulfill certain criteria:

- It should be accurately constructed not to bias the calibration results,
- it should be large to cover a great portion of the instrument's field-of-view, and
- it should be of a simple shape, so it can be approximated by a geometric primitive (rotational paraboloid).

In the original implementation, the calibration was done for each scan separately, without using two-face measurements. On the contrary, the realization implemented within this thesis processes all scans simultaneously in a bundled adjustment. Furthermore, the two-face measurements are explicitly introduced in the adjustment using the functional model of TLS observations described in Equations (3.1)-(3.3). The advantages of new implementation are discussed in detail in Section 5.2. The calibration adjustment is realized as a strict solution of a nonlinear least-squares minimization problem based on the Gauss-Helmert-Model (Mikhail, 1976). The core of the functional model is the geometrical parametrization of the rotational paraboloid:

$$\frac{X_j^{i\,2} + Y_j^{i\,2}}{4 \cdot f_j} - Z_j^{i\,2} = 0, \tag{3.14}$$

where X_j^i, Y_j^i, Z_j^i are the coordinates of the point *i* for the scan *j* in the coordinate system describing the paraboloid in its normal position (Holst et al., 2012). This equation is related to the local scanner coordinate system as:

$$\boldsymbol{XYZ_j^i} = \begin{bmatrix} \boldsymbol{X_j^i} \\ \boldsymbol{Y_j^i} \\ \boldsymbol{Z_j^i} \end{bmatrix} = \boldsymbol{R_y}(\boldsymbol{\tau y}) \cdot \boldsymbol{R_x}(\boldsymbol{\tau x}) \cdot \boldsymbol{xyz_j^i} + \boldsymbol{T_v}, \tag{3.15}$$

where $\boldsymbol{R_y}(\tau y)$ and $\boldsymbol{R_x}(\tau x)$ are the rotation matrices, $\boldsymbol{T_v} = [X_v, Y_v, Z_v]$ is the translation vector and $\boldsymbol{xyz_j^i}$ is the vector of the TLS observation triplet *i* from scanner station *j* influenced by random and systematic errors (Eq. 3.8). Hence, the parameters defining the rotational paraboloid in the local scanner coordinate system of a scanner station *j* are:

$$\boldsymbol{x_{RP}}^j = [\boldsymbol{X_v}, \boldsymbol{Y_v}, \boldsymbol{Z_v}, \boldsymbol{\tau x}, \boldsymbol{\tau y}, \boldsymbol{f}]^{\boldsymbol{T}}. \tag{3.16}$$

In the bundled calibration adjustment, the rotational paraboloid parameters for all scans are estimated simultaneously together with a single set of the calibration parameters, which are expected to be constant during one measurement campaign (argued in Section 5.4). The calibration parameters that are estimated within the paraboloid-based calibration adjustment equal the ones in Eq. (3.11-3.13), except for the excluded parameter x_2 (Tab. 3.1). The estimable parameters are determined based on the conducted sensitivity analysis (publication B1). Hence, this calibration approach is not comprehensive but covers the majority of the calibration parameters relevant for high-end panoramic TLSs. To cope with the large data size of the acquired measurements, the point clouds are necessarily subsampled to a regular grid as proposed in Holst & Kuhlmann (2014a). The eventual outliers are removed within this subsampling step. The stochastic model of the calibration adjustment is based on the values for TLS polar measurements provided in the manufacturer's specifications.

4 Content of Relevant Publications

In this chapter, the publications that form the basis of this cumulative thesis are briefly summarized. Figure 4.1 classifies these publications according to their content and the scientific context. Based on their primary focus, they are grouped into three topics and referred to as publications A-, B- and C-.

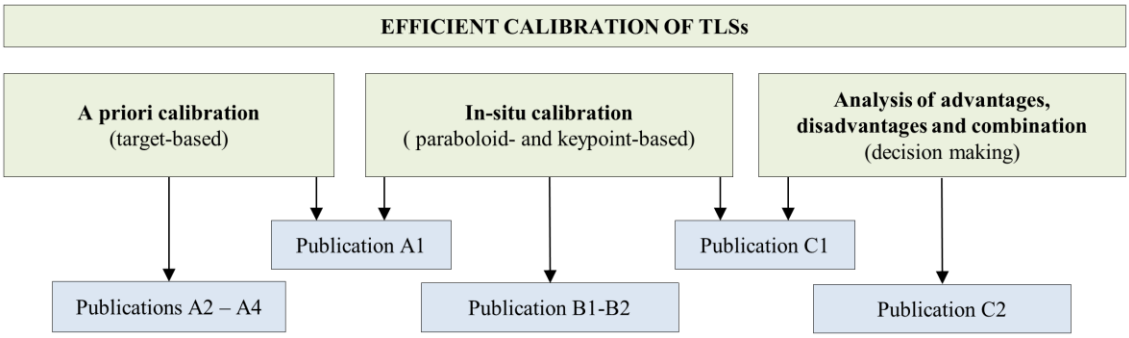

Figure 4.1: Content assignment of the relevant publications to clarify their respective contribution to the dissertation.

The publication A1 presents the results of the preliminary investigation setting up the basics of both advancements in the a priori and in-situ calibration. The publications A2-A4 deal with optimizing the efficiency of the prevailing a priori calibration approach, the target-based self-calibration. Further, the publications B1 and B2 (also partially C1) deal with the advancements within in-situ calibration approaches. More precisely, publication B1 deals with the enhancements of a paraboloid-based self-calibration, while publication B2 introduces new keypoint-based calibration that addresses the efficiency-related shortcomings identified within the publication B1. Furthermore, the publication C1 introduces certain improvements to the keypoint-based calibration approach. Finally, the publications C1 and C2 analyze the advantages and disadvantages of the investigated calibration approaches. Moreover, they bring a discussion of their relevance for the end-users, concentrating on decision making, the selection of the appropriate approach and/or their combination. The main aspects of the publications are addressed again in Chapter 5, where their context within the main objectives of this thesis (Section 1.2) is emphasized.

Publication A1

- Medić, T., Holst, C., & Kuhlmann, H. (2017) Towards System Calibration of Panoramic Laser Scanners from a Single Station. Sensors, 2017, 17, 1145.

The publication A1 presents the preliminary analysis of the state-of-the-art in the target-based self-calibration with several simple modifications. Two main aims of the publication were:

- Setting up the functional model of the calibration adjustment that was used in the following experiments,
- and analyzing how important is the extensive number of scanner stations within the calibration field.

First, a different parametrization of the TLS angular measurements is introduced to allow direct implementation of the two-face measurements in the calibration adjustment (Section 3.1.1). Second, at that time novel functional model of the calibration parameters developed by NIST for the laboratory component-wise TLS calibration was investigated, adjusted for the high-end panoramic TLSs and implemented in the target-based self-calibration (Section 3.1.3). These steps defined the complete functional model that was later used for optimizing the efficiency of the a priori target-based self-calibration in publications A2-A4 (Section 5.1).

Moreover, stirred by the latter modifications, a new target-based self-calibration algorithm based on only two-face measurements form a single scanner station, the two-face method (Section 3.2.2), was introduced. Namely, in the majority of the previously conducted experiments, the two-face measurements were only introduced in the TLS calibration as coarse two-face measurements, where the instrument is physically rotated for 180° around its standing axis. So far, there were only two documented simplified calibration experiments where explicit two-face

measurements were used for the TLS calibration (Muralikrishnan et al., 2014; Neitzel, 2006). However, they were never used in the comprehensive target-based self-calibration.

The implemented modifications of the functional model and the new calibration algorithm were tested in an initial target-based self-calibration experiment. The calibration field was realized in a machine hall with dimensions of 70 x 25 x 9 meters, where 300 targets were well distributed over the whole volume. Targets were scanned from three stations with five scans (two two-face scans and one single face scan). In the experiment, the high-end panoramic TLS Leica ScanStation P20 was investigated and the measurement acquisition lasted approximately five hours (five scans with the highest measurement resolution). The functional model of the calibration adjustment was initially realized as the network method (Section 3.2.1). Additionally, the two-face method (Section 3.2.2) was applied to the measurements from one scanner station. The stochastic model equaled the usually employed ones in the literature, i.e. based on manufacturer's specifications and refined with the VCE (Section 3.2.1), which can be justified in this case due to high abundance of observations.

The comparison of the two-face method with the full-blown network-method of the target-based self-calibration proved that the majority of the relevant calibration parameters can be successfully estimated using only the two-face measurements from a single station. This is in a stark contrast with the usual realizations of the target-based self-calibrations. The differences in the achieved measurement accuracy with both calibration methods were marginal, while the two-face method requires several times shorter scanning time. This analysis had a significant impact on the following investigation of the most sensitive measurement configurations for the TLS calibration conducted in publication A3 (see also Section 5.1). Namely, this served as the confirmation that the two-face measurements should be treated as the primary information source for the TLS calibration of all parameters that can be estimated this way. Additionally, this led to the two-face method founding a basis for the new 2D keypoint-based calibration approach developed herein (publications B2 and C1).

Finally, the measurement configuration from the empirical experiment was replicated in the simulated environment, where estimating the synthetic calibration parameters confirmed that all parameters of the newly implemented functional model (based on the NIST model) can be estimated within the target-based self-calibration. These results served as the confirmation of the implemented functional model which was furtherly used for optimizing and designing the efficient calibration field through the publications A2-A4.

Publication A2

- Medić, T., Holst, C., Janßen, J., Kuhlmann, H. (2019b) Empirical stochastic model of detected target centroids: Influence on registration and calibration of terrestrial laser scanners, J. Appl. Geodesy, 13 (3), 179-197.

In the publication A2, the usually employed stochastic models for the target-based self-calibration (Section 3.2.1) and target-based registration of TLS point clouds were disputed. Namely, they are typically based on the manufacturer's specifications for single point measurement accuracy, which are eventually refined with the VCE. However, these stochastic models are not accurate, at least not before the refinement, because the target-based algorithms use target centers and not raw single-point measurements. The target centers are derived from multiple measurements, using the image representation of EDM intensity values and different target centre estimation algorithms (Section 3.2). Hence, they have different uncertainty characteristics in comparison to the raw single point measurements. Not accounting for these differences can have two adverse effects:

- First, for the optimization and design of the efficient calibration fields, the stochastic model needs to be a priori well-defined as it cannot be iteratively refined based on the empirical data, e.g. through VCE. Hence, an inaccurate stochastic model can bias the optimization results.
- Second, in the general case of TLS calibration and registration, if the initial definition of the stochastic model is far from truth, especially considering relative weighting between the observation groups, the adjustment procedure can be biased even in the case of using VCE. This point is especially critical if the number of observations within the adjustment is small due to small sample for the variance refinement.

Therefore, to confirm the abovementioned statements, the precision of the target center estimation was empirically investigated. Furthermore, the values from the empirical investigation are used to form the stochastic models of TLS calibration and registration adjustments to detect and quantify the adverse effects of potentially incorrect stochastic models. Using the target centre precision for the stochastic model of the TLS calibration and registration is

discussed in detail and arguably justified in the publication A2, while a dispute about this simplification is given in Section 6.3.

The empirical precision was estimated as a standard deviation of repeatedly estimated target centers of 15 targets on different distances (2, 5, 10, 15, 20, 35, 50, 75, 100 m) with different angles of incidence (from 0° to 60°). The targets were measured with the Leica ScanStation P20, with two highest scanning resolutions (0.8 and 1.6 mm at 10 meters), see Leica Geosystems AG (2015). The target centers were estimated with two different software solutions, once with Leica Cyclone and once with the in-house developed algorithm (Section 3.2) derived in Janßen et al. (2019). All targets measured on the same distance are considered to be a part of the same observation group. Hence, their standard deviations are combined using the pooled standard deviation to increase the statistical power (Lomax & Hans-Vaughn, 2012). The most relevant results of the latter investigation can be summarized as follows:

- If the usually employed stochastic models based on manufacturer's specifications are not refined through VCE, the uncertainty of the parameters estimated within the adjustment is over-estimated.
- Typically used representations of the target centre uncertainty are overly simplified. The uncertainty depends on the measurement configuration (distance and angle of incidence), both in the case of range and angular measurements. Hence, representing it with three constant scalar values is not generally applicable.
- Target centre uncertainty depends on the scanning resolution to some degree and it strongly depends on the target centre estimation algorithm.
- Disregarding the latter three points has adverse effects on the tasks of planning, processing and the analysis of TLS point cloud registration and calibration.

Based on the latter results, it was confirmed that the target centre precision depends on multiple factors such as scanner settings, measurement configuration and the target center estimation algorithm. To account for that, several adaptations were made in the subsequent experiments. First, a simple empirical stochastic model in the form of the look-up tables was used for the sensitivity analysis and the design of the efficient calibration field in publications A3 and A4 (see Section 5.1). The in-house developed target centre estimation algorithm was used in the following experiments, as it provided higher measurement precision than the commercial solutions and it almost completely alleviated the impact of the angle of incidence on the measurement precision (Janßen et al., 2019). Also, the scanning resolution was adjusted to find the best compromise between the scanning time and the measurement precision (see Section 5.1). Considering the later adaptations helped optimizing the efficiency of the target-based self-calibration.

Publication A3

- Medić, T., Kuhlmann, H., Holst, C. (2019d) Sensitivity Analysis and Minimal Measurement Geometry for the Target-Based Calibration of High-End Panoramic Terrestrial Laser Scanners, Remote Sens., 11 (13), 1519.

The publication A3 makes a step further in the efficiency optimization of the target-based calibration approach. It deals with sensitivity analysis aiming at finding the best measurement configurations for detecting and estimating each individual calibration parameter. This step is necessary for approach optimization to reduce the numerical complexity of the problem (see Section 2.1.2). Namely, defining the most cost-efficient measurement configuration for the target-based TLS calibration has an unlimited number of solutions with multiple degrees of freedom, such as the possible number and position of targets, as well as the number, position and orientation of the scanner stations in 3D space. Hence, narrowing down the possible solutions on the subset of well-defined sensitive measurement configurations makes the optimization problem tackled in publication A4 solvable. Additionally, the separation of the sensitivity analysis on the individual calibration parameters allowed the justified reduction of the problem from 3D to 2D.

The sensitivity analysis of the measurement configurations towards estimating individual calibration parameters was realized by investigating the signal to noise ratios (SNRs). Here, the signal represents the impact of the mechanical misalignment on the TLS observations, i.e. the magnitude of the resulting systematic error, based on the well-defined functional model from publication A1. The noise represents the empirical target center precision determined in publication A2. The SNR is analyzed for different target(s)-to-scanner measurement configurations, where the position of only one target is observed for the two-face sensitive parameters (when applicable) and the change of the distance between two targets is observed for the remaining calibration parameters (Table 3.1). As a result, the most sensitive measurement configurations for 10 calibration parameters relevant for the high-end panoramic TLSs (Eq. 3.4-3.6) were derived and the possibility of their implementation in realistic conditions was discussed.

In addition to the sensitivity analysis, and also as a demonstration of its usefulness, the minimal measurement configuration sensitive to all calibration parameters was derived. It was compared with the TLS test-fields used for the measurement quality assessment (see Section 1.1) and it proved that the typical test-fields are sensitive to all relevant mechanical misalignments. Finally, the shortcomings of this minimal measurement configuration were highlighted concerning the objective A presented in Section 1.2, i.e. estimating the trustworthy calibration parameters with a pre-defined quality. Although the configuration was found to be sensitive, it had low reliability, low precision and too high correlations between the calibration parameters for the successful calibration. This analysis made a final groundwork for defining the optimization goals that need to be perused when designing the efficient target-based calibration field (publication A4).

Publication A4

- Medić, T., Kuhlmann, H., & Holst, C**.** (2020b) Designing and Evaluating a User-Oriented Calibration Field for the Target-Based Self-Calibration of Panoramic Terrestrial Laser Scanners, Remote Sens., 12 (1), 15.

In the publication A4, the goals for designing the efficient TLS target-based calibration-field were decisively defined and discussed in detail. The goals are summarized in the Section 1.2, under the objective A, and they focus on precision, reliability, parameter correlations and the efficiency. Based on these goals, a locally optimal TLS calibration-field was derived through the series of simulation experiments.

The simulations were realized according to the functional model attested in the publication A1 and the stochastic model in the form of the look-up tables defined in the publication A2. The simulations were based on the trial and error analysis considering only the sensitive measurement configurations identified within the sensitivity analysis in publication A3. The simulation trials started with the minimal measurement configuration sensitive to all calibration parameters, which was also derived in the publication A3. The number of targets was iteratively increased by 1 when aiming to improve the estimates of two-face sensitive calibration parameters, or by two when aiming to improve the estimates of the remaining parameters (Table 3.1). In the simulation process, 85 different target locations and four different scanner stations in several hundred different set-ups were considered, reaching the maximum configuration complexity when incorporating 24 targets.

The simulation results indicated that 14 targets observed from 2 scanner stations using two-face measurements are sufficient for the comprehensive and successful calibration of high-end TLSs. This is eight times smaller number of targets in comparison to the typical calibration field presented and simulated in Chow et al. (2013) consisting of 120 targets. Consequently, the derived calibration-field design was implemented and evaluated on several different panoramic terrestrial laser scanners. The results achieved were mostly following the simulated values and the improvement in the measurement accuracy was in the same range as the improvements achieved in the literature. The advancement of the implemented calibration field lies in the fact that the number of observations necessary for the calibration was approximately an order of magnitude smaller in comparison to the previous implementations. The most important results concerning the efficient target-based self-calibration are presented and discussed in detail in Section 5.1.

Additionally, within this publication, the a posteriori application of the calibration parameters estimated on a calibration-field was investigated. It successfully improved the point cloud accuracy in the following measurement campaigns beyond the manufacturer's factory calibration, even for the brand new and recently factory calibrated instruments. However, the point cloud accuracy improvement was degraded in comparison to the in-situ improvement realized within the calibration field, in the moment of the calibration. This placed the focus on the problem of the stability of the calibration parameters, which was already discussed in the literature (see Section 2.1.2). To account for that, the stability of the estimated calibration parameters was investigated in detail in the publication C2 (see also Section 5.4).

Publication B1

- Holst, C., Medić, T., & Kuhlmann, H. (2018a) Dealing with systematic laser scanner errors due to misalignment at area-based deformation analyses, J. Appl. Geodesy, 12 (2), 169-185.

Within the publication B1, the influence of the TLS mechanical misalignments on a concrete task of deformation monitoring of a main reflector of the VLBI radio telescope was investigated. For the deformation analysis, the main reflector is approximated with a rotational paraboloid and the deviations from the designed geometry are

investigated. It was identified that the instrument-related systematic errors lead to large and systematically distributed post-fit residuals, an inaccurate estimate of the observed object's shape and an inaccurate estimate of the object's position and orientation. Additionally, it was identified that the state-of-the-art approach of the in-situ paraboloid-based calibration introduced in Holst & Kuhlmann (2014a) could be insufficient to alleviate all adverse effects. The main reason for this is the shortcoming of the approach identified in Section 2.2.1. Namely, the high correlation between some geometrical parameters of the modeled object and the calibration parameters can cause biased results of both in-situ calibration and, consequently, the deformation analysis.

Therefore, to improve the results of the deformation analysis several strategies were tested and compared. The strategies consider: the inclusion of the two-face measurements, the in-situ paraboloid-based self-calibration of each scanner station individually as introduced in Holst & Kuhlmann (2014a), the bundled self-calibration with all scanner stations together as introduced herein (see Section 3.4), as well as the combination of two-face measurements and the mentioned self-calibration approaches. The best results were obtained when the two-face measurements were explicitly introduced in the adjustment using the functional model derived in publication A1, when the bundled in-situ paraboloid-based calibration was used, and when only a subset of the most relevant calibration parameters defined in publication A1 was targeted.

The inclusion of two-face measurements strongly supports the estimation of the calibration parameters within the in-situ calibration, as most of the calibration parameters are two-face sensitive (see Section 3.1.3). This reduces the correlations between the calibration parameters and the geometrical parameters of the measured object's, mitigating the eventual bias in the parameter estimation. Moreover, bundling multiple scanner stations within one calibration adjustment strongly improves the measurement configuration with the same outcome. When the unbiased in-situ self-calibration is assured, the estimated calibration parameters correctly absorb the systematic trend of the post-fit residuals assuring correct analysis of the a posteriori variances and the correct statistical testing results. Hence, this strategy successfully alleviates all adverse effects indicated in the beginning.

The results and conclusions of this study a43 discussed focusing on the transfer to a general case of the areal-based deformation monitoring with TLSs, and also, the main considerations regarding the in-situ TLS calibration are presented in Section 5.2. Despite the successful application of the strategy, several shortcomings were identified. The main shortcoming is the evident limitation of the approach on the geometrically describable man-made object with the a priori known shape. This shortcoming is shared by all in-situ calibration approaches described in the literature. Hence, it was tackled in the following work within this thesis (publication B2).

Publication B2

- Medić, T., Kuhlmann, H., & Holst, C. (2019a) Automatic in-situ self-calibration of a panoramic TLS from a single station using 2D keypoints, ISPRS Ann. Photogramm. Remote Sens. Spatial Inf. Sci.,IV-2/W5,413-420.

In the publication B2, a new efficient in-situ calibration approach was introduced that allows automatic calibration of panoramic TLSs from a single station. This approach overcomes the main shortcoming of the existing in-situ calibration strategies identified in the publication B1 (see also Section 2.2.1). Namely, it does not require a priori identified geometrically describable man-made structures in the surroundings, making it more efficient and generally applicable.

The calibration approach is based on the two-face calibration method derived in the publication A1 and described in Section 3.2.2. The main difference is that here, instead of the dedicated TLS targets, the keypoints that are automatically detected in the environment are used as observations. The keypoints are detected using the photogrammetric feature detection algorithm and the correspondences between the matching keypoints are built using the photogrammetric feature matching algorithm. The whole calibration approach is described in Section 3.3.

The approach was tested in a large indoor hall on a dataset acquired with the high-end panoramic TLS, Leica ScanStation P20, in normal (non-laboratory) working conditions. The estimated calibration parameters were compared against the results of the attested target-based two-face calibration method and the impact of applying the calibration parameters on the point cloud accuracy was investigated. The estimated calibration parameters were directly comparable concerning the parameter values, their precision and parameter correlations. Additionally, applying the estimated parameters successfully removed the detectable systematic trends in the point clouds.

It can be concluded that the proposed in-situ calibration approach successfully mitigated majority of the relevant TLS misalignments, without the need for any preparatory works. This derived solution is primarily interesting for the environments where the man-made objects cannot be found in abundance, e.g. outside the urban regions. The impact on the point cloud quality, some properties of the derived calibration approach as well as the general considerations are discussed in more detail in Section 5.3.

Despite the successful application of the approach, several shortcomings were identified. First, the detected keypoints were not well distributed within the instrument's field-of-view, hindering the possibility of detecting eventually missing calibration parameters. Second, the range observations to the detected keypoints had low precision making several calibration parameters impossible to estimate. These problems were further tackled in publication C1, where the initial implementation of the calibration approach was enhanced.

Additionally, as this calibration approach relies on two-face measurements from a single station, it cannot be used for the comprehensive calibration. The possible solutions regarding this problem are discussed in Section 6.4. The last shortcoming is that the calibration success strongly depends on the measurement configuration found during a measurement campaign, which cannot be controlled. Hence, this calibration approach cannot guarantee the comprehensive calibration with the pre-defined quality criteria (Section 1.2). Hence, to achieve the optimal calibration results, it needs to be combined with a comprehensive a priori calibration, what is investigated in the publications C1 and C2 (see also Section 5.5).

Publication C1

- Medić, T., Kuhlmann, H., & Holst, C. (2020c) Empirical evaluation of terrestrial laser scanner calibration strategies: manufacturer-based, target-based and keypoint-based, Contributions to International Conferences on Engineering Surveying, INGEO&SIG 2020, Springer (accepted manuscript, ahead of print).

The publication C1 examined the advantages and disadvantages of several calibration possibilities the end-users have at hand to calibrate their terrestrial laser scanners. The investigated possibilities were: the a priori target-based calibration (publications A1-A4), the in-situ keypoint-based calibration (publication B2) and the a priori manufacturer's factory calibration (see Section 1.1).

The investigation focused on the analysis of two common datasets, the indoor measurements of a large hall and the outdoor measurements of a building façade, acquired with a high-end panoramic TLS, the Z+F Imager 5016. In order to get a better insight on how the user-oriented calibration approaches compare with the manufacturer's calibration, the dataset of the large hall was depleted of the factory calibration. The analysis concentrated on comparing the point cloud accuracy before and after applying the calibration parameters.

The most important results and the general considerations regarding the relevance for the end-users are presented and discussed in detail in Section 5.5. In short, the results indicated that, if necessary, both user-oriented calibration approaches can substitute the factory calibration, if the functional model of the calibration parameters is a priori known are comprehensive. Also, the results demonstrated that the most accurate point clouds are acquired when all three calibration approaches are appropriately combined, which successfully makes the use of the main advantages of each approach. Finally, within this study, several improvements of the keypoint-based calibration approach (Section 3.3) were introduced to tackle the shortcomings identified in the publication B2.

Publication C2

- Medić, T., Kuhlmann, H., & Holst, C**.** (2020a) A priori versus in-situ terrestrial laser scanner calibration in the context of the instability of calibration parameters, Contributions to International Conferences on Engineering Surveying, INGEO & SIG 2020, Springer (accepted manuscript, ahead of print).

Finally, the publication C2 investigated the stability of the calibration parameters, which was identified as a major drawback of the a priori target-based self-calibration approach in the publication A4 (see also Section 2.1.2). The stability of the calibration parameters was investigated on the calibration field for the efficient target-based calibration of panoramic terrestrial laser scanners developed through the publications A1-A4. As the aim of the calibration fields is typically the a priori calibration, the stability of the estimated parameters is of high relevance.

The investigation focused on the analysis of the calibration parameter changes within the time series of several calibration days (2-6 calibrations per day) within half a year (8-9 calibration days) for two high-end panoramic TLSs, the Leica ScanStation P50 and the Z+F Imager 5016. The efficient calibration approach developed in the previous publications allowed the realization of nearly 40 calibration experiments for the latter two instruments within the given time frame. A short-term (within a day) and a long-term (between days) parameter stability were investigated separately due to a different scale and the relevance for the end-users. The analysis was based on estimating the empirical correlations between the estimated calibration parameters and the variables such as the instrument's working time, ambient temperature and internal instrument's temperature (when possible).

The results indicated that the changes can be traced and partially modeled based on the internal warming-up of the instrument and the ambient temperature. Moreover, the variability of nearly half of the parameters can be reduced if the instrument's working time and the ambient temperature are measured and mathematically considered. By applying simple correction models, the short-term parameter instability can be reduced by 24% on average, while the long-term instability by 43% on average. Additionally, the calibration parameters of the dynamic dual-axis compensators (see Section 3.1.1) were also investigated in a similar manner. The results confirmed that the compensator index offsets (see Section 3.1.3) are highly correlated with the ambient temperature.

The magnitudes of the parameter changes and the relevance for the TLS calibration in general are presented and discussed in detail in Section 5.4. Additionally, based on these results, the advantages and disadvantages of the a priori calibration are analyzed, and the strategies for achieving an adequate measurement accuracy are discussed. These findings aim at helping the end-users to decide if they require additional instrument calibration for their measurement task. In the case they do, the demonstrated experiments can help to select the optimal strategy regarding their respective efficiency and accuracy demands.

5 Summary of the Most Important Results

In the previous chapter, the relevant publications that form the basis of this thesis were briefly summarized in a publication-wise manner. Within this chapter, the major findings and aspects of the latter publications are presented in a topic-wise manner concerning the objectives presented in Section 1.2. Within topic "**A**" regarding the a priori TLS calibration, Section 5.1 answers the question: "*How to design a target-field for the efficient a priori TLS target-based self-calibration*?". Within topic "**B**" concerning the in-situ calibration, Section 5.2 answers the question: "*How to assure successful in-situ TLS calibration*?", while Section 5.3 introduces the *new efficient in-situ calibration approach* that tackles the identified shortcomings of the existing approaches. Finally, topic "**C**" deals with the analysis and comparison of the calibration approaches. Herein, Section 5.4 summarizes the findings that brings the *better understanding of the calibration parameters' stability*, as the key limiting factor of the a priori calibration, while the results and conclusion of the approaches comparison is presented in Section 5.5, which leads to the *better understanding of advantages and disadvantages of each calibration approach*.

5.1 "A" Designing a target-field for efficient a priori TLS calibration

As elaborated in Section 2.1.1, the target-based self-calibration is at the moment the best-suited approach for the a priori TLS calibration that can fulfill the criteria defined within objective A in Section 1.2. In short, the demanded characteristics for a widely accepted calibration approach are to be efficient and easily reproducible, comprehensive, as well as informative and trustworthy. The efficiency is identified as the main shortcoming of the existing implementations in Section 2.1.2. Therefore, this work focuses on increasing the efficiency of the target-based calibration to support the transfer from the scientific community to a wide number of users in the commercial sector.

The main contribution of this thesis is the stepwise solution of the problem that can be easily reproduced by qualified engineers. The implemented workflow can be separated on four key steps (publications A1-A4):

- Step 1: Choice of an adequate functional model,
- Step 2: Choice of an adequate stochastic model,
- Step 3: Problem simplification that assures solvable optimization and design,
- Step 4: Optimization of the calibration field that assures efficient and trustworthy calibration results.

By following these four steps, a calibration field was designed, implemented and evaluated to confirm the feasibility of the suggested workflow. Additionally, an easy reproducibility was demonstrated by a simple simulation demonstration. The summary of the most relevant results of this investigation is given in the following text.

Step 1: Choice of an adequate functional model

Solving the task of designing an efficient calibration field (FOD problem) requires clearly defined and accurate functional model of the calibration adjustment (Section 2.1.2). As this was not entirely fulfilled in the literature, in the publication A1 (Medić et al., 2017), this functional model is investigated and adapted for the target-based self-calibration of the high-end panoramic TLSs as explained in Sections 3.1.1 and 3.1.3. In short, the functional model of calibration parameters is based on the genuine instrument's geometry and only the most relevant parameters are kept. This resulted in 10 relevant calibration parameters (Eq. 3.4-3.6) making the functional model at the same time accurate, to avoid biased optimization results and not over-parameterized, which makes the derivation of the efficient calibration solution possible. Additionally, the angular parametrization (Section 3.1.1, Eq. 3.1-3.3) was implemented in the way that allows the explicit introduction of the two-face measurements, which were proven to be an indispensable source of information for the calibration in the publication A1 (Medić et al., 2017).

The results within the study proved that the selected parameters based on the genuine TLS geometry can be successfully estimated within the target-based self-calibration (Medić et al., 2017). All parameters were found significant at least for some of multiple investigated instruments, pointing out that considering all 10 parameters was necessary (Medić et al., 2020b). Finally, the point clouds of the calibrated instruments showed no noticeable remaining systematic errors, indicating the comprehensiveness of the defined functional model for high-end TLSs (Medić et al., 2020b).

Step 2: Choice of an adequate stochastic model

Additionally, a well-defined stochastic model is another mandatory prerequisite for optimizing the calibration procedure (Section 2.1.2). As stated in Section 3.2.1 and analyzed in publication A2 (Medić et al., 2019b), the usually employed stochastic models are based on the vague values given in the instrument specifications. Therefore, they are not sufficiently precise, at least not before the refinement through VCE. This can lead to the biased results when optimizing the calibration field design.

In order to define a more realistic stochastic model for designing the efficient calibration field, the precision of the target center estimation was empirically investigated in publication A2 (Medić et al., 2019b) for a particular scanner and a measurement setup (Figure 5.1). Figure 5.1 presents notable differences between the values from manufacturer's specifications (red lines) and the empirical precision of the target centers (black curves) in the direction of ranges (left), in the direction of horizontal angles expressed in angular units (middle) and expressed in metric units (right), calculated as $r \cdot \tan \sigma_{\varphi}$. The vertical angles are excluded as there was no notable difference to horizontal angles. The empirical values are significantly different from theoretical ones, and they are distance-dependent. To account for that, the stochastic model for the optimization of the calibration field design was defined in the form of the distance-dependent look-up tables. An important piece of information for designing a calibration field is that there is a global minimum of the angular measurement uncertainty (Figure 5.1, middle), which is accounted for in the look-up tables.

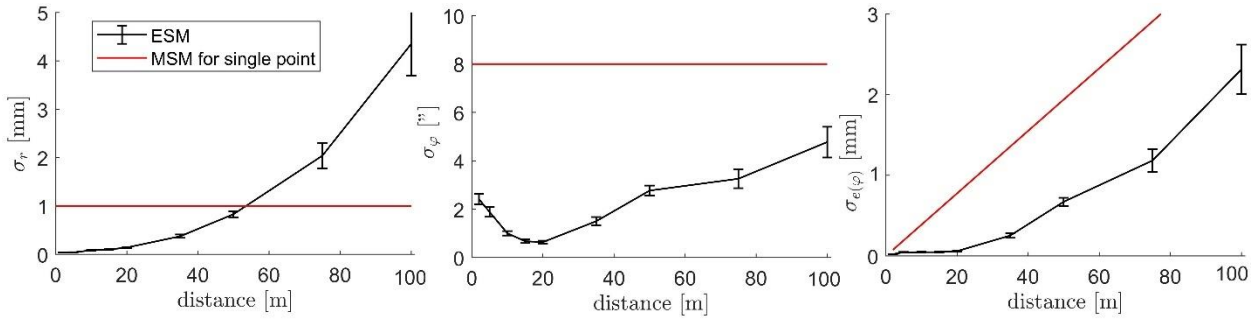

Figure 5.1: Values from the manufacturer's specifications, i.e. manufacturer's stochastic model - MSM (red) vs. empirical target center precision, i.e. the empirical stochastic model - ESM (black) for Leica ScanStation P-series, scanning resolution 1.6 mm at 10 meters; left – range measurements, middle – horizontal angles in arc seconds, right – horizontal angles in millimeters; error bars denote 1 sigma value.

For the empirical experiments on the implemented calibration field, an alternative stochastic model was required (not instrument dependent look-up tables), the one that would be applicable to multiple scanners and that would fit the observed target center precision behavior. If both range and angular measurements are observed in the metric units (Figure 5.1, left and right), the uncertainty remains approximately constant up to the distance of 20 meters. Therefore, the a priori knowledge of the calibration field dimensions was used (maximal distances not notably larger than 20 meters) and a stochastic model for the empirical experiments was derived in the following form:

$$\boldsymbol{\Sigma} = \begin{bmatrix} {\sigma_{r\,[mm]}}^2 \boldsymbol{I} & & \\ & (\tan^{-1}\frac{\sigma_{e(\varphi)\,[mm]}}{r_i})^2 \boldsymbol{I} & \\ & & (\tan^{-1}\frac{\sigma_{e(\theta)\,[mm]}}{r_i})^2 \boldsymbol{I} \end{bmatrix} \tag{5.1}$$

where Σ is a diagonal covariance matrix, $\sigma_{r\,[mm]}$ is the standard deviation of ranges, while $\sigma_{e(\varphi)\,[mm]}$ and $\sigma_{e(\theta)\,[mm]}$ are the standard deviations of angular measurements expressed in metric units. The additional modification was necessary, as the higher noise in angular measurements was observed for targets located on very high elevations (close to the instrument's zenith). This phenomenon was not examined in detail within the thesis due to time constraints (see Section 6.3). However, it was considered in the stochastic model by additionally splitting observations of horizontal and vertical angles on two observation groups, one for lower and one for higher elevated targets.

This way the stochastic model that more accurately fits the true target center uncertainty is derived and used for designing and evaluating the calibration field. Additionally, one of the results of the investigation was that the target precision does not differ significantly between different scanning resolutions, at least up to the distances of 20 meters (Medić et al., 2019b). These results indicate that it is possible to achieve great time savings by using lower scanning resolution without any loss of the measurement precision, which is important information for the efficient TLS calibration. Based on these results, the following experiments rely on the second-highest measurement resolution (1.6 mm at 10 meters) to achieve notable time savings of approximately four times.

Step 3: Problem simplification

The FOD of the calibration field is a numerically complex problem and it is not readily solvable with the existing optimization methods (Section 2.1.2). Hence, this step focuses on the problem simplification to make it resolvable. Simplifying the FOD problem of the calibration field design was achieved with the sensitivity analysis of the measurement configurations towards detecting mechanical misalignment, which was realized by investigating the signal to noise ratios (SNRs) in publication A3 (Medić et al., 2019d). An exemplary sketch of one derived sensitive measurement configuration for estimating the calibration parameter x_{5z} (Equation 3.6) is given in Figure 5.2. In this concrete case, the length between two targets needs to be observed from two scanner stations, where from the first one the parameter under investigation does not influence the length, while from the second station it maximally influences the length. All derived measurement configurations are documented in Medić et al. (2019d) and (2020d). These configurations represent the main constructive elements, i.e. the building blocks, which need to be adequately combined to allow the comprehensive and efficient TLS calibration. This approach of designing the calibration field drastically reduces the complexity of the optimization problem.

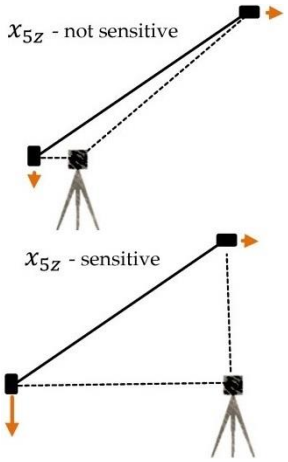

Figure 5.2: Insensitive and sensitive measurement configuration for estimating the parameter x_{5z} using the change of the distance between 2 targets measured from 2 scanner stations (orange arrow – magnitude and direction of related systematic error).

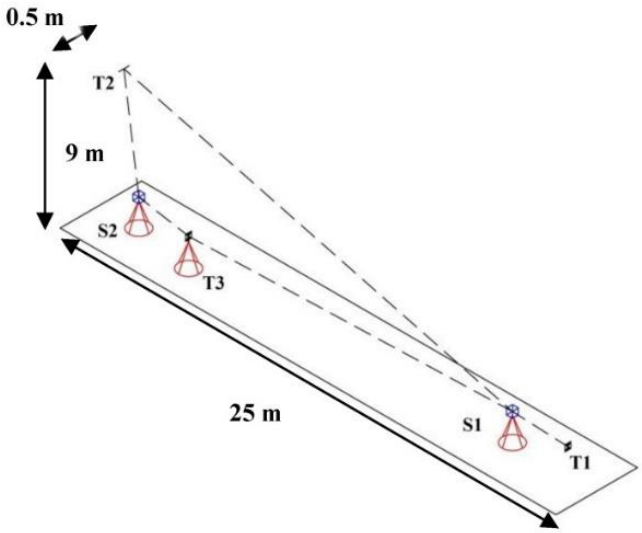

Figure 5.3: Minimal measurement configuration sensitive to all 10 relevant CPs: scanner stations (S1 and S2), targets (T1, T2, and T3).

Based on this sensitivity analysis, the minimum number of targets and scanner stations necessary for estimating all 10 relevant calibration parameters was derived in Medić et al. (2019d) by the series of simulation experiments. In short, only 3 targets measured from two scanner stations using two-face measurements are necessary to achieve the latter aim (Figure 5.3). It can be observed that the measurement configuration sensitive towards estimating the parameter x_{5z} (Figure 5.2) is also contained in the minimal measurement configuration presented in Figure 5.3. The presented measurement configuration is contained within the measurement configuration recommended for TLS quality assurance in the relevant ISO norm (International Organization for Standardization, 2018) and in the TLS test-field design proposed in Neitzel et al. (2014). Hence, these results serve as proof that the existing TLS testing procedures are sensitive to all calibration parameters relevant for the calibration of high-end TLSs. The later statement holds, if the measurements from both scanner stations are made in two-faces (Section 3.1.1). For a more detailed comparison of these results with the recommended TLS test-field designs, readers are referred to the

publication A3 (page 72 of the thesis attachment). This minimal measurement configuration served as the backbone of the calibration field designed in the following (last) step.

Step 4: Optimization

The final step is defining the well-thought optimization goals, i.e. the minimization functions that would assure the trustworthy calibration results. Generally, the quality of the geodetic network is characterized by its precision, reliability, and cost, i.e. efficiency, (Amiri-Simkooei et al., 2012). Based on the previous work on the topic of TLS calibration, an additional criterion is adopted —the correlations of the calibration parameters. In short, as the aim is the efficient target-based self-calibration, the main goal is to minimize the efforts of the calibration field assembly, maintenance, data acquisition and processing. Hence, the goal is to achieve the minimum number of targets p and scanner stations s without the requirements of the costly reference values. To assure the adequate parameter quality, the thresholds given in Table 5.1 are defined in publication A4 (Medić et al., 2020b).

Table 5.1: The optimization goals for designing the efficient TLS calibration field ($\boldsymbol{s}$ – # scanner stations, $\boldsymbol{p}$ – # targets, $\boldsymbol{\sigma_x}$ – a posteriori standard deviation of the CPs, $\boldsymbol{\nabla x}$ – related impact factors, $\boldsymbol{\rho_x}$ – max. correlations of the CPs).

efficiency	$\boldsymbol{s, p \rightarrow min.}$
precision	$\sigma_x \leq \bar{\sigma}_{r\,[mm]}, \bar{\sigma}_{\varphi\,[\,''/mm\,]}, \bar{\sigma}_{\theta\,[\,''/mm\,]}$
reliability	$\nabla x \leq \bar{\sigma}_{r[mm]}, \bar{\sigma}_{\varphi[\,''/mm\,]}, \bar{\sigma}_{\theta[\,''/mm\,]}$
correlations	$\rho_x \leq 0.8$

The adopted precision threshold is that the σ_x of each calibration, parameter needs to be equal to or smaller than the mean random measurement noise (expected target center precision within the calibration field). The threshold was proven as reasonable based on the achieved calibration results (Medić et al., 2020b), but its choice is argued within Section 6.1. The same threshold applies to the maximal impact of the undetected outliers on the calibration parameter estimates, indicated by the impact factors (∇x), which assures the reliability of the calibration results (Baarda, 1968). This measure is of high relevance when designing an efficient measurement configuration with a minimal number of observations. Namely, in typical calibration fields in the literature, the sheer number of observations assures high reliability without placing a special focus on the problem. Finally, the correlations (ρ_x) between the calibration parameters should be as low as possible (Lichti, 2010b) to avoid the eventual parameter bias. The threshold of 80% correlation is selected, as in all attempts of designing an efficient calibration field, this was the lowest value that could be achieved for so many functionally similar parameters (Medić et al., 2020b)**.**

To validate the defined optimization goals, the calibration field design was obtained by the series of simulation experiments, using the least computationally expensive heuristic method, the man-made trial and error analysis (see Chapter 4, publication A4). The number of possible solutions is reduced based on the results of the sensitivity analysis. In addition to the presented criteria, there was an additional constraint that the calibration field needs to be implemented within a given facility, which is typically the case. Hence, the number of possible measurement configurations is realistically constrained. As the optimization requires one definite stochastic model, the design of the calibration field within this works focuses on the values defined for Leica ScanStation P50, BOTA8 targets and the in-house developed target center estimation algorithm (Section 3.2). The concrete threshold values are 0.5" for the standard deviations and the impact factors of the tilt (angular) calibration parameters and 0.1 mm for the offset (metric) calibration parameters (Medić et al., 2020b).

The final simulation result for the high-end panoramic TLSs is presented in Figure 5.4. The best simulation result that fulfilled the optimization criteria from Table 5.1 was the network of 14 targets measured from two scanner stations (S1 and S2) using two-face measurements (overall four scans). The network is symmetric, and it is realized by four repetitions of the minimal measurement configuration (Figure 5.3) with four additional targets perpendicular to the line connecting scanner stations S1 and S2. The latter targets have increased elevation angles at higher distances and they had a strong positive impact on the calibration solution.

The calibration approach for the non-high-end TLSs slightly deviates from the latter description, primarily due to the missing possibility of two-face measurements. In their case, the measurement configuration is identical to the

one depicted in Figure 5.4. However, overall eight scans are necessary to reach the defined optimization goals, where the instrument needs to be coarsely manually rotated around its standing axis (Medić et al., 2020b).

It is worth noting that within the derived calibration field it is possible to identify the measurement configuration that strongly resembles the TLS test-field design recommended by the relevant ISO norm (International Organization for Standardization, 2018). Moreover, it is possible to find several independent instances of such a measurement configuration (e.g. Figure 5.4, targets 3, 5, 9 and 11 or targets 2, 6, 10 and 13). Hence, the derived calibration field design takes advantage of high-sensitivity of the latter configuration towards relevant mechanical misalignments, which was proven by the sensitivity analysis conducted in Medić et al. (2019d). Moreover, inducing the mentioned repetitiveness was necessary to additionally assures high measurement reliability and lower parameter correlations (as the same measurement configuration is observed using different instrument orientations), which are imposed as necessary criteria for the trustworthy calibration. These results imply that the usually employed TLS test-fields also carry the potential for the TLS calibration tasks. This hypothesis should be furtherly investigated in the future. Unfortunately, such an investigation was omitted within this work due to time-constraint.

Evaluation of the workflow and the implemented calibration field

The presented workflow for the design of the efficient calibration fields was tested by implementing the simulated calibration field design and calibrating multiple instruments. The simulated design was reconstructed with centimeter-level accuracy for both BOTA8 targets and scanner station locations (deemed sufficient based on the simulations). For the evaluation, six TLSs were calibrated in publication A4 (Medić et al., 2020b): Leica ScanStation P20, P50, and Z+F Imager 5016 (all three high-end), as well as the Faro Focus3D X 130, Leica BLK360, and Leica HDS6100.

The improvement in observation residuals is the most common evaluation of the calibration success in the literature (Abbas et al., 2014a; Chow et al., 2012; Garcia-San-Miguel & Lerma, 2013; Lichti, 2007) and, therefore, these values are presented herein. Garcia-San-Miguel & Lerma (2013) analyzed and summarized the success of all TLS calibration experiments, presenting significant improvements of 36%–48% for ranges, 30%–80% for horizontal angles, and 31%–74% for vertical angles. The values achieved herein (Tab. 5.2) fit well in the latter intervals. The mean values are 28%, 60%, and 50% for ranges, horizontal, and vertical angles, respectively, where only range measurements fall marginally short in comparison to the previous experiments.

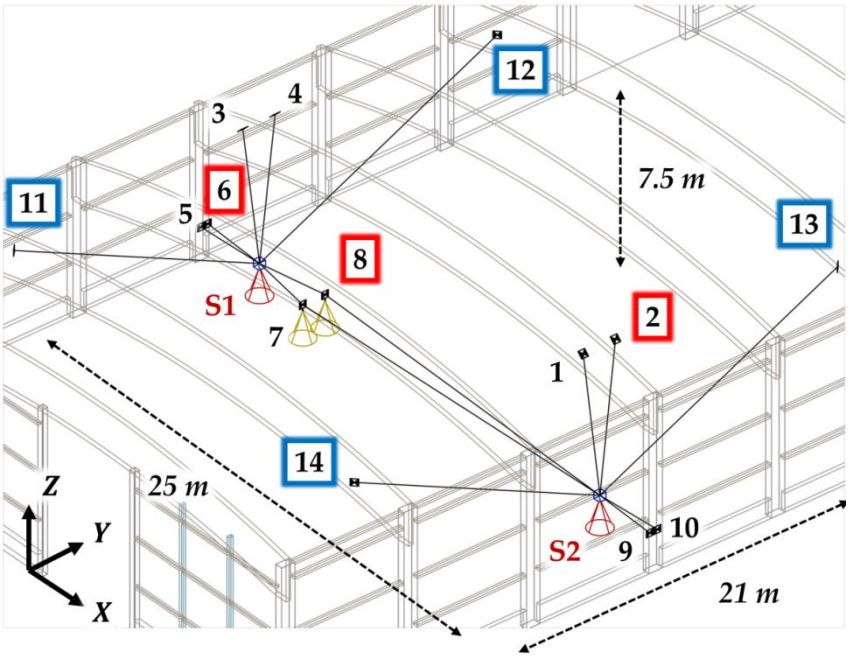

Figure 5.4: The calibration field design with a total of 14 targets (scanner stations S1 and S2; red frames—targets necessary for minimum measurement configuration corresponding to Fig. 5.3; blue frames—additional targets at higher elevation).

The biggest gain in comparison to the previous experiments is that the number of observations in the reviewed studies falls within the range of 390–4680, with a mean of 2390. Herein, the number of observations is 168 for high-end TLSs or 336 for the remaining ones. This is a significant decrease of up to an order of magnitude. Hence, the presented results demonstrate that the designed calibration field assures comparable measurement improvements with a notably reduced number of observations, and, therefore, much more efficient.

Table 5.2: Observation residuals in the calibration adjustment without applying CPs (no CPs), after applying CPs (CPs), and improvement in observation residuals (%).

	P50			**P20**			**Imager 5016**		
	σ_r **[mm]**	σ_φ **["]**	σ_θ **["]**	σ_r **[mm]**	σ_φ **["]**	σ_θ **["]**	σ_r **[mm]**	σ_φ **["]**	σ_θ **["]**
no CPs	0.15	93.73	18.36	0.28	26.14	8.79	0.12	32.07	4.82
CPs	0.06	24.72	1.86	0.25	13.39	4.47	0.06	17.73	3.40
%	56.76	73.62	89.87	10.87	48.79	49.22	48.98	44.70	29.50
	HDS6100			**FOCUS 3D**			**BLK360**		
	σ_r **[mm]**	σ_φ **["]**	σ_θ **["]**	σ_r **[mm]**	σ_φ **["]**	σ_θ **["]**	σ_r **[mm]**	σ_φ **["]**	σ_θ **["]**
no CPs	0.27	84.02	17.23	0.11	218.02	21.50	2.16	58.05	25.40
CPs	0.20	26.31	8.88	0.10	70.60	11.26	1.72	24.07	16.08
%	24.24	68.69	48.45	5.87	67.62	47.60	20.34	58.53	36.68

Additionally to the investigation of the measurement residuals, it was necessary to validate if applying the estimated calibration parameters improves the accuracy of whole point clouds, both for the in-situ case (point clouds acquired during the calibration) and in the later use (unrelated objects measured with a time offset). Herein, the point cloud accuracy is evaluated based on the differences between the 1st and 2nd scan of the two-face measurements (Section 3.1.1), which should in a perfect case have a central tendency of zero with a low dispersion – corresponding to the random measurement noise (Mikhail, 1976). This evaluation strategy relies on the presumption that all systematic influences except the ones originating from the mechanical misalignments act identically on both point clouds. Hence, they are canceled out by building the differences. To increase the sensitivity of the testing approach and reduce the point cloud noise, the M3C2 point cloud comparison algorithm is used (Lague et al., 2013). It should be noted that this evaluation strategy is not completely comprehensive. Namely, it validates 9 out of 10 calibration parameters, because the rangefinder offset cannot be controlled (Medić et al., 2020b).

Moreover, this evaluation strategy limits the analysis to the high-end TLSs allowing two-face measurements (Medić et al., 2020b). The exemplary results for the ScanStation P50 are presented in Figures 5.5 and 5.6. The notable improvements are observed both for the point clouds of the calibration field captured during the calibration, as well as for the point clouds of the unrelated object. In the in-situ case, the systematic trend in the point cloud differences is completely eliminated indicating the comprehensiveness of the calibration approach (see histograms in Figure 5.6). However, the achieved improvements for the later use of the calibration parameters were lower, indicating the problem of the calibration parameters' stability. These results were consistent for all high-end TLSs (Medić et al., 2020b).

Within the investigations, it was also confirmed that the defined optimization goals regarding the a priori defined parameter quality were mostly fulfilled. Moreover, the empirical values were mostly consistent with the simulated ones. Only notable discrepancy became apparent by the consecutive calibrations of the Leica ScanStation P50. There, nearly a linear drift over time for some calibration parameters was observed, causing an unexpectedly large deviation in values and indicating the problem of parameter stability.

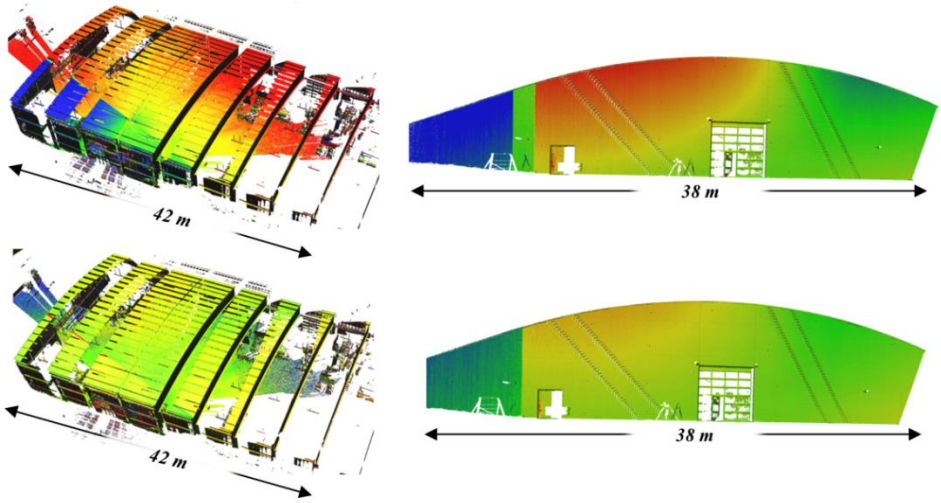

Figure 5.5: Point cloud differences (M3C2) between 1st and 2nd scans of two-face measurements, before (top) and after (bottom) the calibration for Leica ScanStation P50 (left – point cloud acquired during calibration, right – unrelated object measured two weeks from calibration). Color values are analogous to the values in Figure 5.6.

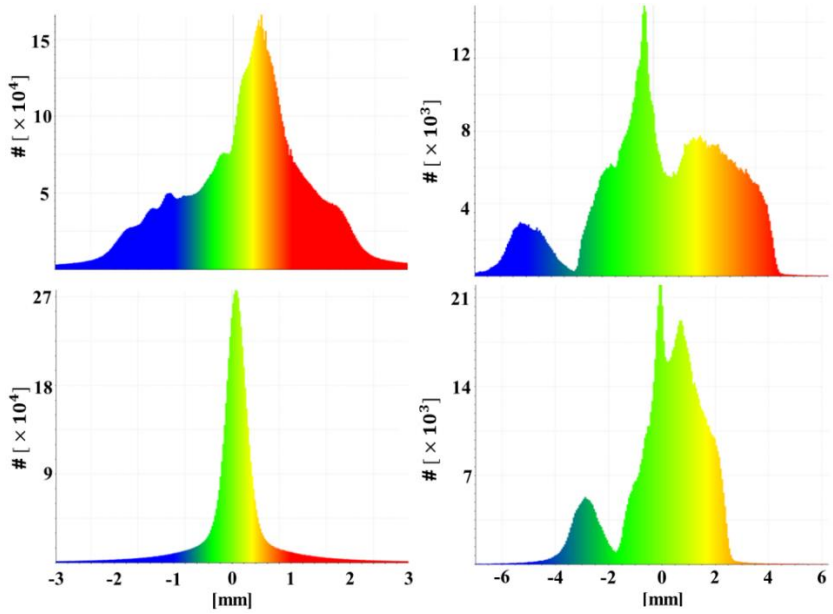

Figure 5.6: Histograms of the point cloud differences (M3C2) for Leica ScanStation P50 before (top) and after (bottom) the calibration (left – point cloud acquired during calibration, right – unrelated object measured two weeks from calibration)

Concluding remarks

To conclude, these results demonstrate that applying the presented simple stepwise workflow can be used for designing the target-based calibration fields that fulfill the criteria defined within the objectives of this thesis (Section 1.2). The calibration field allows efficient and comprehensive calibration delivering the trustworthy and informative calibration parameters with the pre-defined and complete quality criteria (precision, correlations, and reliability). The problem of parameter stability was highlighted as the major limitation of the results with the a priori target-based instrument calibration. Hence, the extent of this problem was furtherly investigated in Section 5.4 in order to gain a better understanding of the calibration parameters' stability.

The implemented calibration field is the second such facility for the TLS calibration in Europe (1st is Zöller & Fröhlich facility in Wangen, Germany) and the only non-commercial one. As it provides the attested comprehensive TLS calibration, it can be used as a benchmark for the development of further calibration approaches. However, the objective of this thesis is not the development of a single functional calibration facility. Rather, the objective is supporting the efficient TLS calibration for a large number of end-users. Namely, one of the defined goals was easy reproducibility by qualified engineers regarding their own needs and constraints. Hence, achieving this goal is demonstrated in the following simple simulation-based example.

Reproducibility

In this demonstration, the Institute of Geodesy and Geoinformation (IGG) at the University of Bonn needs to implement the calibration field in front of the institute building to allow easy frequent usage. A permanent installment of all targets is not possible in the lively street. Hence, for the sake of efficiency, it is necessary to make a different trade-off between the number and mounting of targets and the scanning time.

By analyzing the constraints of the given environment, available equipment and desired quality of the calibration parameters (equals to the ones defined in the optimization step), a single calibration field design is derived by combining the building blocks, i.e. sensitive measurement configurations for each calibration parameter (derived in the problem simplification step). The calibration field is intended for the calibration of high-end panoramic TLSs and it consists of two scanner stations (S1 & S2) and eight targets (1-8) sketched in Figure 5.7. Two two-face scans from each scanner station are expected (overall 8 scans) with a rotation of the instrument around its standing axis between the scans for 90°. That leads to the anticipated measurement time of approximately two hours. In order to evaluate the derived calibration field design, a single simulation without iterative corrections and adjustments of the measurement configuration was made (simulation equals the one in the optimization step). The results of the simulations are presented in Table 5.3.

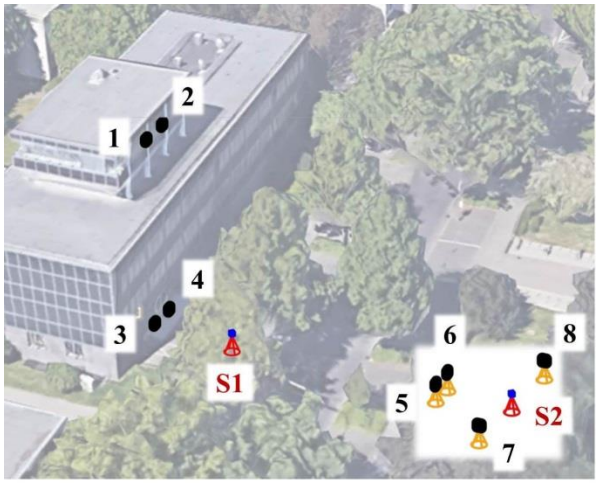

Figure 5.7: The sketch of the simulated calibration field in front of the IGG building consisting of 8 targets (black squares) and two scanner stations (blue square on a red cone)

Table 5.3: The simulation results for the outdoor calibration field design in front of the IGG building (goals: $\hat{\sigma}_x$ and $\leq$ $\mathbf{0.5"}$ **or** $\mathbf{0.1}\ mm$, $\rho_{x(max)} \leq \mathbf{0.8}$).

AP	x	$\hat{x}$	$\hat{\sigma}_x$	$\rho_{x(max)}$	∇x
x_{10} [mm]	-2.00	-2.02	0.01	0.18	0.01
x_2 [mm]	-0.20	-0.20	0.00	-0.31	0.01
x_3 [mm]	-0.20	-0.20	0.00	-0.79	0.00
x_6 ["]	-8.00	-8.02	0.04	-0.79	0.04
x_{1z} [mm]	-0.20	-0.21	0.03	0.81	0.04
x_7 ["]	8.00	8.03	0.51	0.81	0.61
x_{5z} ["]	-8.00	-7.74	0.30	0.73	0.23
x_{1n} [mm]	-0.20	-0.21	0.01	-0.61	0.01
x_{5n} ["]	-8.00	-7.79	0.15	-0.61	0.19
x_4 ["]	-8.00	-8.09	0.05	-0.42	0.04

As can be seen, all parameters are estimated unbiasedly with the desired precision and reliability of 0.5" for the tilt parameters and 0.1 mm for the offset parameters, as well as with the desired correlations (marginal deviations in a few instances). This simple simulation example demonstrates the feasibility of the presented workflow for the calibration field design in practice. Hence, the efficient calibration fields can be easily reproduced by qualified engineers by considering the adequate functional and stochastic model, known sensitive measurement configurations and well-defined optimization criteria.

5.2 “B” Assuring successful in-situ TLS calibration

For the majority of the in-situ calibration approaches, the problem can appear if the objects that are functionally modeled within the in-situ calibration adjustment (e.g. planes, cylinders or paraboloids) are at the same time the main subjects of the measurement campaign, e.g. the subjects of the deformation analysis (Section 2.2.1). Namely, if the measurement configuration is not adequate, the latter can lead to high correlations and eventually biased solutions of both the TLS calibration as well as the deformation analysis (Holst et al., 2018a).

In order to tackle the problem, it is necessary to assure the separability between the calibration parameters and the parameters defining the geometry of the measurement subject. Hence, in the publication B1 (Holst et al., 2018a), different strategies for assuring the latter goal were analyzed on a specific example of deformation monitoring of the VLBI radio telescope with the simultaneous paraboloid-based calibration (Section 3.4). These calibration strategies are directly transferable for assuring the successful in-situ TLS calibration in the general case, which is discussed in the following text.

Specific deformation monitoring example

In short, the VLBI radio telescope can change its orientation to be optimally adjusted for observing certain radiation sources. When changing the elevation angle concerning the local zenith, the telescope undergoes geometrical changes due to the influence of gravity, see e.g. Holst et al. (2012) and (2019a). For the deformation analysis, the telescope needs to be observed with a TLS at different elevation angles between 0° and 90°, it needs to be approximated with a rotational paraboloid (Section 3.4), and the changes in the focal length f_j (Eq. 5.14-5.16) needs to be assessed. When scanning, the main reflector covers different portions of the instrument’s field-of-view at different elevation angles, as the instrument's vertical axis is always in the direction of the local gravity vector (Holst et al., 2012). Hence, the resulting measurement configuration of each scan is different.

The in-situ TLS calibration is necessary to assure the unbiased calibration analysis as the instrument’s systematic errors surpass the measurement noise, which can be observed in the systematically distributed best-fit paraboloid residuals (Figure 5.8, left). Several strategies for mitigating the systematic effects, primarily based on the paraboloid-based calibration adjustment (Section 3.4), are analyzed and compared (Table 5.4). They are segregated by using or not using two-face measurements, using or not-using in-situ calibration, when calibrating then using the bundled calibration of all scans together or local calibration of each elevation angle individually.

Table 5.4: Different strategies to mitigate the instrument related systematic errors in measurements

Strategy	Description
1	In-situ paraboloid-based calibration for each elevation angle (each scan) separately using only single-face measurements
2	Bundled in-situ paraboloid-based calibration for all elevation angles (all scans) together using only single-face measurements
3	Approximation of rotational paraboloid using two-face measurements without in-situ calibration
4	In-situ paraboloid-based calibration for each elevation angle separately using two-face measurements
5	Bundled in-situ paraboloid-based calibration for all elevation angles together using two-face measurements

The results of the deformation analysis of the focal length (f_j in Equation 3.16) change for all five strategies are presented in Figure 5.9. When considering strategies without using two-face measurements, the first and the second scan of two-face measurements are analyzed separately for the comparison purpose (red lines for first scans, green lines for second scans). The a priori expectation based on the physical models is that the focal length gradually decreases with lower elevation angles. If no strategy is used to account for the TLS misalignments (▪▪▪▪▪▪ and ▪▪▪▪▪▪), the estimated focal lengths deviate notably from the assumption of a smooth elevation-dependent decrease. This also holds for Strategy 1, which is the current state-of-the-art (Holst et al., 2015), and Strategy 4. Both strategies are based on the in-situ calibration of each elevation angle independently. Hence, not bundling all scans

together in one adjustment leads to a deficient measurement configuration, which further leads to high (nearly perfect) correlations between the focal length and some calibration parameters causing the biased results.

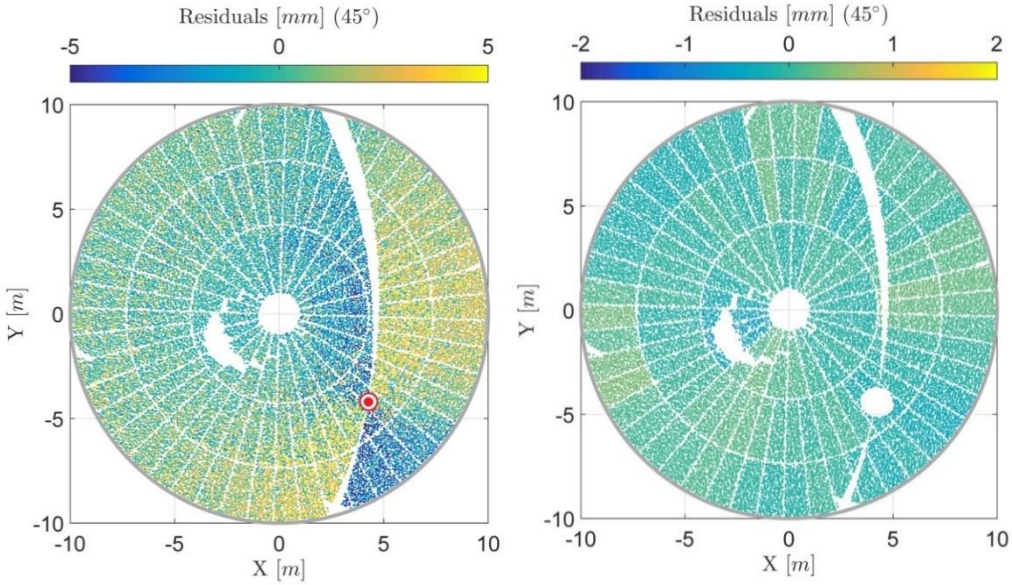

Figure 5.8: The observation residuals of the best-fit rotational paraboloid adjustment before (left) and after (right) successful in-situ calibration, at the telescope's elevation angle of 45° (red dot is the intersection of the TLS's z-axis with the main reflector).

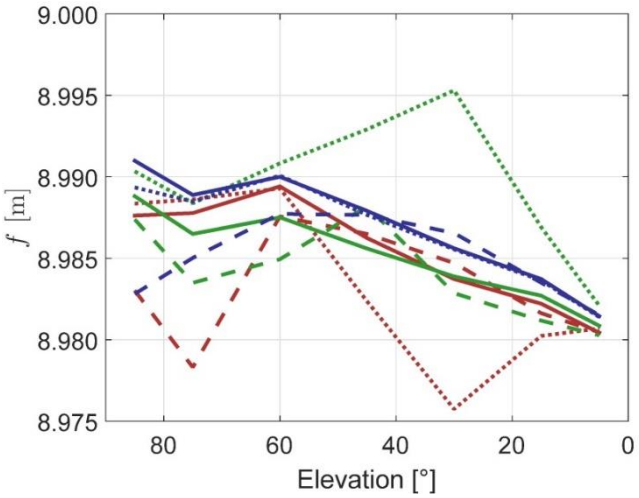

Figure 5.9: Estimated changes of the focal length with different telescope's elevation angles; no strategy with 1st (▪▪▪▪▪▪) and 2nd (▪▪▪▪▪▪) scan of two-face measurements, Strategy 1 with 1st (▬ ▬) and 2nd (▬ ▬) scan, Strategy 2 with 1st (▬▬▬) and 2nd (▬▬▬) scan, Strategy 3 (▪▪▪▪▪▪), Strategy 4 (▬ ▬) Strategy 5 (▬▬▬).

Strategy 2 and 5 come much closer to the expected smooth decrease of the focal length (deviation at 75° appeared due to instability of the TLS mounting). However, their results are noticeably different. Strategy 5 can arguably be considered as the most accurate one due to introducing the two-face measurements. Interestingly, Strategy 3 delivers nearly identical results to Strategy 5, despite using no in-situ calibration strategy. The consequent question is: Is it necessary to implement the bundled in-situ calibration at all or just scanning using two-face measurements is sufficient?

This can be answered by analyzing the post-fit residuals for the latter two strategies. The residuals of Strategy 5 (considered as the best one) are presented in Figure 5.8 (right), while the residuals of one scan of Strategy 3 are the ones already presented in Figure 5.8 (left). Hence, if the systematic errors in observations are not accounted for within the functional model of the calibration adjustment, they are fully absorbed in observation residuals. This has

two disadvantages. One is that the further deformation analysis of individual smaller elements of the main reflector is not possible, as eventual smaller deformations are over-shadowed by the instrumental errors. The second one is that the residuals are not normally distributed. Hence, the a posteriori variance analysis will be incorrect.

Transfer to the general case of the in-situ TLS calibration

Several generally applicable conclusions can be drawn from the latter investigation. Generally, using two-face measurements can completely remove the influence of all two-face sensitive instrumental systematic errors, which is the great majority. Namely, 9 out of 10 relevant calibration parameters (Equations 3.4-3.6) are at least partially two-face sensitive in the case of the high-end instruments. Therefore, just by measuring in two-faces can improve the accuracy of deformation analysis.

However, there are several limitations of the approach. First, this approach requires a doubled measurement time. Second, the calibration parameters not sensitive to two-face measurements could still bias the results. Hence, they should be additionally estimated, either in-situ or a priori. Third, the local deformations of a smaller spatial scale could remain undetected, if they are over-shadowed by the systematically biased observation residuals. Fourth, to utilize the two-face measurements in the deformation analysis, it is necessary to build some correspondences between the first and the second scan of two-face measurements. This can be achieved, as in the latter experiment, by assigning the a priori knowledge of the geometrical shape of the measured object to both point clouds. This way the systematic errors from both point clouds act with the opposite signs on the estimation of geometrical shape parameters of the measured object. Hence, they cancel each other out, and, therefore, the parameter estimation is unbiased. Finally, if the systematic errors are still present in the adjustment procedure while estimating the object's shape parameters, the a posteriori variance analysis and further statistical testing will be biased. Therefore, the in-situ calibration is a preferable solution, as it mitigates most of the aforementioned limitations.

When analyzing different in-situ calibration strategies (Table 5.4) there are two prerequisites for successful results. First, explicitly introducing the two face measurements notably helps to decouple the calibration parameters and the object geometrical parameters, which helps to assure the unbiased deformation analysis. Second, the success of the calibration strongly depends on the measurement configuration within the measurement campaign. The more versatile the measurements during the deformation analysis are, the better is the possibility of estimating TLS calibration parameters. The necessary presumption is that the calibration parameters do not change significantly during one measurement campaign (argued in Section 5.4). That allows all scans collected during one assignment to be bundled in one adjustment procedure with enhanced sensitivity concerning the TLS calibration.

There are two important prerequisites for this procedure. First, the object of interest needs to be scanned several times with altering measurement configuration between the scanner and the object. Second, some a priori knowledge about the measured object's shape is required. The first prerequisite is typically accomplished without any extra effort because most deformation monitoring tasks aim at objects that are generally too large to be scanned from a single location, e.g. dams, tunnels and bridges. The second prerequisite is also often fulfilled because objects of interest are frequently man-made buildings, which can be approximated with one or more simple primitives.

Hence, when adequate measurement configuration is achieved the bundled in-situ calibration successfully mitigates the bias in the deformation analysis due to the instrument's misalignments. Moreover, it overcomes some problems of only applying two-face measurements. Namely, in this case, the systematic errors are estimated and removed from the observations. Hence, local deformations (smaller spatial scale) of the object can be detected and the a posteriori variance analysis and statistical testing will be unbiased. However, the problem of requiring a priori geometrical knowledge of the investigated object remains. This makes the presented strategy not universally applicable and less efficient. Hence, this problem is identified as the major one and it is tackled in Section 5.3.

To conclude, the well-realized in-situ calibration strategy surpasses the positive effects of only using two-face measurements. The best strategy for assuring the successful in-situ TLS calibration during the deformation analysis, however, relies on the explicit inclusion of the two-face measurements and also the inclusion of multiple bundled scans to assure sufficiently versatile measurement configuration. This allows good separability between the calibration parameters and the parameters describing the geometrical shape of the object of measurements. Hence, it ensures unbiased results of the high accuracy demanding engineering tasks, such as deformation analysis.

5.3 “B” Developed approach for the efficient in-situ TLS calibration

The dependence on the a priori knowledge about the man-made geometrically describable objects that are well distributed in the measurement surrounding is identified as the major disadvantage of the existing in-situ calibration approaches (Section 2.2.1). The problem was also highlighted within the investigation in the last section (Section 5.2) and it makes the existing calibration approaches not universally applicable. Also, the necessity of implementing the a priori knowledge about the geometrical shape of objects in the surroundings makes the full automation of the calibration process difficult, and, consequently, the approaches are less efficient. As a result, the existing in-situ calibration approaches still have not emerged from the scientific community to the commercial sector.

Therefore, to tackle the highlighted problem, an efficient fully automatic in-situ calibration approach was developed in publication B2 (Medić et al., 2019a) and enhanced in publication C1 (Medić et al., 2020c). The idea behind the approach is to find the objects or points in the measurement surroundings that could act as natural targets instead of using dedicated laser scanning targets. These natural targets must allow precise estimation of their position, as the high measurement precision is a prerequisite of the instrument calibration. Additionally, they need to allow automatic matching of the corresponding points in multiple scans in order to be used as observations in the calibration adjustment.

The perfect tool for achieving these prerequisites was found in the photogrammetric feature detection and matching of the local 2D image keypoints, which were already used for similar tasks (Section 3.3). The only necessary adaptation is representing the TLS observations in the form of spherical images (Section 3.3). However, the limitation of this solution is that for assuring high localization precision and successful matching, the images need to be very similar. In the case of TLS calibration, that means that scans need to be made from the same or very close positions, as the larger distance between the scanner stations introduces different intensity image distortions and perspective changes (discussed in detail in Section 6.4).

The possible solution to the mentioned problem was highlighted in publication A1 (Medić et al., 2017), where nearly identical improvement in the measurement accuracy was achieved by using the two-face method (Section 3.2.2) instead of the full network method (Section 3.2.1) of the target-based self-calibration. There, two-face measurements from a single station allowed the mitigation of nearly all instrument related systematic errors relevant for high-end TLSs. Consequently, the new calibration approach was developed that relies on automatic detection of well-defined salient points, i.e. keypoints, in the environment and automatically builds correspondences of these points between the first and second scan of two-face measurements (Section 3.3). In the following text, the success of the calibration approach is presented, some special properties of the approach are identified, and some concluding remarks are given.

The success of the calibration approach

The approach was tested in the machine hall with the permanently installed calibration-field (Section 5.1) with Z+F Imager 5016. The success of the calibration is evaluated by analyzing the point cloud differences (M3C2) between the 1^{st} and 2^{nd} scan of the two-face measurements (see Section 5.1), before and after applying the calibration parameters (Figure 5.10). It is visible that the calibration notably reduced the differences and almost completely removed the systematic trends, which is especially visible in the histogram of the differences. The achieved improvement is directly comparable to the point cloud improvements of the target-based calibration presented in Section 5.1 (Figures 5.5 and 5.6).

Hence, at first glance, this fully automatic in-situ calibration approach is capable of achieving similar results to the well-thought and designed calibration field for the target-based calibration. This raises the question if the a priori calibration on a dedicated calibration field is necessary at all, and the answer to the question is given in Section 5.5 which focuses on the better understanding of advantages and disadvantages of each calibration approach.

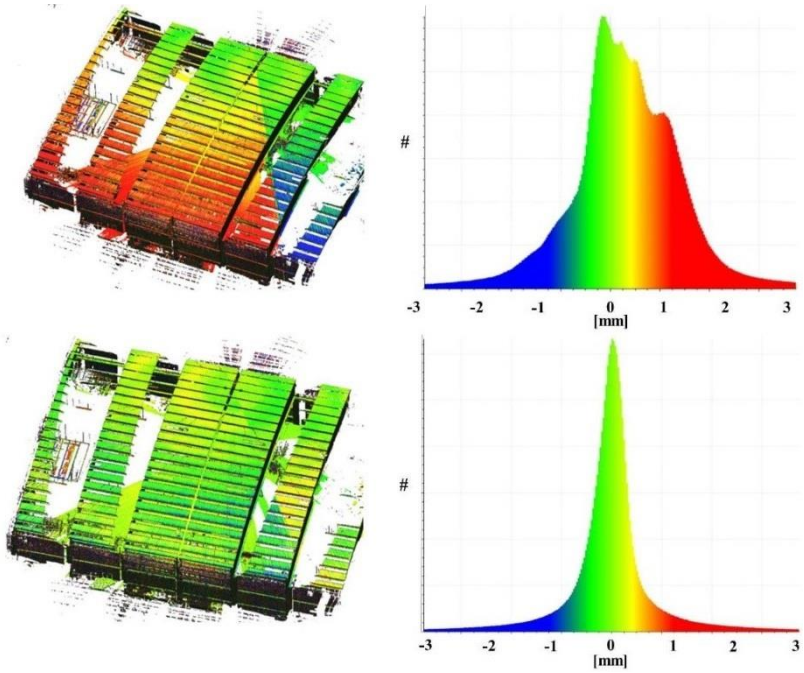

Figure 5.10: Point cloud accuracy improvement by 2D keypoint-based in-situ calibration. The point cloud (M3C2) differences before (top) and after (bottom) the calibration for Imager 5016 (left) and the corresponding histograms (right).

Special properties of the calibration approach

The keypoint-based calibration approach relies on the great number of observations in the calibration adjustment. For example, in the case of the presented calibration of Imager 5016, this number equals approximately 440 000. This high redundancy allows the detection of two-face sensitive mechanical misalignments that are eventually missing in the functional model of the calibration parameters. To investigate this possibility, the scans of Imager 5016 were de-calibrated by the manufacturer in publication C1 (Medić et al., 2020c). To do so, they extracted the raw TLS measurements without applying the mathematical corrections for the systematic errors estimated during the factory calibration (Section 1.1). The keypoint based calibration was repeated and, again, the set of 8 calibration parameters relevant for high-end panoramic TLSs was estimated (see Section 3.2.2). The residuals of the horizontal angles from the calibration adjustment are plotted regarding the instrument's field-of-view and colored according to their magnitude and sign (Figure 5.11, top).

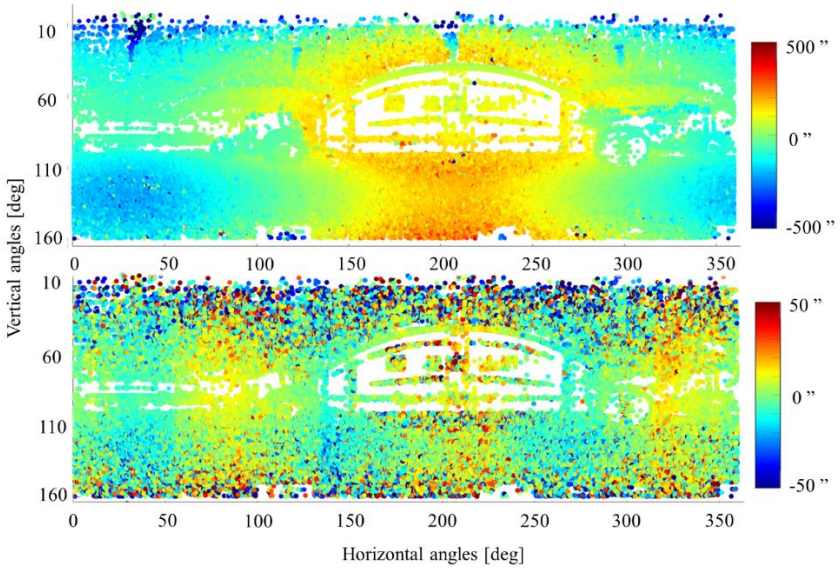

Figure 5.11: Horizontal angle residuals of keypoint-based calibration in the scanner's field-of-view for 8 calibration parameters in Equations 3.11-3.13 (top) and when also accounting for encoder eccentricity (bottom); mind colorbar scales.

As can be seen, positive and negative residuals are clustered together, changing with the sine of the horizontal angles. This indicates the presence of a large systematic error in horizontal angle measurements due to the encoder eccentricity (Muralikrishnan et al., 2015a). To prove this, the calibration parameters for the encoder eccentricity were introduced and the calibration was repeated. Newly estimated residuals for the horizontal angles are presented in Figure 5.11, bottom. Now, the magnitude of the residuals is notably lower and the previously visible trend is removed. However, by removing the latter large trend, a previously undetectable trend appeared, which corresponds again to the sine of the horizontal angle, but with an increased frequency (repeating the patter every 120°). This indicates another encoder related error that can be described with the 3rd order harmonics as a part of the Fourier series (2nd order does not appear as even orders are not sensitive to two-face measurements; furtherly discussed in Section 6.2). When all measurement residuals are analyzed, overall, 14 new significant calibration parameters can be detected. Out of these 14, only 4, had large values and a strong impact on the point cloud accuracy. When these parameters are considered, all visible systematic trends in the observations are removed. Hence, disregarding some mechanical misalignments can be justified for many applications.

Concluding remarks

These results demonstrate the success of the developed 2D keypoint-based calibration approach and highlight some of the useful properties. The approach does not require any a priori knowledge about the observed scene and also it does not require that the objects in the scene are man-made and describable by geometric primitives. This makes it an interesting alternative for the usually employed in-situ approaches, such as the plane- and the cylinder-based approach, especially in an environment where such geometrical shapes cannot be found in abundance. For example, it is an interesting solution for the measurement tasks outside the urban areas, such as deformation monitoring of landslides and slopes.

The calibration approach requires only two scans from a single scanner station, which requires approximately 30 minutes for high-end TLSs without any preparatory works to successfully mitigate the majority of the relevant mechanical misalignments. With the fact that no a priori knowledge about the environment is necessary, this approach can be fully automatic and fast, making it extremely efficient. Also, the high abundance of the observations makes it a useful tool for the calibration of the panoramic TLSs, even when the functional model of the calibration parameters is not a priori well defined.

However, the approach has some shortcomings which will be discussed in detail in Section 5.5. One of the more obvious ones is that, at least with the current implementation, it is limited to estimating only the two-face sensitive calibration parameters (Table 3.1). Hence, further developments should tackle this problem to make the approach comprehensive. Nevertheless, the approach showed great potential. Hence, it can be build-upon to develop the efficient in-situ and full-blown calibration solution, which is searched for in the community. The detailed discussion of the necessary steps for achieving this goal is given in Section 6.4.

5.4 “C” Better understanding of the calibration parameters’ stability

The presumption that the calibration parameters are stable over time is important for the assurance of the point cloud quality regardless of the calibration approach. For the a priori calibration, either user-based or manufacturer’s factory calibration, which happens for example on the calibration field days or months before the measurements, it is presumed that the parameters are stable in a long term. Moreover, the stability of the calibration parameters is also important for the in-situ calibration approaches that bundle more scans captured within a measurement campaign, as pointed out in Section 5.2. However, in this case, the short-term stability, within one measurement campaign (one day) is of relevance.

Therefore, in publication C2 (Medić et al., 2020a) and in Holst et al. (2019b), both the short-term (within one day) and the long-term (within several months) parameter stability for two high-end TLSs, Leica ScanStation P50 and Z+F Imager 5016 were investigated. The key findings of the investigation are presented in the following text, and the conclusions that are drawn can be applied for the TLSs in general.

Investigation and results

The mentioned instruments were repeatedly calibrated on the permanent calibration field presented in Section 5.1 over a period of several months (multiple times within a day). The monitored values during the experiments were the: instrument’s working time (IWT), ambient temperature and the internal instrument’s temperature in the case of

Imager 5016 (for ScanStation P50 not possible). The special focus is naturally placed on the temperature, as it is known that it can influence the instrument's internal geometry (see Section 1.1). As an initial demonstration, only the stability of the mirror tilt x_6, (Eq. 3.5) of ScanStation P50 is presented in Figure 5.12. In Figure 5.12 (left) the parameter values are related to the instrument's working time (IWT) within each day (one colored line per day). The repeatable negative drift of the x_6 with time is apparent. The probable cause is the internal instrument's temperature change, which causes small displacements of the mechanical components due to thermal expansion of different materials.

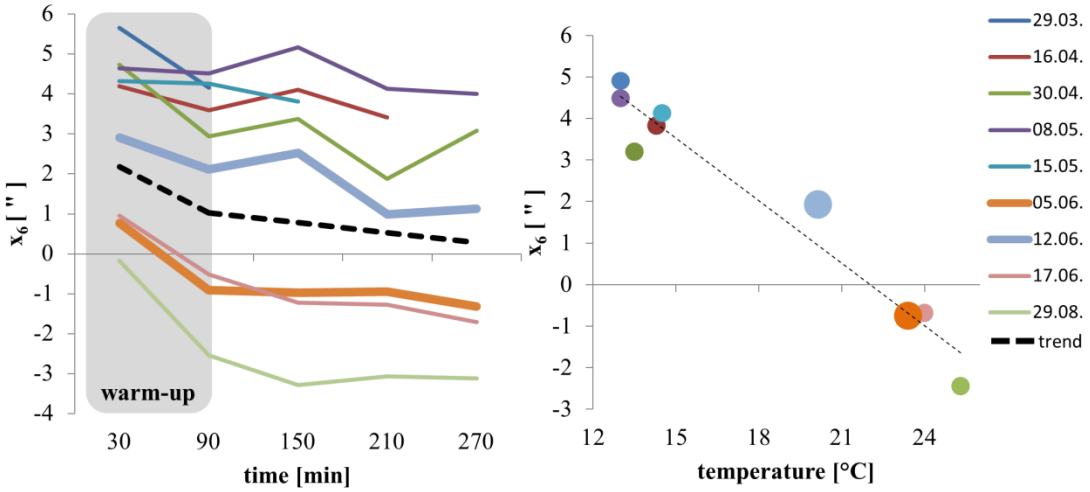

Figure 5.12: Stability of the mirror tilt (x_6) in Leica ScanStation P50 with the instrument's working time (left) and ambient temperature (right), 9 days of repeated calibrations (2-6 consecutive calibrations per day, each lasting approximately 1 hour).

As the user monitoring of the internal temperature is not possible for the majority of the instruments, herein, this short-term drift is modeled considering the IWT time, which is easily measured by the users. From (Janßen et al., 2020), it is known that the instrument's temperature change can be divided into two separate stages. The first stage is the initial warming-up, with a sharp temperature increase that lasts approximately one hour. The second stage is recognizable by a gradual temperature change. Hence, herein, these two stages are modeled as two separate linear trends (simplified due to a few data points per day). The black dashed lines (Figure 5.12, left) present the average trends from all days. The slopes of both trendlines significantly differ from zero, indicating that x_6 drifts over time continuously during measurements. Also, both trendlines are significantly different from each other, confirming that the warm-up period should be considered separately.

Moreover, a clear offset of the x_6 values between different days (colored lines) is visible. This indicates the long-term parameter instability. Figure 5.12 (right) presents the x_6 values against the ambient temperature (averages within a day). Fitting a linear trend (black dashed line) makes the strong correlation between these values apparent. Hence, the x_6 is influenced by the ambient temperature, again, probably due to the thermal expansion of the mechanical components. As the measurement of the ambient temperature is easily achievable for the end-users, the long-term stability focuses on this variable.

Based on the correlation analysis, the calibration parameters that change significantly in the short-term or the long-term are detected for both instruments (50% of the parameters). These parameter changes are linearly modeled as demonstrated above regarding the instrument's working time for the short-term changes (IWT due to no universal availability of the internal temperature measurements) and regarding the ambient temperature for the long-term changes. The values of the modeled changes are summarized in Table 5.5.

Table 5.5: The short-term parameter change with the instrument's working time per 1 hour (Δx/ 1h) during and after warm-up (w.-u.), and the long-term parameter change with the ambient temperature per 1°C (Δx / T [1°C])

	P50				**Imager 5016**			
	$\mathbf{x_7}$ ["]	$\mathbf{x_6}$ ["]	$\mathbf{x_{5n}}$ ["]	$\mathbf{x_{5z}}$ ["]	$\mathbf{x_{10}}$ [mm]	$\mathbf{x_3}$ [mm]	$\mathbf{x_4}$ ["]	$\mathbf{x_{5z}}$ ["]
Δx/ 1h *warm-up*	-5.73	-1.15	0.63	-1.57	-0.04	0.03	-1.51	3.24
Δx / 1h *after w.-u.*	-1.20	-0.25	0.19	-0.12	-0.02	0.01	-0.94	0.71
	$\mathbf{x_7}$ ["]	$\mathbf{x_6}$ ["]	$\mathbf{x_4}$ ["]	$\mathbf{x_{5z}}$ ["]	$\mathbf{x_{10}}$ [mm]	$\mathbf{x_{1z}}$ [mm]	$\mathbf{x_4}$ ["]	$\mathbf{x_{5z}}$ ["]
Δx / T [1°C]	-1.79	-0.54	-0.31	-0.76	-0.03	-0.03	-0.45	-0.84

When considering the short-term stability, the changes during the warming-up are few arcseconds and few tenths of a millimeter per hour, while after the warm-up they are several times smaller. During the warm-up, these values are notably higher than target center precision presented in Section 5.1 (0.5" and 0.1 mm). Hence, this drift cannot be neglected. As the drift after the warm-up is notably smaller, it can become relevant only in the case of extremely long measurement campaigns. Additionally, the results of the investigation indicated that these short-term parameter drifts related to the IWT account for 9-61% of the overall parameter instability. Hence, there is a repeatable drift in the parameter values that can be modeled. Modeling this drift can improve the short-term parameter stability and it can reduce the systematic errors in TLS measurements.

When considering the long-term stability, the magnitudes of the parameter changes per 1°C are up to two arcseconds for tilt parameters and a few hundreds of millimeters for offset parameters. As the temperature differences can easily achieve 15-20°C over the year, this effect can become prominent. The observed magnitudes (per 1°C degree) are in the same order of magnitude as the precision of the target centers making this effect significant. Again, the results indicated that modeling the temperature-related parameter changes can account for up to 73% of the overall long-term instability. Hence, this effect cannot be neglected. When the ambient temperature readings are substituted with the internal instrument temperature in the case of Imager 5016, the results are nearly identical. Namely, after the initial warming-up, the difference between internal and ambient temperature has a constant offset.

Additionally, within these experiments, the stability of the dynamic dual-axis compensator measurements was investigated (Section 3.1.2), as these measurements can significantly bias both TLS measurements and the estimates of the calibration parameters (Section 3.1.3). Thus, it is important to assure that the compensator measurements are unbiased as well. Both TLSs were equipped with the compensator and they allowed in-situ calibration of the compensator index errors in the longitudinal (C_L) and transversal (C_T) direction (Section 3.1.3). When the repeatedly estimated values of the index errors were analyzed, both C_L and C_T were found to be significantly correlated with the ambient temperature for both instruments. The linear change per 1°C was found to be in the same order of magnitude as the change of the calibration parameters, so it cannot be neglected. The temperature changes were responsible for 24-69% of the overall C_L and C_T instability. Thus, functional modeling of this effect can notably improve their stability.

Concluding remarks for parameter stability in general

The presented results indicate that the TLS calibration parameters are generally unstable to a large amount. A large portion of this instability can be traced back to the changes in the instrument's internal temperature, which is mainly influenced by the internal heating up during the measurements and the ambient temperature. General consideration for demanding engineering tasks is that the instrument should be properly warmed-up (at least 60 minutes) before the data acquisition. Additionally, it is important to timely calibrate the dynamic compensator by the in-situ calibration approaches provided by the manufacturers, because the compensator bias changes with the temperature, which can cause systematic errors in measurements. This in-situ calibration should be done after the instrument's warming up period. For the long measurement campaigns, the everlasting parameter drift after the warm-up should not be neglected. Hence, it is advisable to repeat the in-situ calibration procedure (compensator included) based on the accuracy demands or even develop a dynamic temperature-dependent functional model of calibration parameters. In the latter case, it would be interesting to investigate the possibility of using the instrument's own warming-up for estimating a temperature-dependent functional model within a single calibration. However, this is out of the scope of this work due to the time constraint.

In order to better highlight the parameter changes and their uncertainty in the long-term, Figure 5.13 presents the empirical standard deviations of some calibration parameters over time. The first entry is calculated as the standard deviation of the parameter within one calibration experiment (1 day), while the remaining standard deviations are considering more consecutive calibration experiments (parameter values of 2, 3, …, 9 calibration days together). The 11 days time offset is the median time passed between the consecutive calibration experiments (more in Medić et al. 2020a).

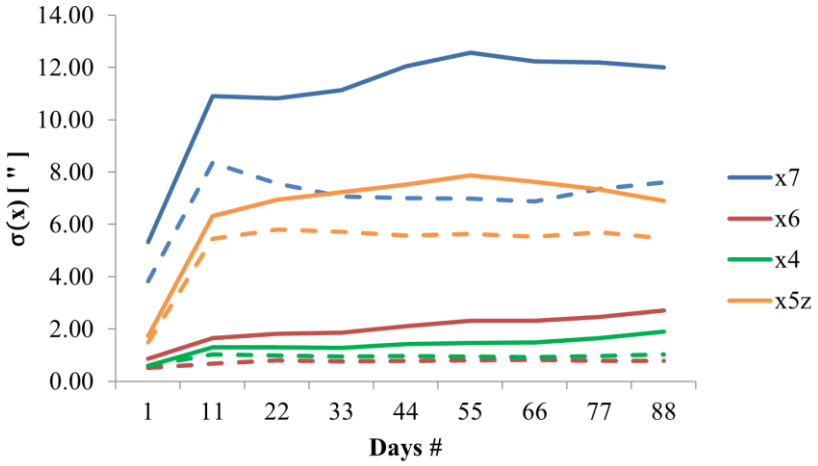

Figure 5.13: Empirical standard deviations of the ScanStation P50 tilt calibration parameters regarding time, before (solid lines) and after (dashed lines) applying the temperature correction; e.g. the values for the mirror tilt x_6 are calculated based on the values presented in Figure 5.12 before and after removing the modeled trends.

A strong sudden increase in the standard deviation is observable if standard deviations within 1 day are compared with the standard deviations of more days grouped together. Additionally, there is a little difference if the standard deviations are calculated by grouping only two consecutive calibrations (approximately 11 days apart) or all days together (spawning through 3 months). This especially holds if the temperature correction is applied (dashed lines), where the line is almost completely flat after the initial jump. Consequently, a sudden increase in the uncertainty (instability) of the calibration parameters can be expected if they are used one or several days after the calibration. However, this increase in the uncertainty stops here and the uncertainty of the parameters (not the value) is stable over a longer period of time if the temperature-related parameter correction is applied.

Therefore, an in-situ calibration is highly recommended for all calibration parameters that can be estimated based on the given measurement geometry. The remaining parameters should be a priori estimated on the dedicated calibration field and corrected for the temperature influence if the correction is applicable. Based on the data availability, this can be realized either by monitoring the instrument's internal temperature or by measuring the instrument's working time and the ambient temperature. If the in-situ calibration is not possible, relying on the a priori calibration is the best alternative. For realizing the instrument's maximal accuracy potential, the a priori calibration should be performed directly before the measurement campaign (within the same day). Such an approach could be well suited for industrial applications, where a dedicated calibration hall could be situated in the proximity of the measurement subject. Unfortunately, such an approach is hardly feasible for geodetic deformation monitoring tasks.

The presented results also indicate that in the long-term, the parameter instability is primarily related to the atmospheric conditions, and not particularly related to the time passed since the last calibration. Therefore, the measurement at the extreme environmental conditions should be avoided, as the extrapolation of the temperature influence on the calibration parameters is expected to be inaccurate. If inevitable, it is recommended to calibrate the instrument at similar conditions, rather than in a controlled laboratory environment.

5.5 "C" Better understanding of the advantages and disadvantages of the calibration approaches

As stated within the introduction of this work in Section 1.1, the knowledge of TLS calibration is primarily limited to manufacturers and the small circle of scientists. Hence, one of the main aims of the thesis is to support the acceptance of the user-oriented TLS calibration approaches from the broader community in the commercial sector (Section 1.2). Therefore, in publication C1 (Medić et al., 2020c), different options for the TLS calibration are analyzed and compared to assure a better understanding of their advantages and disadvantages. This information is expected to help the end-users in the decision-making process when answering the questions: "*Do I need to calibrate my instrument again*?" and "*Which approach is the most suitable for my cause*?".

To that aim, two user-oriented self-calibration approaches, the target-based and the keypoint-based approach are analyzed and compared with the manufacturer's factory calibration. The manufacturer's factory calibration and the target-based calibration present two options the TLS users have for the a priori calibration, while the keypoint-based calibration is one example of the existing in-situ calibration approaches. The analysis is based on scans of two common measurement objects acquired with the Z+F Imager 5016: a large hall as an example of indoor measurements (the implemented calibration field), and a building façade as an example of outdoor measurements.

Again, for the analysis of the point cloud accuracy, the point cloud differences (M3C2) between the 1st and 2nd scan of two-face measurements are analyzed. The first dataset, the point clouds of the calibration field, is depleted from the manufacturer's calibration to analyze how the user-oriented calibration approaches measure up to the manufacturer's calibration. The second dataset, the point clouds of a building façade, is used to analyze to what extent can different calibration strategies, including their combination, influence the point cloud accuracy. In this case, the manufacturer's calibration remained. In the following text, the results of these two specific examples are discussed and the conclusions that can be transferred to TLS calibration, in general, are drawn.

Specific examples

Dataset 1 (a large hall with the calibration field)

The de-calibrated point clouds of the calibration field are analyzed in four cases: without the manufacturer's calibration, with the manufacturer's calibration, with target-based calibration, and with keypoint-based calibration (Figure 5.14). As can be seen, all calibration approaches notably improved the point cloud accuracy. Namely, before any calibration, the differences were in the level of centimeters (up to 5 cm). When the point clouds were calibrated, with any of the three methods, all differences dropped below the values given in the manufacturer's specifications (+/- 3 mm). The point cloud accuracy after both user-oriented calibrations now even surpasses the manufacturer's calibration (visible in histograms). This is not surprising, as the factory calibration was a few months before the measurements, while the target- and keypoint-based calibrations were both, in this case, realized in-situ. Hence, these results reflect again on the important issue of the parameter instability over time discussed in Section 5.4.

In the case of the target-based and the keypoint-based calibration, the originally used functional models of the calibration parameters (10 CPs from Equations 3.4-3.6 or 8 CPs from Equations 3.11-3.13) are extended with four additional highly-influential calibration parameters which were empirically observed using the keypoint-based calibration (Section 5.3, Figure 5.11). This was necessary, as the angular encoders related errors became prominent after the manufacturer's factory calibration was removed. Namely, the presumption for the functional model of 10 most relevant calibration parameters for high-end TLSs is that the encoder related errors are either methodologically removed by using the encoders with multiple reading heads or they are a priori calibrated, e.g. on a rotary table (Section 3.1.3). If these additional parameters are not introduced, the point cloud differences in the case of both user-oriented calibration approaches exceed the values given in the manufacturer's specifications (up to 15 mm).

Hence, the user-oriented calibration can be improved by introducing further calibration parameters, which points out the first big advantage of the keypoint-based calibration. Namely, the target-based calibration field is specifically designed to estimate the a priori defined set of the calibration parameters with pre-defined quality criteria, where the number of observations is strictly limited to a necessary minimum for the sake of efficiency. On the contrary, the keypoint based calibration delivers a huge number of well-distributed observations (Section 5.3), which allows the detection of missing calibration parameters. Additionally, these results demonstrate that adding only four additional calibration parameters removes most of the systematic errors in the case of the not-factory-calibrated instrument.

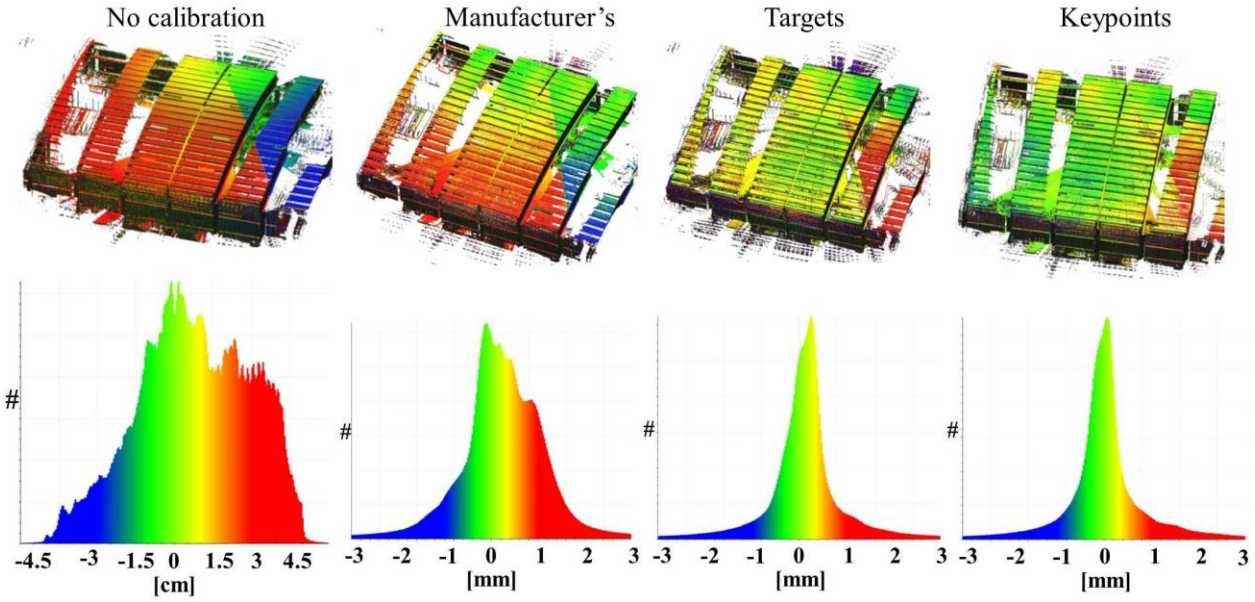

Figure 5.14: Point cloud differences (M3C2) between 1st and 2nd scan of two-face measurements of a machine hall: (1) with and (2) without manufacturer's factory calibration, (3) target- and (4) keypoint-based calibration and the corresponding histograms (mind the different scale of M3C2 differences for the case (1) without any calibration)**.**

The user-based calibration is typically used to re-calibrate the already factory calibrated instrument to account for changes in the calibration parameters. When the target-based or keypoint-based calibration is applied on top of the manufacturer's calibration the point cloud differences are even lower. In this case, disregarding four empirically observed additional calibration parameters had no noticeable influence on the point cloud accuracy. Hence, the following conclusions can be made.

First, using the user-based calibration approaches to re-calibrate the instrument (for in-situ cases) further improves the point cloud accuracy beyond the manufacturer's calibration. Second, the improvement achieved by both calibration approaches is similar. Hence, involving tens of thousands of observations does not bring noticeable benefits. This means that in-situ keypoint-based calibration could be realized by only processing a portion of the whole instrument's field-of-view. This could lead to smaller computational requirements, speed the calibration process substantially and allow nearly real-time and on-board estimation of the calibration parameters using the instrument's processing unit. Third, the functional model of the calibration parameters can be safely truncated for the factory-calibrated instruments.

Dataset 2 (building façade)

A building façade was measured from approximately 25 meters, there is no calibration field for the target-based calibration in the surroundings and the measurement configuration found on site is not ideal for the keypoint-based calibration. The analysis focuses on the comparison of the manufacture's factory calibration, the a priori calibration (target-based), the in-situ calibration (keypoint-based), as well as their eventual combination. In this case, both user-oriented calibration approaches are applied to the previously factory-calibrated instrument, as expected in practice. The point cloud differences and corresponding histograms are presented in Figure 5.15 and 5.16.

There are visible systematic errors in the point clouds when only the manufacturer's calibration is used (values within the manufacturer's specifications). If the calibration parameters estimated a priori on the calibration field are additionally applied, the point cloud differences are smaller and more normally distributed. Hence, applying the parameters estimated roughly two months in advance improves the point cloud quality beyond the manufacturer's calibration.

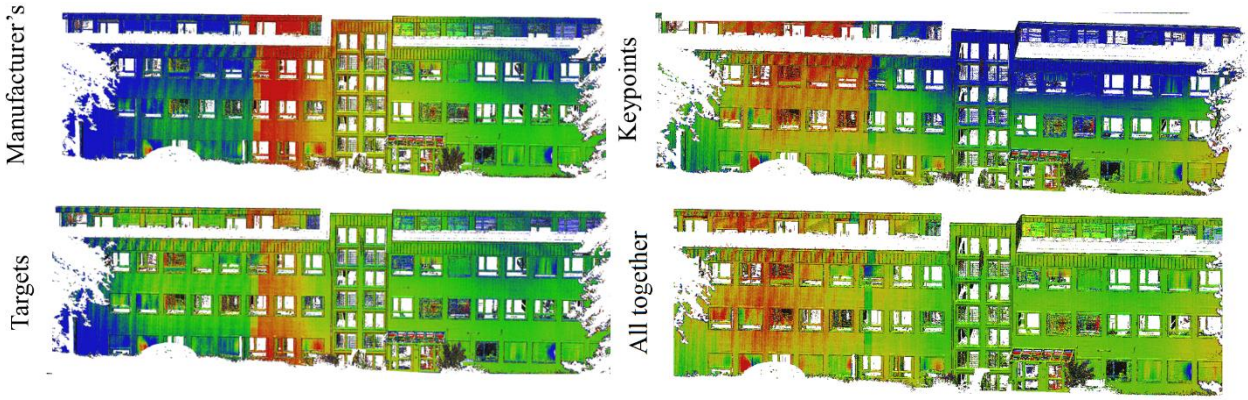

Figure 5.15: Point cloud differences (M3C2) of a façade: for: factory calibration only, additionally enhanced with target-based, keypoint-based or both calibration approaches combined (solid blue/red: +/- 1.5mm).

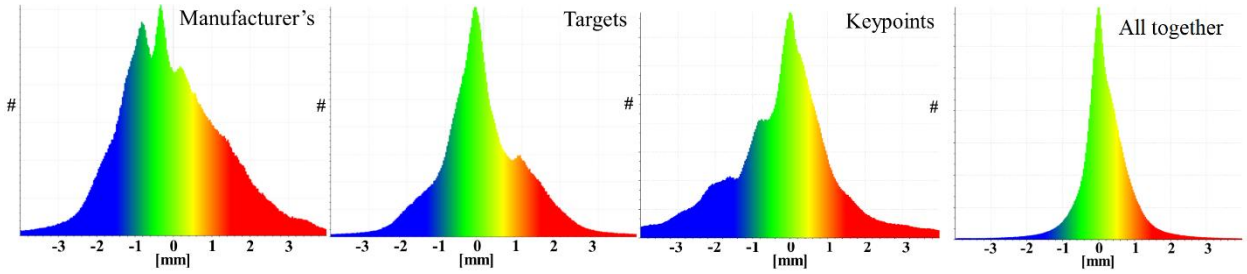

Figure 5.16: Histograms of the point cloud differences presented in Figure 5.29.

Furthermore, eight parameters (Eq. 3.11-3.13) were estimated in-situ using the keypoint-based approach. The histograms show that the results achieved are comparable to the a priori target-based calibration, indicating no further benefit of the in-situ calibration with the up-to-date parameters. Moreover, the point cloud in Figure 5.15 (top right) shows the remaining systematic trend in the case of the keypoint-based calibration, which increases with the vertical angle. This arguably indicates that the in-situ calibration as a stand-alone solution was not particularly successful in this case. A deeper look into the results revealed that some calibration parameters were almost perfectly correlated (6 out of 8 shared 98% correlations). Additionally, some offset parameters had unrealistically high values of several millimeters, which is an order of magnitude higher than expected for the factory-calibrated instrument. Hence, the keypoint-based calibration results were probably suboptimal due to the insufficient measurement configuration. This insufficient configuration led to the extreme parameter correlations and caused biased parameter estimates, highlighting the problem of the fortuitous character of the in-situ calibration.

The tilt and offset parameters (Section 3.1.3) with similar functional relationships with the TLS observations (Eq. 3.4-3.6) are hardly separable if the sufficient variation in the distances for similar elevation angles cannot be achieved (Medić et al., 2019d). To account for that, the offset parameters estimated a priori on the calibration field are used as given values, as it is difficult to accurately estimate them in the given working environment. Afterward, the keypoint-based calibration is used to estimate the remaining tilt parameters. The results for this combined approach (Figure 5.15 bottom right) demonstrate a much smaller point cloud differences with a notably narrower distribution (Figure 5.16, far right). Hence, this indicates that the adequate combination of the a priori and in-situ calibration strategies on top of the factory-calibrated instrument can deliver the highest measurement accuracy.

Concluding remarks and the relevance for the end-users

The presented results for point cloud differences in sections 5.1, 5.3 and 5.5 all demonstrate that the measurement accuracy of high-end TLSs is at a level of few millimeters and generally following the values given in the manufacturer's specifications (approximately 3 mm for Leica ScanStation P-series and Z+F Imager series). Therefore, for the majority of applications, the manufacturer's factory calibration upon the instrument assembly is sufficient to assure adequate measurement quality and the possibilities for the users' instrument calibration are of no concern.

However, some remaining systematic trends of smaller magnitudes can still be observed and furtherly reduced by user-oriented calibration approaches. This points out that the further calibration of the instrument is primarily relevant for the tasks demanding extraordinary measurement accuracy on the limit of the instrument's possibilities, such as geodetic deformation monitoring and the quality assurance in the large-scale metrology. Consequently, the following discussion is relevant only for the high accuracy demanding measurement tasks.

Directly comparing the in-situ success of user-oriented calibration against the manufacturer's showed that they can achieve comparable results. Hence, if necessary, the user-oriented calibration could substitute the costly manufacturer's calibration to some extent. However, each of the calibration approaches has certain advantages. The ultimate advantage of the manufacturer's calibration is that they have an in-depth knowledge of the instrument assembly that surpasses one of the end-users. Hence, the manufacturer's functional model of the calibration parameters is more comprehensive, and the calibration procedure is optimized for the estimation of all mechanical misalignments.

However, this approach is made a priori in the manufacturer's facilities, upon the instrument's assembly. Hence, the parameters are likely to partially change over time. Therefore, the main advantage of user-oriented calibration is that it is more up to date, so it can account for small geometrical changes that occurred in the instrument. Thus, for achieving the highest accuracy, the manufacturer's factory calibration is necessary to account for all mechanical misalignments, while the user-based calibration should be used to account for changes of the most relevant misalignments that can notably influence the point cloud accuracy.

When comparing the a priori target-based and the in-situ keypoint-based user-oriented calibration approaches, some important advantages and disadvantages should be considered. The target-based approach is more comprehensive and trustworthy as the calibration field can be specifically designed to accurately estimate all relevant calibration parameters with pre-defined quality criteria. The main disadvantage of the approach is that it is intended for the a priori instrument calibration, similarly to the manufacturer's calibration. Hence, it also suffers from the instability of the calibration parameters. The second disadvantage concerns the herein implemented calibration field that aims at a cost-efficient solution with minimal time and effort necessary for the calibration. Namely, if the functional model of the calibration parameters for the specific instrument is not a priori well defined, this approach can hardly be used to detect and model missing calibration parameters.

The keypoint-based calibration can be considered as a complementary for the target-based calibration. Namely, the main advantages of this approach are the possibility of the in-situ use, delivering up-to-date calibration parameters on-the-spot and that it has highly redundant observations, allowing the detection and estimation of eventually missing calibration parameters. On the contrary, it cannot be used to estimate all relevant calibration parameters for high-end instruments and it strongly depends on the geometry of the environment found during the measurement campaign. Hence, it cannot guarantee comprehensive calibration with pre-defined quality criteria due to its fortuitous character.

To summarize, the generally optimal workflow comprises the manufacturer's exhaustive calibration upon the instrument's assembly, a priori target-based calibration in regular time intervals as a cost-efficient alternative for the costly factory re-calibration. Finally, the in-situ calibration should account for the remaining small changes for all calibration parameters that can be estimated regarding the limitations of the given measurement geometry.

6 Further Considerations

The presented investigations aimed at the enhancement and development of methods for the efficient calibration of high-end panoramic terrestrial laser scanners. Within these investigations, further questions arose due to the achieved results or due to the restrictions and adopted simplifications, which have not been considered in detail so far. This chapter is intended to address some of these questions and outline, based on the contributions made in this thesis, possible further advancements in the respective field. The first four sections discuss more general problems related to the TLS calibration, while the remaining sections discuss very specific possibilities for the enhancement of the solutions derived within this work.

Section 6.1 identifies the necessity of further investigations to answer the question: *How accurate should TLS measurements really be*? Section 6.2 deals with the necessary extensions of the self-calibration approaches to achieve a generally applicable efficient solution for all TLSs. Section 6.3 identifies the deficiencies of the uncertainty model of TLS measurements that could potentially negatively impact the calibration results. Section 6.4 identifies the necessary steps towards the development of the full-blown calibration solution, which would be of great benefit to the community. Then, concerning the more specific problems, Section 6.5 describes several possibilities for the automation of the well-established target-based self-calibration approach. Section 6.6 discusses the possibilities to challenge and eventually improve the optimization and design of the calibration field derived within this study. Finally, Section 6.7 discusses the potential benefit of the multifunctional character of the implemented calibration field.

6.1 The sensitivity of deformation monitoring towards misalignments

The implemented calibration field is designed to assure calibration parameters with certain accuracy (Section 5.1). This accuracy is directly related to the measurement precision, more specifically, to the achievable precision of the target center estimation. The following investigations suggested that the achieved parameter accuracy was sufficient to almost completely remove the detectable systematic influences in the point clouds, in the case of the in-situ applications, see Section 5.1 and 5.5, as well as Heinz et al. (2018). In the case of the a posteriori use, the accuracy of the parameters was found to be overshadowed by their instability due to different influences (Section 5.4). Hence, there is no reason to presume that the calibration field should assure more accurate calibration parameters. However, the adopted accuracy threshold is rather based on intuition rather than objective optimization.

Defining the non-subjective accuracy threshold for the calibration parameters is a non-trivial task without a universal solution. The general goal is that the influence of the remaining systematic errors after the calibration should be sufficiently small to be insignificant, so it can be considered as a part of the random noise. Achieving this goal depends on two aspects. First, the magnitude of the random noise depends on multiple factors, such as measurement geometry and surface properties of the measurement subject (Soudarissanane, 2016), scanner and scanning settings, as well as denoising and preprocessing strategies which are commonly applied for the tasks such as deformation monitoring (e.g. M3C2 algorithm used through Chapter 5). Hence, the resulting random noise is not homogenous and describable by a single scalar value.

Second, the calibration requirements depend on the specific engineering task. Namely, different tasks demand different measurement accuracy which directly influences how accurate the calibration parameters should be. Additionally, the accumulated impact of all mechanical misalignments depends on the size, shape, and position of the object of interest in the scanner's field-of-view and it is not constant, it changes within the field-of-view and regarding the distance. Hence, the accuracy of the calibration parameters that should be achieved strongly depends on the demands of each individual user.

Therefore, to derive exact and non-subjective calibration requirements the latter effects should be jointly considered for specific applications individually. To quantify these effects, different engineering tasks, such as deformation monitoring of water dams, for example, should be simulated and all influences forward modeled. This way, it would be possible to investigate how sensitive are the results of e.g. deformation monitoring on the remaining influence of the mechanical misalignments after the calibration. Such forward modeling should also account for all uncertainty influences that will be discussed in the following section.

This analysis could especially benefit the in-situ calibration approaches, as it would be possible to a priori define which mechanical misalignments should be accounted for and to which amount. For example, if the whole object of interest can be measured using a narrow field-of-view, there is a high chance that the majority of the calibration parameters act homogeneously on all measurements not significantly biasing the results of the deformation monitoring. This is especially important for the hybrid TLSs, as they have notably reduced field-of-view in the vertical direction, where most of the known systematic errors have the highest impact.

Moreover, such forward modeling could also be used for viewpoint-planning to minimize the influence of mechanical misalignments on the measurement results by selecting the appropriate instrument location. Hence, a detailed analysis based on the forward modeling of TLS systematic errors on realistic examples is necessary to better understand the relevance of rigorous calibration.

6.2 Efficient calibration of all existing instrumental errors

The design of the calibration field in this study aims primarily at the calibration of high-end panoramic TLSs, as they are most often used for highly demanding engineering tasks. Hence, the accuracy requirements are the most rigorous in their case. Achieving the measurement accuracy even beyond the one assured by the manufacturers helps these instruments to come closer to the accuracy level of acclaimed total stations and laser trackers. This makes them as competitive alternatives due to several distinct properties, such as the high measurement rates allowing time savings and the dense coverage of nearly full field-of-view, allowing gains in comprehensiveness.

For the majority of TLS applications, using high-end TLSs and achieving the accuracy beyond the one already assured by the manufacturers is unnecessary. Moreover, the lower accuracy requirements allow a less rigorous initial factory calibration as well as less expensive measurement units and instrument components. This unavoidably leads to a higher number of overall mechanical misalignments that can significantly systematically bias the measurements of non-high-end instruments. For example, if the angular encoders are not calibrated extensively, e.g. on a rotary table, or they do not comprise multiple reading heads, a large number of misalignments (Table 3.1) can reach magnitudes above the measurement noise. Similar applies to the EDM unit if the comprehensive calibration is omitted.

Regardless of generally less stringent accuracy demands, the instruments not falling into the category of high-end TLSs are also often the subject of compulsory quality assurance. For example, in Germany, the Society for Measurement and Automatic Control (GMA) published a legally enforceable guideline for the accuracy evaluation of 3D optical measuring systems based on area scanning at regular intervals (VDI/VDE 2634), see e.g. Kersten et al. (2009). For many applications, such as 3D city modeling and land cadaster, TLSs need to achieve certified accuracy, which is, depending on individual regulations, validated on TLS test-fields (International Organization for Standardization, 2018). If the instrument fails the test procedure, the only possibility for the end-users is a costly repeated factory calibration. Hence, for the further benefit of a large number of end-users in the commercial sector, the solutions derived in this thesis should be adapted and furtherly extended for the larger assortment of TLSs. This primarily implies development of the calibration fields and/or approaches that are sensitive towards larger set of mechanical misalignments relevant for non-high-end TLSs.

Angular encoder errors

As mentioned in Section 5.3, angular encoder errors can be represented as the elements of the Fourier series, e.g. Muralikrishnan et al. (2010). As the magnitude of the systematic errors strongly decreases with higher-order harmonics, typically only the first and second orders are considered, representing angular encoder eccentricity and scale errors (Table 3.1). However, this is not necessarily true for the instruments completely depleted of the manufacturer's calibration (Figure 5.11, bottom).

In the case of horizontal angle encoders, due to the TLS measurement principle, the "odd" orders of the harmonics are sensitive to two-face measurements. Hence, they can be easily detected by the keypoint-based calibration approach (as demonstrated in Section 5.3) or by distributing a large number of targets within the instrument's horizon. So, they can be detected without any additional effort. The "even" order harmonics are not two-face sensitive and more difficult to estimate. The easiest approach would be to use well-distributed targets (or keypoints) in the instrument's horizon and to observe them form the same station multiple times by coarsely rotating the scanner around its standing axis. This way, the position of the target is determined using different parts of the

angular encoders. Hence, the distances between target pairs will slightly change between each scan. The reference values of these distances are not necessary, as they can be estimated as the mean distance of all scans due to the periodic nature of encoder errors (Muralikrishnan et al., 2010)

In the case of the vertical angle encoder errors, the "cosine" related part of the errors is two-face sensitive, while the "sine" part is not. Hence, the "cosine" part is easily estimable if a sufficient number of targets is well distributed within one vertical plane, i.e. one cross-section of the indoor facility, passing through the origin of the TLS local coordinate system. However, the "sine" part is much more problematic, as it would require a rotation of the instrument within this vertical plane, which is impossible due to the gravity. Namely, for the majority of the instruments, this is strongly limited, as a strong tilt could interfere with the normal functioning of the device and it could lead to permanent damage.

Hence, an alternative option would be to have an uncalibrated test length (at least several meters long) combining two targets that would be observed in numerous positions within one vertical profile. For the eventual automation, this test lengths should be mechanically moved within the vertical profile over one circumference with a radius of at least five meters to achieve sufficient sensitivity. However, this concept defies the goal of cost-efficient self-calibration. The second option would be observing a large number of targets or keypoints densely distributed within one vertical plane, from several scanner stations spread within this vertical plane. However, this approach requires extensive sensitivity analysis to assure calibration success.

EDM systematic errors

The eventual scale error in the EDM unit could be efficiently estimated by target-based calibration, with an additional inside-out tests, see e.g. Medić et al. (2019d), such as the one used for the estimation of the rangefinder offset (x_{10}). For this aim, the additional test should have an optimized distance between the targets, optimized target size and design, as well as an optimized scanning resolution and number of repetitions. These adjustments can be led by the signal-to-noise ratio sensitivity analysis as demonstrated in Section 5.1.

The cyclic error is hard to estimate with the presented self-calibration approaches efficiently. A large number of targets on different distances is necessary to successfully separate between the rangefinder offset, scale and cyclic errors, e.g. (Lichti, 2007). However, the potential for efficient self-calibration exists. Namely, when larger objects are measured, the cyclic error causes a systematic trend in measurements that can have a recognizable pattern in the resulting point cloud (Dorninger et al., 2008). Figure 6.1 presents such a measurement behavior for an older-generation phase-shift panoramic TLS, Surphaser 25HSX-IR, that was observed in one of the experiments conducted at IGG. Similar behavior was also observable for the Leica HDS 7000 in Bergstrand et al. (2019) during the deformation monitoring of a VLBI telescope. As can be seen, it is possible to visually separate the geometry of the measured object and systematic trend in measurements. Hence, by signal aliasing between the object geometry and the systematic errors, the cyclic error could be accurately extracted without requiring expensive reference values or a comparator track/bench. This additional effort could be easily realized as a single component calibration, before the comprehensive self-calibration routine to assure the unbiased estimate of the remaining parameters.

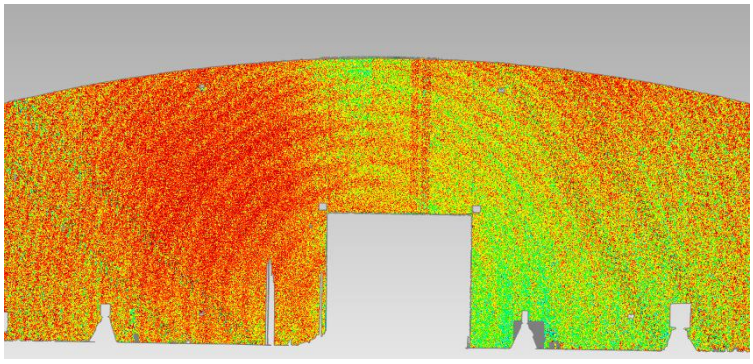

Figure 6.1: The point cloud differences (M3C2) of Surphaser 25HSX-IR and Leica ScanStation P20 (reference) after the registration (magnitudes up to 2 mm).

The intensity, i.e. reflection, dependent rangefinder offset (see Figure 6.2, left) is also documented in the literature (Clark & Robson, 2004; Hanke et al., 2006; Kersten et al., 2005; Pfeifer et al., 2007; Zámecnikova et al., 2014),

mostly for older series of TLSs. However, this systematic error is never considered in self-calibration approaches. One of the reasons for this is probably that this error is well estimated within the factory calibration (Figure 6.2, right) and presumably stable concerning the other systematic errors investigated in Section 5.4. This especially holds for the latest TLS models, while some remaining artifacts could have been observed for some relatively recent generations of the instruments in the locations where the laser beam footprint samples inhomogeneous surfaces with strong changes in the reflectivity (Figure 6.2, middle). However, for the sake of comprehensiveness, e.g. in the case of the instruments depleted of factory calibration, this systematic error could be easily estimated within the self-calibration routines. First, the absolute rangefinder offset (x_{10}) should be estimated using the abovementioned inside-out test by processing only e.g. white parts of the target surface, as a reference. Afterward, the relative range offsets to different colors should be estimated by simultaneously scanning the planar patches with different surface reflectivity, for example, different shades on a grayscale.

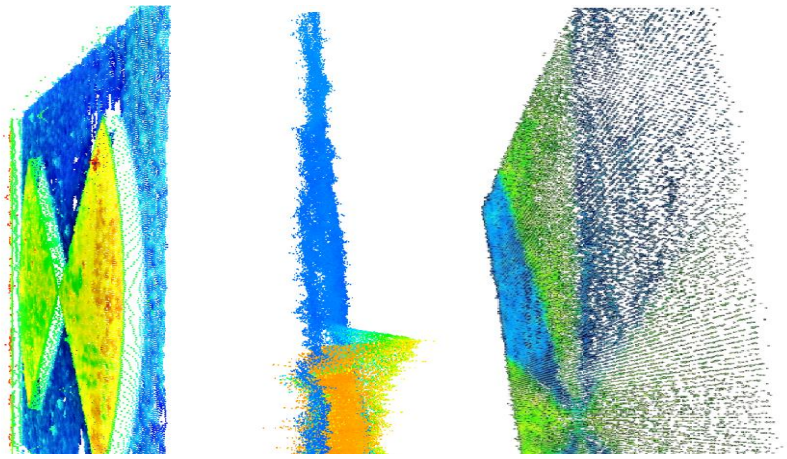

Figure 6.2: Intensity related rangefinder offset for an older TLS model depleted of factory calibration reaching magnitudes of approximately 12 mm – Surphaser 25HSX-IR (left), the remaining artifacts when sampling inhomogeneous surfaces (an edge of black and white regions in a TLS target) with a more recent instrument – Leica ScanStation P20 (middle), no noticeable systematic errors for the latest high-end instrument – Leica ScanStation P50 (right).

Other systematic errors and sensors

The systematic errors due to the horizontal and vertical axis wobble have been considered within the self-calibration experiments (Chow et al., 2013; Lichti, 2007), but it was disregarded within this work due to relatively small magnitudes in the case of high-end instruments. Moreover, the functional model of this systematic error is not well defined and a priori known. Rather, it is empirically estimated within the calibration adjustment relying on the high number of redundant observations and some a priori knowledge about the error source. Namely, the axes wobble in TLSs was investigated within the literature (Reshetyuk, 2009; Schulz, 2007; Zogg, 2008) and it is known to be related to the legions, i.e. size and number of balls in the ball bearing (Kerschner, 1980; Walsh, 2015), and it can be modeled as a Fourier series (Harvey & Rüeger, 1992). However, exact harmonic orders are not a priori known, which poses a problem for the optimization of the TLS target-based calibration with the aim of efficiency. Therefore, additional research efforts are necessary for the efficient mitigation of this systematic error, where novel calibration approaches relying on a high number of automatically detected and matched keypoints have the highest potential.

Finally, besides EDM unit and angular encoders, future development of the self-calibration approaches should aim at incorporating all measurement sensor that are the integral parts of terrestrial laser scanners, such as cameras and dynamic compensators, as well as the simultaneous calibration of instrument's specific stochastic models that would be applied in later point cloud processing algorithms. Furthermore, completely new sensitivity analysis and the efficient calibration field design should be derived for the hybrid TLSs due to their different working principle, field-of-view and set of relevant mechanical misalignments.

6.3 Extended TLS uncertainty model for better calibration results

The models of TLS measurement uncertainties, both deterministic and stochastic, used in the reviewed literature and within this thesis are still incomplete and they should be extended in the future as disregarding some uncertainty sources can bias the calibration results.

Compensator uncertainty

One of the most influential uncertainty sources which is typically disregarded is the dynamic dual-axis compensator (Section 3.1.2), which can be demonstrated on the example of two types of high-end panoramic TLSs: Leica ScanStation-P series and Z+F Imager-series. The specifications of the ScanStation P-series (Leica Geosystems AG, 2017) indicate compensator accuracy values that are three times higher than the precision of the target center estimation presented in Section 5.1 (1.5" vs. ~0.5"). Also, the specifications of the Imager 5016 (Z+F GmbH, 2016) indicate the same accuracy values for the compensator and angular measurements (~14.4"). Moreover, the measurement error of the dual-axis compensator in the lateral direction (Section 3.1.2) influences the horizontal angle measurements with the tangents of the elevation (vertical) angle, reaching infinity at the instruments zenith (Ghilani, 2017). Hence, already a random measurement noise of the compensator should not be disregarded.

However, there is an additional uncertainty originating from the estimation of the compensator index error (Section 3.1.3). Namely, after the manufacturer's in-situ compensator calibration, the measurements are expected to be unbiased and the uncertainty of this calibration procedure is disregarded. Additionally, the compensator index error is known to be strongly instable and temperature-dependent (Section 5.4), which is also not accounted for. Therefore, these uncertainty sources should be further investigated, their magnitudes estimated and their influence on TLS measurements examined by forward modeling. Finally, they should be accounted for within stochastics models.

Target center estimation uncertainty

Within this work, for the sensitivity analysis and the design of the calibration field (Section 5.1), the stochastic model in the form of look-up tables for a particular scanner was used to describe the uncertainty of the target center estimation. However, this can be hardly considered as a generally applicable solution. In the future, it would be beneficial to further investigate if there is a functional model that could explain the general uncertainty of the target centers, as it is the case for the EDM measurement noise (Schmitz et al., 2019; Wujanz et al., 2017). Such a functional model would be valuable for eventual iterative updates of the stochastic models based on the empirical data, e.g. through a variance components estimation (Förstner & Wrobel, 2016), as the look-up tables are not well suited for this method. Such a solution could further improve the results of the target-based self-calibration algorithms that rely on VCE for the refinement of stochastic models.

Moreover, an increase of the measurement uncertainty with increasing elevation (vertical angle θ) was observed in this study, and it was partially accounted for in the implemented stochastic model (Section 5.1). However, the phenomenon has not been furtherly investigated due to time constraints. The influence of the compensator measurement noise can be excluded as the only reason for this, as the phenomenon appears even when this sensor is turned off during the measurements.

It can be presumed, based on the spherical nature of TLS measurements, that the measurement uncertainty reaches extreme values close to the pole (zenith) where the laser beam footprints of the neighboring measurements almost completely overlap, making the measurements nearly perfectly correlated (Figure 6.3). This phenomenon is expected to mostly impact the horizontal angle measurements, which can be explained by the law of spherical cosine. For example, for the Leica ScanStation P50, at the vertical angle θ of 5° and a distance of 10 meters, where the laser beam footprint size is roughly 1 cm (Leica Geosystems AG, 2017; Schmitz et al., 2020b), nearly 70 consecutive measurements in horizontal direction have their laser beam footprints overlapped (sketch in Figure 6.3), which strongly influences the effective number of measurements (Schmitz et al., 2020a).

To give support for this hypothesis, Figure 6.4 presents the distribution of the horizontal angle residuals of the keypoint-based calibration implemented in Section 5.3. As can be seen, the residuals are the smallest close to the instrument's horizon and larger when moving towards poles (local zenith and nadir). The red curve represents the standard deviation of the residuals with different vertical angles, where the standard deviation of keypoint residuals on high elevations is up to four times larger than on the horizon. Besides the mentioned reduction of the effective

number of measurements, the reason for this phenomenon could be the increased impact of the disregarded low-level systematic errors on higher elevations, such as axes wobble and the encoder errors of a higher order. Regardless of the cause, the stochastic model should account for these elevation-dependent oscillations.

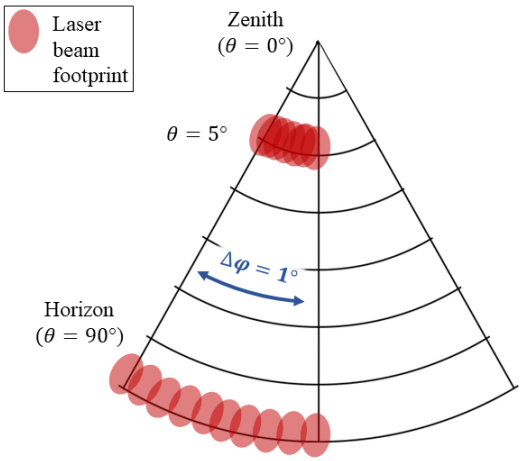

Figure 6.3: Sketch of the overlapping laser beam footprints at different elevations in the scanner's field-of-view

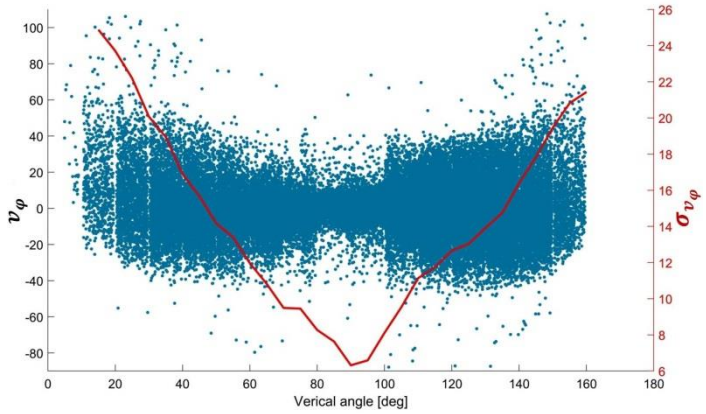

Figure 6.4: The horizontal angle residuals of the keypoint-based calibration adjustment and corresponding standard deviations at different elevations in the scanner's field-of-view (in arcseconds)

Finally, the TLS observations are systematically displaced over time due to internal temperature changes, which influence the mechanical misalignments and the EDM unit, see Section 5.4 and Janßen et al. (2020). Hence, for longer measurements, their variance should be time-dependent and adjusted accordingly. This could be assessed, for example, by applying the Allan variance calculation (Allan et al., 1974) on the time series of the repeated target center measurements over longer time periods.

External error sources

The external error sources are often considered negligible in the case of terrestrial laser scanning. Within this work, this is arguably justified due to the indoor measurements on the calibration field of relatively small dimensions (Section 5.1). However, when the high target center estimation precisions of 0.5" in angular and 0.1 mm in range measurements are considered, several external influences could have a significant impact.

The potentially influencing factors are the angle of incidence between the measured surface and the incoming laser beam, the horizontal and vertical refraction, as well as disregarding the earth curvature and the atmospheric correction. Although small in magnitude, when typical TLS working ranges are considered, the influence of the refraction and abovementioned corrections can reach values that are in the same order of magnitude as the target center precision (Witte & Schmidt, 2000).

On the other hand, the angle of incidence is proven to have a significant impact on the EDM measurements, what is documented in many studies, however, sometimes with contradictory conclusions regarding the magnitude and the direction (Chaudhry et al., 2019; Gordon, 2008; Kersten et al., 2009; Schäfer, 2017; Zámecnikova & Neuner, 2017). As a precaution, in the TLS calibration, all measurements with steep angles of incidence are removed from the calibration adjustment, e.g. Lichti (2007). However, the systematic influence on the remaining non-perpendicular measurements could still significantly bias the calibration results.

Besides, the incidence angle could also systematically bias the angular measurements in the target-based or keypoint-based calibration adjustment. Namely, the position of the target center or the keypoint in angular direction is estimated using the recoded intensity values of the EDM unit, which could also be biased by steep incidence angles. This could especially be problematic when the laser beam footprint samples a non-homogenous surface with strong variations in the reflectivity, which is often the case in the latter examples, e.g. edges of black and white regions on the target. Moreover, such edges are typically crucial information in determining the target or keypoint position. Hence, this possibility should be further investigated.

To conclude, it would be beneficial to forward model the abovementioned external influences and to investigate if they can bias the calibration results. If they turn out to be significant, they should be stochastically or deterministically modeled to alleviate the impact on the calibration. Moreover, some effects could be reduced if they would be introduced in the calibration adjustment as additional parameters. This way they could be estimated within the adjustment as by-product mitigating their influence on the results.

Correlations

Finally, in all documented calibration approaches the stochastic model comprises a diagonal covariance matrix, completely disregarding the strong correlations between densely sampled TLS observations, primarily due to insufficient knowledge. Hence, a better understanding of TLS correlations would benefit the task of TLS calibration, mainly by improving the a posteriori uncertainty evaluation of the estimated calibration parameters (Holst et al., 2012; Holst & Kuhlmann, 2014b; Jurek et al., 2017; Kermarrec et al., 2019a; Zhao et al., 2019).

The correlations have already been traced in individual test measurements (Koch et al., 2010; Koch & Kuhlmann, 2009) and substantial research efforts are invested in further advancements (Kauker et al., 2016; Kauker & Schwieger, 2017; Schmitz et al., 2020a). However, strategies for a general estimation of correlations in terrestrial laser scanning are still non-existent. To conclude, the advancements in this field are also important for the TLS calibration and this issue is of the highest relevance for the in-situ calibration approaches relying on numerous densely sampled observations, e.g. keypoint-based, plan-based or paraboloid-based calibration.

6.4 Future of TLS self-calibration

Improving keypoint-based calibration

As the immediate advancement of the self-calibration, there is a large potential in the further development of the keypoint-based calibration approach, which was proven to be a powerful tool for estimating the two-face sensitive calibration parameters (Section 5.3). The next big challenge is enabling the successful finding of the corresponding keypoints, i.e. feature matching, for the point clouds collected from distant scanner stations. Achieving this would allow the keypoint-based calibration to become fully automatic and comprehensive.

In order to accomplish the latter aim following problems need to be tackled: the distortion of the intensity values with changing measurement configuration (Tan & Cheng, 2016), the perspective distortion of the image due to different viewpoints (Yu et al., 2018), as well as the re-scaling and blurring influencing the image when the keypoint is observed from different distances (Lindeberg, 2012). As an additional improvement, other cartographic projections instead of the spherical projection could be used to eventually reduce the distortion of the intensity image in the regions close to poles, see e.g. (Markiewicz & Zawieska, 2019). This could increase the number and the precision of keypoints in these extreme regions, which are of high relevance for TLS calibration.

Moreover, the keypoint detection and matching algorithms suffer from many regulating parameters that are typically subjectively adjusted, which leads to suboptimal algorithm performance. In the future, it is necessary to develop efficient machine-learning routines with well-defined score functions that would provide the optimal tuning of these adjustable parameters. This would undoubtedly lead to further significant improvements in the calibration results. The latter problem is a strong motivation for substituting the men-designed keypoint detection and description algorithms with the data-driven ones developed by deep learning approaches, which do not suffer from similar disadvantages, see e.g. Gojcic et al. (2018). However, they share their own set of weaknesses, primarily due to necessity of large amounts of labeled training data, which is typically not available for such specific tasks as TLS calibration, as well as the difficulty of uncertainty estimation, which is crucial for the quality assurance of the calibration results.

Proposed full-blown calibration solution

For the full-blown TLS calibration solution, it is necessary to exploit all available information sources of the acquired point clouds. The 2D keypoints used within this work are only one example of such an information source. Namely, each keypoint or a point belonging to a geometrical feature, like a linear segment or a planar patch, that can be detected automatically in the point cloud, can be misplaced due to the TLS misalignments. Hence, tracking their relative position changes between several point clouds can further aid the calibration, similarly to the existing in-situ calibration approaches listed in Section 2.2, e.g. plane-based self-calibration from Gielsdorf et al. (2004).

The estimate of their position in space also depends on the precision of TLS measurements and detection algorithms, which can be represented with the uncertainty (i.e. confidence) ellipsoids. The orientation and size of the uncertainty ellipsoid can be estimated using the analysis of principal components and variances of the investigated point cloud segments (Jolliffe, 2002). All segments that have at least one ellipsoid axis with comparably low magnitude can be precisely positioned in space at least in one direction. Hence, such segments hold an information source that can aid the calibration approach. The 2D keypoints found in the intensity image have their position accurately determined in the direction of horizontal and vertical angles by analyzing the variances of intensity values within an image segment. Similarly, the points lying on the geometrical features can be accurately positioned in space, either also in two directions (on a linear segment the point position is only uncertain along the line) or at least in one direction (the point position in a planar patch is accurately fixed only in the direction of a plane normal), which could significantly contribute to the calibration results (Blomley et al., 2014; Maalek et al., 2018).

However, these uncertainty ellipsoids should be transformed from the arbitrary orientation in space, defined by the PCA, into the coordinate system of TLS measurement uncertainty (direction of range, horizontal and vertical angle measurements). This way, the points lying on the detected linear segments or planar patches could be introduced in the calibration adjustment as TLS observations with adequate stochastic information. Including these additional features in the calibration adjustment could be especially helpful for the calibration from multiple scanner stations, as planes and lines are ought to be more robust towards perspective changes. Additionally, such a full-blown calibration solution could provide an increased sensitivity toward detecting and decoupling a larger number of calibration parameters, allowing accurate and unbiased estimations of even low-level systematic errors.

Alternatives

Alternatively to the proposed solution based on the detection and matching of the distinct objects in the point cloud, there are completely different strategies that focus on processing the point clouds as a whole. For example, the algorithms minimizing Rényi quadratic entropy of the point clouds (or similar) are successfully used for the calibration of the mobile scanning systems (Hillemann et al., 2019; Sheehan et al., 2012). Such approaches could be transferable to the calibration of terrestrial laser scanners. Finally, there is also the possibility of a hybrid solution by dissecting the point cloud into voxels with well-defined geometrical and semantic information. Such well-defined voxels would allow reliable detection of correspondences between two or more point clouds, see e.g. (Li, 2018). Hence, this way, the whole point cloud could be used for the calibration as in the case of minimizing the Rényi quadratic entropy, where each voxel could be interpreted as one well-defined keypoint. However, it should be noted that such point-cloud based approaches suffer from a difficult uncertainty estimation, which is crucial for trustworthy calibration results.

On-board and near-real-time calibration solution

The described calibration approaches rely on handling large amounts of data, they require great computational power and hours of off-line post-processing. For example, the 2D keypoint based calibration approach implemented in Section 5.3 requires approximately three hours of processing on a powerful desktop PC. However, the optimal solution that the industry requires is evaluation of the in-situ calibration, on-the-spot and in near-real-time, using the on-board processing unit of TLS itself. The problem is that for the delicate task of TLS calibration, a high measurement resolution, which assures high precision, is mandatory and it leads to large data amounts.

The solution to this problem is a selective high-resolution scanning, which requires an adequate analysis of the given measurement configuration before the calibration. This can be realized by the initial coarse scanning that would reveal the geometry of the surroundings, followed by the sensitivity analysis. An example of such sensitivity analysis would be simulating the regular grid of sparse observations that can be realized concerning the given geometry. Afterward, the impact of these observations on the estimation of the calibration parameters could be quantified based on impact factors, which are also used in Section 5.1. Namely, the impact factors point out the observations that have the highest contribution in estimating the searched parameters within the calibration adjustment (Baarda, 1968; Baarda, 1967). Hence, the simulated observations with the highest impact factors could indicate at the parts of the surroundings that need to be measured at high resolution to allow successful calibration.

If the given configuration is not sensitive enough to determine all relevant calibration parameters, an efficient optimization approach should be utilized to find out where should TLS be re-positioned within the surroundings to increase the sensitivity. The application of the heuristic optimization algorithms, like SA, PSO or GA (Section 2.1.2), could, in this case, be reasonable, as the computational problem is strongly limited by the given geometry of

the surroundings and the refinement of the instrument positioning is limited only to relocations on the surface of the ground (2D problem).

Finally, if the given geometry does not allow the accurate and unbiased estimation of all calibration parameters, the same sensitivity analysis should be the basis of the refinement of the functional model and exclusion of undetectable mechanical misalignments. The latter part of the approach was already successfully used in the refinement of the deformation monitoring measurement configurations in the case of leveling networks and terrestrial laser scanning (Holst et al., 2013; Holst & Kuhlmann, 2014b). There, instead of the impact factors or the measure of the outer reliability, the partial redundancies or the measure of the internal reliability are utilized (Baarda, 1968). However, the modification of the approach to incorporate the measures of the outer reliability was already discussed in the literature (Holst, 2015).

The latter workflow could be implemented also to boost the other in-situ calibration approaches. For example, in the case of the paraboloid-based calibration (Section 5.2), such sensitivity analysis could be used to identify at which positions the subject of deformation monitoring should be scanned to allow successful decoupling of the object's geometrical parameters and the calibration parameters. Moreover, such sensitivity analysis could be used to derive the optimal measurement set-up of the ad-hoc target-based calibration-fields, such as ones used for the Leica Check and Adjust in-situ calibration procedure.

6.5 Automation of target-based self-calibration

The current implementations of the target-based calibration approach should be more automatized to furtherly promote the integration of the user-oriented calibration in the commercial sector. This can be achieved by supplementing the calibration with the automatic detection of targets in the acquired point clouds. Several approaches for this cause are already developed in the literature (Abmayr et al., 2008; Akca, 2003; Liang et al., 2014; Loy & Eklundh, 2006; Yi et al., 2018). However, they are not completely robust, they do not have perfect recall and also they require manual tuning of control parameters. Hence, future solutions should tackle these challenges and the most promising strategy is completely data-driven detection based on deep learning approaches, as they are well suited for the task (instance segmentation).

After the successful target detection, the target centers should be precisely estimated using algorithms such as one described in Janßen et al. (2019), which are capable of the elimination of the falsely detected targets based on the achieved correlation values. Furthermore, the coarse registration is necessary to define approximate values for the parameters that are searched in the calibration adjustment. This step is necessary, as the calibration adjustment unavoidably relies on the linearization by a first-order Taylor approximation. Probably the best solution for this would be the implementation of the 4 points congruent sets algorithms (Aiger et al., 2008; Ge, 2017) that were proven to be very robust and computationally effective for such tasks.

Finally, if the target detection step was an integral part of the calibration routine, the 2D keypoint-based calibration could be easily integrated with the target-based calibration. Namely, within this step, it would be possible to detect keypoints without large additional computational requirements and all observed quantities could be integrated within one calibration adjustment with adequate weighting. In the case of the a priori calibration, this would lead to comprehensiveness due to target-based calibration and improved calibration parameter precision due to redundant observations from keypoints. However, this increase in precision is doubtfully beneficial for the later parameter use, as it is known that the parameter stability is limited. A larger gain could be achieved in the case of the in-situ combination of both approaches, where the targets could be used to supplement eventually deficient measurement configuration, which would lead to both more comprehensive and accurate calibration results.

6.6 Challenging the calibration field design

The design of the calibration field implemented in this study is based on a man-made trial and error analysis supported by the sensitivity analysis described in Section 5.1. Additionally, within the mentioned section, it was demonstrated how this approach can be adapted for the efficient design of new calibration fields. However, such an approach can only deliver near to the optimal solution, which could certainly be refined. Moreover, it would benefit from further automation, as it would eliminate the currently existing requirement that the calibration field is designed by qualified engineers.

Several already applicable solutions could be used for challenging the derived calibration field design and for the automation of the designing procedure. The first possibility is to use heuristic optimization approaches that are already used for the TLS viewpoint-planning tasks as described in Section 2.1.2. However, to make the numerical problems solvable they could focus on the optimal combination of the finite set of the sensitive measurement configurations derived in Section 5.1. The second possibility would be to use the sensitivity analysis based on the impact factors, which would be strongly numerically simplified by considering only the measurement configurations defined by the a priori given geometry of the surroundings, as proposed in Section 6.4.

Finally, the third possibility would be to use one of the existing methods for analytical solving of the first-order design problem in the optimization of the geodetic networks (Section 5.1). With this approach, by fixing the a priori known functional and stochastic models, and by defining the desired quality of the searched calibration parameters, it is possible to derive the optimal configuration matrix, which describes the required measurement configuration for achieving the desired results (Amiri-Simkooei, 2007; Kuang, 1996). However, this approach suffers from the problem of difficult interpretation of the derived configuration matrix.

6.7 Multifunctionality of the calibration field

The calibration field designed and implemented in this study (Section 5.1) has a potential for the comprehensive calibration of different instruments relying on the polar measurement principle and comprising angular encoders and EDM units. Namely, the functional models of total stations (Lichti, 2007), laser trackers (Muralikrishnan et al., 2009) and terrestrial laser scanners (Eq. 3.4-3.6) are nearly identical.

Hence, the calibration field has a potential for multifunctionality with minimal adaptations. For the accurate calibration of laser trackers and total stations, the TLS targets can simply be substituted with corner cube reflectors. Achieving such a multifunctional calibration field has several potential advantages. It can be a polygon for a direct and unbiased comparison of the achievable measurement accuracy of these instruments. Additionally, it can be used to assess the interoperability of these instruments and check the consistency of their measurement results. Finally, it could help to objectively asses and compare the stability of the internal instruments' geometries due to changeable mechanical misalignments, which is identified as the significant source of the measurement uncertainty (Section 5.4). Therefore, it can help in providing proof if terrestrial laser scanners can compete with the industry-standard instruments in high accuracy demanding engineering tasks.

Such direct comparison could help TLSs to verify if their measurement products can be back-to-back with the established measurement technologies and aid them in the infiltration of the commercial applications with high accuracy demands such as deformation monitoring and large-scale industrial metrology.

7 Conclusion and Outlook

Terrestrial laser scanners (TLSs) commonly suffer from systematic errors in measurements due to mechanical misalignments of the internal instrument components. These systematic errors often surpass the magnitudes of the random measurement noise making their impact on acquired point clouds significant. This issue is of high relevance for engineering applications with high demands toward accuracy, such as deformation monitoring in the field of geodetic/surveying engineering, as well as industrial quality control and assurance in the field of large-scale metrology. These fields of application predominantly rely on well-established measurement technologies, the total stations and laser trackers. Hence, assuring high measurement accuracy for terrestrial laser scanners is a necessary prerequisite for their better acceptance in these practices. The whole subject of matter is of high relevance for TLSs, as in other applications with lower accuracy demands, such as 3D mapping of the environment, they are becoming gradually substituted by the mobile mapping systems due to their lower efficiency.

The solutions for dealing with instrument-related systematic errors exist in the scope of the repeated factory calibration at manufacturer's facilities or in the scope of user-oriented self-calibration used in scientific circles. However, both solutions suffer from certain disadvantages hindering their wider acceptance in the commercial sector. In both cases, the main limiting factors are associated with the costs, time and necessary effort. Hence, increasing the efficiency of the existing calibration strategies or developing new efficient calibration strategies would strongly benefit the large community of end-users. Therefore, the main objective of this thesis is to increase the efficiency of the user-oriented self-calibration to support the wider acceptance of the practice.

The existing user-oriented calibration approaches are segregated on the a priori calibration, before the measurement campaign, and the in-situ calibration, during the measurement campaign, each having certain advantages and disadvantages. Hence, within this work, they are first investigated and analyzed separately, while afterward they are compared, and their advantages and shortcomings are examined to support the selection of appropriate strategy. The investigations primarily aim at the high-end TLSs used in highly demanding engineering tasks, but the results are transferable to a large amount to all panoramic TLSs. Based on these studies, and in line with the questions and considerations placed in the objectives, three main aspects, which are addressed in different publications, can be highlighted:

- **Improving the efficiency of the existing a priori calibration approaches**
  The established a priori target-based self-calibration approach has so far been carried out using hundreds of quasi-randomly distributed targets scanned from multiple scanner stations, which assured accurate calibration results, but lacked in the efficiency (Chow et al., 2013). Within this thesis, more precise functional and stochastic models of the calibration adjustment were derived, focusing on the most relevant calibration parameters, allowing explicit inclusion of two-face measurements, and describing the measurement uncertainty in detail. These results made the basis for the sensitivity analysis aiming at detecting the most sensitive measurement configurations towards estimating each individual calibration parameter, which provided the building-blocks for efficiently designing the calibration field.

  Finally, the permanent calibration field was designed and implemented allowing several times more efficient calibration, while assuring trustworthy calibration results. Although this is the first such non-commercial facility in Europe, the main contribution lies in the applied workflow, which can be easily reproduced by qualified engineers for establishing new calibration fields concerning their individual demands and constraints.

- **Improving and developing further efficient in-situ calibration approaches**

  This works also continues the efforts of *the further development of existing concepts for TLS-based deformation analysis*, where the aspect of the accurate in-situ scanner calibration is emphasized as necessary for assuring the unbiased deformation monitoring results (Holst, 2015). By analyzing different in-situ calibration strategies, the bundled calibration adjustment incorporating two-face measurements and sufficient variations in the measurement configurations is identified as necessary for the accurate deformation analysis on all spatial scales (both local and global object's deformations).
  Moreover, the first fully automatic in-situ calibration approach was introduced as the response to the efficiency related deficiencies of the existing in-situ calibration strategies identified within this work. The

approach assures an efficient calibration relying on automatically detected and matched salient keypoints in the surroundings, eliminating the requirements of compulsory man-made objects and a priori knowledge about the environment.

- **Investigating the advantages and disadvantages of the approaches**

  The achieved efficient TLS calibration allowed series of multiple calibrations to investigate, for the first time in detail, the stability of the calibration parameters which brought important insight regarding the limitations of the a priori calibration on dedicated calibration fields. Additionally, for the first time, the influence of the estimated parameters on the accuracy of the point clouds was analyzed and it was proved that applying the a priori estimated calibration parameters can improve the point cloud accuracy beyond the manufacturer's calibration. Moreover, it is proven that the self-calibration approaches can reach comparable results as the factory calibration upon the instrument assembly, indicating that, if necessary, the costly manufacturers' calibration can be avoided. Finally, the understanding of advantages and disadvantages of different calibration approaches was expanded, pointing out the most suitable workflows for the user-calibration regarding different possibilities of the a priori and in-situ calibration approaches.

Although the effectiveness of the developed methods has already been demonstrated, the work on the efficient TLS calibration cannot be considered as complete, and several aspects are still to be resolved. First, this work focuses on the efficient calibration of high-end panoramic TLS, as this matter is of the highest relevance for industry requirements. These devices can be significantly influenced only by a smaller subset of the overall number of mechanical misalignments. Hence, to get a more general solution, the results presented in this work should be furtherly expanded to account for all known systematic errors in TLSs. Moreover, the solutions should be transferred to the hybrid terrestrial laser scanners.

Second, the approaches presented herein can be furtherly improved by aiming at a full-blown calibration solution that would be at the same time fully automatic, comprehensive as well as efficient. In other words, it should be fast, realizable on the working site using on-board TLS hardware and delivering a solution in near-real-time. Moreover, the level of automation should allow even inexperienced end-users to assure the required measurement quality. Despite the substantial work that needs to be made, the first steps toward the aim are achieved by introducing the keypoint-based calibration approach, which proved itself to be a promising candidate for further advancements. Additionally, the possibilities for these advancements are discussed in detail to contribute to future developments.

Third, the uncertainty models for terrestrial laser scanners are still simplified to a certain amount, which also impacts the task of TLS calibration. Many influencing factors are disregarded due to insufficient knowledge that could potentially bias the calibration results. Their influence on the TLS calibration needs to be investigated by forward modeling and if they are identified as significant, their influence should be mitigated by appropriate techniques.

Finally, the main purpose of TLS calibration is to assure the adequate measurement accuracy for high demanding tasks, such as deformation monitoring. Hence, it is necessary to furtherly investigate how sensitive and susceptible are real deformation monitoring tasks on the systematic influence of mechanical misalignments. Moreover, by extensive simulations and forward modeling, it should be identified which mechanical misalignments are the most influential, which can be disregarded, which accuracy needs to be achieved and how important is the calibration in general. Answering the simple question of, *how accurate TLS measurements should really be*, is not trivial and should be in the focus of manifold publications.

Only when all these questions are answered, the terrestrial laser scanners will be accepted in highly demanding engineering tasks without a doubt about their capabilities. This way they will establish themselves as a competitive solution for various tasks aiming at areal measurements and approximation of large surfaces with the highest accuracy requirements. If this is not achieved, there is a reason to believe that they will become just a passing solution for large scale 3D mapping, the field which is continuously getting taken over by different mobile mapping systems. These systems will soon be able to deliver comparable measurement accuracy to TLSs, however with much higher acquisition speed.

Overall, the present thesis helped to improve the efficiency of the TLS calibration procedures, while still assuring trustworthy calibration results in the scope of accuracy and reliability. Thus, this thesis contributes to the development and optimization of measurement concepts, as well as the assurance of measurement quality, which are pointed out as some of the core competencies of the engineering geodesy (Kuhlmann et al., 2014).

8 List of Further Publications

This chapter gives a chronological overview of further publications in which the author of this dissertation was involved. The publications listed here are excluded from the main contributions as they are not directly related to this thesis, they are already covered by the relevant publications summarized in Chapter 4 or the author of the thesis participated only as a coauthor.

Peer-reviewed publications:

- Janßen, J., Medić, T., Kuhlmann, H., Holst, C. (2019) Decreasing the uncertainty of the target center estimation at terrestrial laser scanning by choosing the best algorithm and by improving the target design, *Remote Sens.*, 11 (7), 854

- Schmitz, B., Holst, C., Medić, T., Lichti D. D., Kuhlmann, H. (2019) How to Efficiently Determine the Range Precision of 3D Terrestrial Laser Scanners?, *Sensors*, 19 (6), 1466

Non-peer reviewed publications:

- Heinz, E.; Medić, T.; Holst, C.; Kuhlmann, H. (2018) Genauigkeitsbeurteilung von Laserscans anhand realer Messobjekte. In: *DVW e.V. (Hrsg.): Terrestrisches Laserscanning 2018 (TLS 2018). DVW-Schriftenreihe*, Band 93, Wißner Verlag, Augsburg, S. 41-56.

- Medić, T., Holst, C., Kuhlmann, H. (2019c) Improving the Results of Terrestrial Laser Scanner Calibration by an Optimized Calibration Process, *in: Photogrammetrie - Laserscanning - Optische 3D-Messtechnik, Beiträge der Oldenburger 3D-Tage 2019*, Hrsg: Luhmann, T., Schumacher, C., Wichmann Verlag, Berlin, S. 36-50.

- Holst, C., Medić, T., Nothnagel, A., Kuhlmann, H. (2019a) Analyzing shape deformation and rigid body movement of structures using commonly misaligned terrestrial laser scanners: the radio telescope case, *4th Joint International Symposium on Deformation Monitoring (JISDM)*, 15th - 17th May 2019, Athens, Greece.

- Holst, C., Medić, T., Kuhlmann, H. (2019b) TLS-Kalibrierung: in-situ und/oder a priori?, In: *DVW e.V. (Hrsg.): Terrestrisches Laserscanning 2019 (TLS 2019). DVW-Schriftenreihe*, Band 96/2019, Wißner Verlag, Augsburg, S. 89-104.

- Medić, T., Kuhlmann, H. & Holst, C. (2020d) Optimizing the Target-based Calibration Procedure of Terrestrial Laser Scanners, *Allgem. Verm. Nachr*, 1/2020, 3-12, Wichmann Verlag, Berlin.

List of Tables

List of Figures

List of Abbreviations and Acronyms

BOTA8	Bonn Target 8
CP	calibration parameter
DIN	Deutsches Institut für Normung
EDM	electronic distance measurement
EOP	Exterior orientation parameter
FOD	first order design
FoV	Field of View
GHM	Gauß-Helmert Model
GMA	Gesel/schaft Mess- und Automatisierungstechnik
GNSS	Global Navigation Satellite System
IGG	Institute of Geodesy and Geoinformation
IMU	Inertial measurement unit
ISO	International Organization For Standardization
IWT	Instrument working time
LT	laser tracker
M3C2	Multiscale Model to Model Cloud Comparison
MAD	median absolute deviation
NIST	National Institute of Standards and Technology
OP	Object point
RMS	root-mean-square
RMSE	root-mean-squared error
SNR	signal-to-noise ratio
SOD	second order design
TLS	Terrestrial Laser Scanner
TOD	third order design
TS	total station
VCE	Variance component estimation

VDE	Verband der Elektrotechnik, Elektronik und Informationstechnik
VDI	Verein Deutscher Ingenieure
VLBI	very-long-baseline interferometry
WFD	Wave Form Digitizer
ZOD	zero order design

References

Abbas, M. A., Lichti, D. D., Chong, A. K., Setan, H., & Majid, Z. (2014a). An on-site approach for the self-calibration of terrestrial laser scanner. *Measurement: Journal of the International Measurement Confederation*, *52*(1), 111–123. https://doi.org/10.1016/j.measurement.2014.03.009

Abbas, M. A., Setan, H., Majid, Z., Chong, A. K., & Lichti, D. D. (2014b). Improvement in measurement accuracy for hybrid scanner. *IOP Conference Series: Earth and Environmental Science*, *18*, 12066. https://doi.org/10.1088/1755-1315/18/1/012066

Abbas, M. A., Setan, H., Majid, Z., Idris, K. M., Ariff, M. F. M., Chong, A. K., & Lichti, D. D. (2014c). The Effect of Datum Constraints for Terrestrial Laser Scanner Self - Calibration The Effect of Datum Constraints for Terrestrial Laser Scanners Self - Calibration. In *FIG Congress 2014, Kuala Lumpur, Malaysia 16-21 June 2014*.

Abbas, M. A., Lichti, D. D., Chong, A. K., Setan, H., Majid, Z., Lau, C. L., et al. (2017). Improvements to the accuracy of prototype ship models measurement method using terrestrial laser scanner. *Measurement: Journal of the International Measurement Confederation*, *100*, 301–310. https://doi.org/10.1016/j.measurement.2016.12.053

Abbas, M. A., Majid, Z., Azmi, M., Chong, A. K., Lau, C. L., Idris, K. M., & Mustafar, M. A. (2019). Scale Factor Effect in Terrestrial Laser Scanner Datum Transformation. In *IOP Conference Series: Earth and Environmental Science* (Vol. 385, p. 12043). IOP Publishing.

Abmayr, T., Härtl, F., Hirzinger, G., Burschka, D., & Fröhlich, C. (2008). A correlation based target finder for terrestrial laser scanning. *Journal of Applied Geodesy*, *2*(3), 131–137.

Aiger, D., Mitra, N. J., & Cohen-Or, D. (2008). 4-points congruent sets for robust pairwise surface registration. In *ACM SIGGRAPH 2008 papers* (pp. 1–10).

Akca, D. (2003). Full Automatic Registration of Laser Scanner Point Clouds. *Optical 3D Measurement Techniques IV, I.*, 330–337.

Allan, D. W., Shoaf, J. H., & Halford, D. (1974). Statistics of time and frequency data analysis. In *Time and frequency: theory and fundamentals* (p. 151).

Amiri-Simkooei, A. R. (2007). Analytical first-order design of geodetic networks. *Iranian Journal of Engineering Sciences*, *1*(1), 1–11.

Amiri-Simkooei, A. R., Asgari, J., Zangeneh-Nejad, F., & Zaminpardaz, S. (2012). Basic Concepts of Optimization and Design of Geodetic Networks. *Journal of Surveying Engineering*, *138*(4), 172–183. https://doi.org/10.1061/(ASCE)SU.1943-5428.0000081

Amiri Parian, J., & Gruen, A. (2010). Sensor modeling, self-calibration and accuracy testing of panoramic cameras and laser scanners. *ISPRS Journal of Photogrammetry and Remote Sensing*, *65*(1), 60–76. https://doi.org/10.1016/j.isprsjprs.2009.08.005

Baarda, Willem. (1968). A Testing Procedure for Use in Geodetic Networks. *Netherlands Geodetic Commission*, *2*(5).

Baarda, Willem. (1967). *Statistical concepts in geodesy* (Vol. 2). Rijkscommissie voor Geodesie.

Bae, K., & Lichti, D. D. (2007). On-site self-calibration using planar features for terrestrial laser scanners. *Int. Arch. Photogramm. Remote Sens. Spat. Inf. Sci*, *36*, 14–19.

Baselga, S. (2011). Second order design of geodetic networks by the simulated annealing method. *Journal of Surveying Engineering*, *137*(4), 167–173.

Becerik-Gerber, B., Jazizadeh, F., Kavulya, G., & Calis, G. (2011). Assessment of target types and layouts in 3D laser scanning for registration accuracy. *Automation in Construction*, *20*(5), 649–658. https://doi.org/10.1016/j.autcon.2010.12.008

Bergstrand, S., Herbertsson, M., Rieck, C., Spetz, J., Svantesson, C.-G., & Haas, R. (2019). A

gravitational telescope deformation model for geodetic VLBI. *Journal of Geodesy*, *93*(5), 669–680.

BiPM, I. E. C., IFCC, I., IUPAC, I., & ISO, O. (2012). The international vocabulary of metrology—basic and general concepts and associated terms (VIM). *JCGM*, *200*, 2012.

Blomley, R., Weinmann, M., Leitloff, J., & Jutzi, B. (2014). Shape distribution features for point cloud analysis – a geometric histogram approach on multiple scales. *ISPRS Annals of Photogrammetry, Remote Sensing and Spatial Information Sciences*, *II–3*(September), 9–16. https://doi.org/10.5194/isprsannals-ii-3-9-2014

Böhm, J., & Becker, S. (2007). Automatic marker-free registration of terrestrial laser scans using reflectance. In *Proceedings of the 8th Conference on Optical 3D Measurement Techniques, Zurich, Switzerland* (pp. 9–12).

Chan, T. O., & Lichti, D. D. (2012). Cylinder-Based Self-Calibration of a Panoramic Terrestrial Laser Scanner. *International Archives of Photogrammetry, Remote Sensing and Spatial Information Sciences*, *XXXIX*(September), 169–174. https://doi.org/10.5194/isprsarchives-XXXIX-B5-169-2012

Chan, T. O., Lichti, D. D., & Belton, D. (2015). A rigorous cylinder-based self-calibration approach for terrestrial laser scanners. *ISPRS Journal of Photogrammetry and Remote Sensing*, *99*, 84–99. https://doi.org/10.1016/j.isprsjprs.2014.11.003

Chaudhry, S., Salido-Monzú, D., & Wieser, A. (2019). Simulation of 3D laser scanning with phase-based EDM for the prediction of systematic deviations. In *Modeling Aspects in Optical Metrology VII* (Vol. 11057, p. 110570H). International Society for Optics and Photonics.

Chow, J. C. K., Ebeling, A., & Bill, T. (2010a). Low cost Artificial Planar Target Measurement Techniques for TLS. *FIG Congress 2010 Facing the Challenges - Building the Capacity*, (April 2010), 13.

Chow, J. C. K., Lichti, D. D., & Teskey, W. F. (2010b). Self-calibration of the Trimble (MENSI) GS200 terrestrial laser scanner. *International Archives of Photogrammetry, Remote Sensing and Spatial Information Sciences*, *XXXVIII–5*, 161–166.

Chow, J. C. K., Teskey, W. F., & Lovse, J. W. (2011a). In-situ Self-calibration of Terrestrial Laser Scanners and Deformation Analysis Using Both Signalized Targets and Intersection of Planes for Indoor Applications. In *14th FIG Symposium on Deformation Measurements and Analysis*. Hong Kong, China.

Chow, J. C. K., Lichti, D. D., & Glennie, C. L. (2011b). Point-based versus plane-based self-calibration of static terrestrial laser scanners. *The International Archives of the Photogrammetry, Remote Sensing and Spatial Information Sciences*, *38*(5/W12), 121–126. https://doi.org/10.5194/isprsarchives-XXXVIII-5-W12-121-2011

Chow, J. C. K., Lichti, D. D., & Teskey, W. F. (2012). Accuracy assessment of the FARO Focus 3D and Leica HDS6100 panoramic- type terrestrial laser scanners through point-based and plane-based user self-calibration. *Proceedings of the FIG Working Week: Knowing to Manage the Territory, Protect the Environment, Evaluate the Cultural Heritage*, (May), 6–10.

Chow, J. C. K., Lichti, D. D., Glennie, C. L., & Hartzell, P. (2013). Improvements to and comparison of static terrestrial LiDAR self-calibration methods. *Sensors*, *13*(6), 7224–7249. https://doi.org/10.3390/s130607224

Clark, J., & Robson, S. (2004). Accuracy of measurements made with a Cyrax 2500 laser scanner against surfaces of known colour. *Survey Review*, *37*(294), 626–638.

Díaz-Vilariño, L., Frías, E., Balado, J., & González-Jorge, H. (2018). SCAN PLANNING AND ROUTE OPTIMIZATION FOR CONTROL OF EXECUTION OF AS-DESIGNED BIM. *International Archives of the Photogrammetry, Remote Sensing & Spatial Information Sciences*.

Dorninger, P., Nothegger, C., Pfeifer, N., & Molnár, G. (2008). On-the-job detection and correction of systematic cyclic distance measurement errors of terrestrial laser scanners. *Journal of Applied Geodesy*, *2*(4), 191–204. https://doi.org/10.1515/JAG.2008.022

Eling, D. (2009). *Terrestrisches Laserscanning für die Bauwerksüberwachung*. Leibniz-Univ., Fachrichtung Geodäsie und Geoinformatik.

Ford, D., Housel, T., Hom, S., & Mun, J. (2016).

Benchmarking Naval Shipbuilding With 3D Laser Scanning, Additive Manufacturing, and Collaborative Product Lifecycle Management. Naval Postgraduate School Monterey United States.

Förstner, W., & Gülch, E. (1987). A Fast Operator for Detection and Precise Location of Distict Point, Corners and Centres of Circular Features. In *Proceedings of the ISPRS Conference on Fast Processing of Photogrammetric Data* (pp. 281–305). Interlaken.

Förstner, W., & Wrobel, B. P. (2016). *Photogrammetric Computer Vision*. Springer International Publishing Switzerland.

Friedli, E., Presl, R., & Wieser, A. (2019). Influence of atmospheric refraction on terrestrial laser scanning at long range. In *Proceedings of the 4th Joint International Symposium on Deformation Monitoring (JISDM), 15–17 May 2019*.

Garcia-San-Miguel, D., & Lerma, J. L. (2013). Geometric calibration of a terrestrial laser scanner with local additional parameters: An automatic strategy. *ISPRS Journal of Photogrammetry and Remote Sensing*, *79*, 122–136. https://doi.org/10.1016/j.isprsjprs.2013.02.007

Ge, X. (2016). *Terrestrial Laser Scanning Technology from Calibration to Registration with Respect to Deformation Monitoring*. Technical University of Munich.

Ge, X. (2017). Automatic markerless registration of point clouds with semantic-keypoint-based 4-points congruent sets. *ISPRS Journal of Photogrammetry and Remote Sensing*, *130*, 344–357.

Ge, X., & Wunderlich, T. (2014). Target Identification in Terrestrial Laser Scanning. *Survey Review*, *47*, 129–140. https://doi.org/10.1179/1752270614Y.0000000097

Ghilani, C. D. (2017). *Adjustment computations: spatial data analysis*. John Wiley & Sons.

Gielsdorf, F., Rietdorf, A., & Gruendig, L. (2004). A Concept for the Calibration of Terrestrial Laser Scanners. *Proceedings of the FIG Working Week. Athens, Greec*, 1–10.

Gojcic, Z., Zhou, C., & Wieser, A. (2018). Learned compact local feature descriptor for tls-based geodetic monitoring of natural outdoor scenes. *International Archives of the Photogrammetry, Remote Sensing and Spatial Information Sciences*, *4*, 113–120.

Gojcic, Z., Zhou, C., & Wieser, A. (2019a). Feature-based approaches for geomonitoring using terrestrial laser scanning point clouds. In *MLEG2019*.

Gojcic, Z., Zhou, C., & Wieser, A. (2019b). Robust pointwise correspondences for point cloud based deformation monitoring of natural scenes. In *4th Joint International Symposium on Deformation Monitoring (JISDM)* (Vol. 5).

Gojcic, Z., Zhou, C., Wegner, J. D., Guibas, L. J., & Birdal, T. (2020). Learning multiview 3D point cloud registration. *ArXiv Preprint ArXiv:2001.05119*.

Gordon, B. (2008). *Zur Bestimmung von Messunsicherheiten terrestrischer Laserscanner*. Technische Universität Darmstadt. Retrieved from http://tuprints.ulb.tu-darmstadt.de/1206/1/Dissertation_BGordon.pdf

Gordon, S., Lichti, D. D., Stewart, M. P., & Tsakiri, M. (2000). Metric performance of a high-resolution laser scanner. In *Videometrics and Optical Methods for 3D Shape Measurement* (Vol. 4309, pp. 174–184). International Society for Optics and Photonics.

Gordon, S., Davies, N., Keighley, D., Lichti, D. D., & Franke, J. (2005). A rigorous rangefinder calibration method for terrestrial laser scanners. *Journal of Spatial Science*, *50*(2), 91–96. https://doi.org/10.1080/14498596.2005.9635052

Grafarend, E. W., & Sanso, F. (1985). *Optimization and Design of Geodetic Networks* (1st ed.). Springer-Verlag Berlin Heidelberg.

Guo, Y., Bennamoun, M., Sohel, F., Lu, M., & Wan, J. (2014). 3D object recognition in cluttered scenes with local surface features: a survey. *IEEE Transactions on Pattern Analysis and Machine Intelligence*, *36*(11), 2270–2287.

Hanke, K., Grussenmeyer, P., Grimm-Pitzinger, A., & Weinold, T. (2006). First experiences with the trimble GX scanner. *ISPRS Commission V Symposium*, 6. Retrieved from

www.isprs.org/proceedings/XXXVI/part5/paper/1238_Dresden06.pdf%5Cnwww.isprs.org/proceedings/XXXVI/part5/

Harmening, C., & Neuner, H. (2020). Using Structural Risk Minimization to Determine the Optimal Complexity of B-Spline Surfaces for Modelling Correlated Point Cloud Data.

Harvey, B. R., & Rüeger, J. M. (1992). Theodolite observations and least squares. *Australian Surveyor*, *37*(2), 120–128.

Heinz, E., Medić, T., Holst, C., & Kuhlmann, H. (2018). Genauigkeitsbeurteilung von Laserscans anhand realer Messobjekte. In *DVW e.V. (Hrsg.): Terrestrisches Laserscanning 2018 (TLS 2018). DVW-Schriftenreihe, Band 93* (pp. 41–56). Wißner Verlag, Augsburg.

Hillemann, M., Weinmann, M., Mueller, M. S., & Jutzi, B. (2019). Automatic Extrinsic Self-Calibration of Mobile Mapping Systems Based on Geometric 3D Features. *Remote Sensing*, *11*(16), 1955.

Holst, C. (2015). Analyse der Konfiguration bei der Approximation ungleichmäßig abgetasteter Oberflächen auf Basis von Nivellements und terrestrischen Laserscans. Universitäts-und Landesbibliothek Bonn.

Holst, C., & Kuhlmann, H. (2014a). Aiming at self-calibration of terrestrial laser scanners using only one single object and one single scan. *Journal of Applied Geodesy*, *8*(4), 295–310. https://doi.org/10.1515/jag-2014-0017

Holst, C., & Kuhlmann, H. (2014b). Impact of spatial point distributions at laser scanning on the approximation of deformed surfaces. *Ingenieurvermessung*, *14*, 269–282.

Holst, C., & Kuhlmann, H. (2016). Challenges and present fields of action at laser scanner based deformation analyses. *Journal of Applied Geodesy*, *10*(1), 17–25.

Holst, C., Zeimetz, P., Nothnagel, A., Schauerte, W., & Kuhlmann, H. (2012). Estimation of focal length variations of a 100-m radio telescope's main reflector by laser scanner measurements. *Journal of Surveying Engineering*, *138*(3), 126–135.

Holst, C., Eling, C., & Kuhlmann, H. (2013). Automatic optimization of height network configurations for detection of surface deformations. *Journal of Applied Geodesy*, *7*(2), 103–113.

Holst, C., Nothnagel, A., Blome, M., Becker, P., Eichborn, M., & Kuhlmann, H. (2015). Improved area-based deformation analysis of a radio telescope's main reflector based on terrestrial laser scanning. *Journal of Applied Geodesy*, *9*(1), 1–13. https://doi.org/10.1515/jag-2014-0018

Holst, C., Neuner, H., Wieser, A., Wunderlich, T., & Kuhlmann, H. (2016). Calibration of Terrestrial Laser Scanners / Kalibrierung terrestrischer Laserscanner. *Allgemeine Vermessungs-Nachrichten (AVN)*, *123*(6), 147–157.

Holst, C., Schunck, D., Nothnagel, A., Haas, R., Wennerbäck, L., Olofsson, H., et al. (2017). Terrestrial laser scanner two-face measurements for analyzing the elevation-dependent deformation of the onsala space observatory 20-m radio telescope's main reflector in a bundle adjustment. *Sensors (Switzerland)*, *17*(8). https://doi.org/10.3390/s17081833

Holst, C., Medić, T., & Kuhlmann, H. (2018a). Dealing with systematic laser scanner errors due to misalignment at area-based deformation analyses. *Journal of Applied Geodesy*, *12*(2), 169–185.

Holst, C., Jurek, T., Blome, M., Marschel, L., Petersen, M., Kersten, T., et al. (2018b). Empirische Ergebnisse von TLS-Prüffeldern: Gibt es Auffälligkeiten? In *DVW e.V. (Hrsg.): Terrestrisches Laserscanning 2018 (TLS 2018). DVW-Schriftenreihe, Band 93* (pp. 9–40). Wißner Verlag, Augsburg.

Holst, C., Medić, T., Nothnagel, A., & Kuhlmann, H. (2019a). Analyzing shape deformation and rigid body movement of structures using commonly misaligned terrestrial laser scanners: the radio telescope case. In *4th Joint International Symposium on Deformation Monitoring (JISDM), Athens, Greece*.

Holst, C., Medić, T., & Kuhlmann, H. (2019b). TLS-Kalibrierung: in-situ und/oder a priori? In *VW e.V. (Hrsg.): Terrestrisches Laserscanning 2019 (TLS 2019). DVW-Schriftenreihe, Band 96/2019* (pp. 89–104). Wißner Verlag, Augsburg.

International Organization for Standardization (ISO). (2018). Optics and optical instruments -- Field

procedures for testing geodetic and surveying instruments -- Part 9: Terrestrial laser scanners. Retrieved from www.iso.org

Janßen, J., Medić, T., Kuhlmann, H., & Holst, C. (2019). Decreasing the uncertainty of the target centre estimation at terrestrial laser scanning by choosing the best algorithm and by improving the target design. *Remote Sensing*, *11 (7)*(7).

Janßen, J., Kuhlmann, H., & Holst, C. (2020). Assessing the temporal stability of terrestrial laser scanners during long-term measurements. In K. A., P. Kyrinovič, J. Erdélyi, R. Paar, & A. Marendić (Eds.), *Contributions to International Conferences on Engineering Surveying, INGEO & SIG 2020*. Dubrovnik, Croatia: Springer line.

Jia, F., & Lichti, D. D. (2017). A comparison of simulated annealing, genetic algorithm and particle swarm optimization in optimal first-order design of indoor TLS networks. *ISPRS Annals of the Photogrammetry, Remote Sensing and Spatial Information Sciences*, *4*(2W4), 75–82. https://doi.org/10.5194/isprs-annals-IV-2-W4-75-2017

Jia, F., & Lichti, D. D. (2018). AN EFFICIENT, HIERARCHICAL VIEWPOINT PLANNING STRATEGY FOR TERRESTRIAL LASER SCANNER NETWORKS. *ISPRS Annals of Photogrammetry, Remote Sensing & Spatial Information Sciences*, *IV*(June 2018), 4–7.

Jolliffe, I. T. (2002). *Principal Component Analysis*. *Principal Component Analysis* (2nd ed.). New York, USA: Springer-Verlag. https://doi.org/10.1007/b98835

Jurek, T., Kuhlmann, H., & Holst, C. (2017). Impact of spatial correlations on the surface estimation based on terrestrial laser scanning. *Journal of Applied Geodesy*, *11*(3), 143–155.

Kang, Z., Li, J., Zhang, L., Zhao, Q., & Zlatanova, S. (2009). Automatic registration of terrestrial laser scanning point clouds using panoramic reflectance images. *Sensors*, *9*(4), 2621–2646.

Kauker, S., & Schwieger, V. (2017). A synthetic covariance matrix for monitoring by terrestrial laser scanning. *Journal of Applied Geodesy*, *11*(2), 77–87.

Kauker, S., Holst, C., Schwieger, V., Kuhlmann, H., & Schön, S. (2016). Spatio-temporal correlations of terrestrial laser scanning. *AVN Allg. Vermess. Nachr*, *6*, 170–182.

Kermarrec, G., Paffenholz, J.-A., & Alkhatib, H. (2019a). How Significant Are Differences Obtained by Neglecting Correlations When Testing for Deformation: A Real Case Study Using Bootstrapping with Terrestrial Laser Scanner Observations Approximated by B-Spline Surfaces. *Sensors*, *19*(17), 3640.

Kermarrec, G., Neumann, I., Alkhatib, H., & Schön, S. (2019b). The stochastic model for Global Navigation Satellite Systems and terrestrial laser scanning observations: A proposal to account for correlations in least squares adjustment. *Journal of Applied Geodesy*, *13*(2), 93–104.

Kerschner, R. K. (1980). Mechanical Design Constraints for a Total Station. *HEWLETT-PACKARD JOURNAL*, *31*(9), 12–14.

Kersten, T., Sternberg, H., & Mechelke, K. (2005). Investigations into the accuracy behaviour of the terrestrial laser scanning system Mensi GS100. *Proceedings of 7th Conference in Optical 3D Measurement Techniques*, *I*, 122–131. Retrieved from http://archive.cyark.orarchive.cyark.org/temp/hcuhamburgkerstenetal2005.pdf

Kersten, T., Mechelke, K., Lindstaedt, M., & Sternberg, H. (2009). Methods for geometric accuracy investigations of terrestrial laser scanning systems. *Photogrammetrie-Fernerkundung-Geoinformation*, *2009*(4), 301–315.

Klapa, P., Mitka, B., & Zygmunt, M. (2017). Study into Point Cloud Geometric Rigidity and Accuracy of TLS-Based Identification of Geometric Bodies. In *IOP Conference Series: Earth and Environmental Science* (Vol. 95, p. 32008). IOP Publishing.

Koch, K.-R., & Kuhlmann, H. (2009). The impact of correcting measurements of laserscanners on the uncertainty of derived results. *ZfV-Zeitschrift Für Geodäsie, Geoinformation Und Landmanagement*, (zfv 1/2009).

Koch, K.-R., Kuhlmann, H., & Schuh, W. D. (2010). Approximating covariance matrices estimated in multivariate models by estimated auto-and cross-covariances. *Journal of Geodesy*, *84*(6), 383–397.

Krarup, T., Juhl, J., & Kubik, K. (1980).

Götterdämmerung over least squares adjustment. In *14th Congress of ISPRS*.

Kregar, K., Grigillo, D., & Kogoj, D. (2013). High precision target determination from a point cloud. *ISPRS Annals of the Photogrammetry, Remote Sensing and Spatial Information Sciences*, *II-5/W2*(November), 11–13. https://doi.org/10.5194/isprsannals-II-5-W2-139-2013

Kuang, S. (1996). *Geodetic network analysis and optimal design: concepts and applications.* Chelsea: Ann Arbor Press.

Kuhlmann, H., Schwieger, V., Wieser, A., & Niemeier, W. (2014). Engineering Geodesy-Definition and Core Competencies. *Journal of Applied Geodesy*, *8*(4), 327–334.

Lague, D., Brodu, N., & Leroux, J. (2013). Accurate 3D comparison of complex topography with terrestrial laser scanner: Application to the Rangitikei canyon (NZ). *ISPRS Journal of Photogrammetry and Remote Sensing*, *82*(February 2013), 10–26. https://doi.org/10.1016/j.isprsjprs.2013.04.009

Leica Geosystems AG. (2015). Leica ScanStation P20 Industry ' s Best Performing Ultra-High Speed Scanner. *Leica Scanstation P20: Datasheet*. Retrieved from http://www.leica-geosystems.co.uk/downloads123/hds/hds/ScanStation_P20/brochures-datasheet/Leica_ScanStation_P20_DAT_en.pdf

Leica Geosystems AG. (2017). Leica ScanStation P30 / P40 Because every detail matters, 2.

Lenda, G., Marmol, U., & Buczek, M. (2017). The effect of partial transparency of spherical targets on TLS point clouds registration accuracy. *KSCE Journal of Civil Engineering*, *00*(0000), 1–11. https://doi.org/10.1007/s12205-017-1907-9

Lerma, J. L., & García-San-Miguel, D. (2014). Self-calibration of terrestrial laser scanners: selection of the best geometric additional parameters. *ISPRS Annals of Photogrammetry, Remote Sensing and Spatial Information Sciences*, *II–5*(June), 219–226. https://doi.org/10.5194/isprsannals-II-5-219-2014

Leutenegger, S., Margarita, C., & Roland, Y. S. (2011). BRISK: Binary robust invariant scalable keypoints. In *Computer Vision (ICCV), 2011 IEEE International Conference on. IEEE* (pp. 2548–2555).

Li, M. (2018). A SUPER VOXEL-BASED RIEMANNIAN GRAPH FOR MULTI SCALE SEGMENTATION OF LIDAR POINT CLOUDS. *ISPRS Annals of Photogrammetry, Remote Sensing & Spatial Information Sciences*, *4*(3).

Li, X., Li, Y., Xie, X., & Xu, L. (2018). Terrestrial Laser Scanner Autonomous Self-Calibration with No Prior Knowledge of Point-Clouds. *IEEE Sensors Journal*, *18*(22), 9277–9285. https://doi.org/10.1109/JSEN.2018.2869559

Liang, Y., Zhan, Q., Che, E., Chen, M., & Zhang, D. (2014). Automatic Registration of Terrestrial Laser Scanning Data Using Precisely Located Artificial Planar Targets. *IEEE Geoscience and Remote Sensing Letters*, *11*(1), 69–73.

Liang, Y., Qiu, Y., & Cui, T. (2016). Perspective intensity images for co-registration of terrestrial laser scanner and digital camera. *International Archives of the Photogrammetry, Remote Sensing and Spatial Information Sciences - ISPRS Archives*, *41*(July), 295–300. https://doi.org/10.5194/isprsarchives-XLI-B3-295-2016

Lichti, D. D. (2007). Error modelling, calibration and analysis of an AM-CW terrestrial laser scanner system. *ISPRS Journal of Photogrammetry and Remote Sensing*, *61*(5), 307–324. https://doi.org/10.1016/j.isprsjprs.2006.10.004

Lichti, D. D. (2009). The impact of angle parameterisation on terrestrial laser scanner self-calibration. *Int. Arch. Photogramm. Remote Sens. Spat. Inf. Sci*, *38*(3/W8), 171–176.

Lichti, D. D. (2010a). A review of geometric models and self-calibration methods for terrestrial laser scanners. *Boletim de Ciências Geodésicas*, *16*, 3–19.

Lichti, D. D. (2010b). Terrestrial laser scanner self-calibration: Correlation sources and their mitigation. *ISPRS Journal of Photogrammetry and Remote Sensing*, *65*(1), 93–102. https://doi.org/10.1016/j.isprsjprs.2009.09.002

Lichti, D. D. (2019). Geometric point cloud quality. *Laser Scanning: An Emerging Technology in Structural Engineering*, *14*, 79.

Lichti, D. D., & Chow, J. C. K. (2013). Inner Constraints for Planar Features. *Photogrammetric Record*, *28*(141), 74–85. https://doi.org/10.1111/j.1477-9730.2012.00700.x

Lichti, D. D., & Franke, J. (2005). Self-Calibration of the iQsun 880 Laser Scanner. In *In Proceedings of the Optical 3-D 927 Measurement Techniques VII,Vienna, Austria* (pp. 122–131).

Lichti, D. D., Gordon, S., & Tipdecho, T. (2005). Error Models and Propagation in Directly Georeferenced Terrestrial Laser Scanner Networks. *JOURNAL OF SURVEYING ENGINEERING*, (November), 135–142. Retrieved from http://citeseerx.ist.psu.edu/viewdoc/download?doi=10.1.1.112.9793&rep=rep1&type=pdf

Lichti, D. D., Glennie, C. L., Al-Durgham, K., Jahraus, A., & Steward, J. (2019). Explanation for the seam line discontinuity in terrestrial laser scanner point clouds. *ISPRS Journal of Photogrammetry and Remote Sensing*, *154*, 59–69.

Lindeberg, T. (2012). Scale invariant feature transform.

Liu, J., & Hubbold, R. (2006). Automatic Camera Calibration and Scene Reconstruction with Scale-Invariant Features. In *International Symposium on Visual Computing* (pp. 558–568). Heidelberg: Springer, Berlin.

Lomax, R. G., & Hans-Vaughn, D. L. (2012). *An Introduction to Statistical Concepts* (3rd ed.). New York: Taylor & Francis.

Loy, G., & Eklundh, J.-O. (2006). Detecting symmetry and symmetric constellations of features. In *European Conference on Computer Vision* (pp. 508–521). Springer.

Maalek, R., Lichti, D. D., & Ruwanpura, J. Y. (2018). Robust segmentation of planar and linear features of terrestrial laser scanner point clouds acquired from construction sites. *Sensors (Switzerland)*, *18*(3). https://doi.org/10.3390/s18030819

Maar, H., & Zogg, H.-M. (2014). *WFD – Wave Form Digitizer Technology White Paper*. Heerbrugg, Switzerland.

Markiewicz, J., & Zawieska, D. (2019). The Influence of the Cartographic Transformation of TLS Data on the Quality of the Automatic Registration. *Applied Sciences*, *9*(3), 509.

Markiewicz, J. S., Markiewicz, Ł., & Foryś, P. (2019). THE COMPARISON OF 2D AND 3D DETECTORS FOR TLS DATA REGISTRATION–PRELIMINARY RESULTS. *International Archives of the Photogrammetry, Remote Sensing & Spatial Information Sciences*.

Medić, T., Holst, C., & Kuhlmann, H. (2017). Towards System Calibration of Panoramic Laser Scanners from a Single Station. *Sensors*, *17*(5), 1145. https://doi.org/10.3390/s17051145

Medić, T., Kuhlmann, H., & Holst, C. (2019a). Automatic in-situ self-calibration of a panoramic TLS from a single station using 2D keypoints. In *ISPRS Annals of the Photogrammetry, Remote Sensing and Spatial Information Sciences*.

Medić, T., Holst, C., Janßen, J., & Kuhlmann, H. (2019b). Empirical stochastic model of detected target centroids: Influence on registration and calibration of terrestrial laser scanners. *Journal of Applied Geodesy*, *ahead of p*.

Medić, T., Holst, C., & Kuhlmann, H. (2019c). Improving the results of terrestrial laser scanner calibration by an optimized calibration process. In *Photogrammetrie Laserscanning Optische 3DMesstechnik - Beiträge der Oldenburger 3D-Tage* (pp. 36–50).

Medić, T., Kuhlmann, H., & Holst, C. (2019d). Sensitivity Analysis and Minimal Measurement Geometry for the Target-Based Calibration of High-End Panoramic Terrestrial Laser Scanners. *Remote Sensing*, *11*(13), 1519.

Medić, T., Kuhlmann, H., & Holst, C. (2020a). A priori versus in-situ terrestrial laser scanner calibration in the context of the instability of calibration parameters. In Kopáčik A., P. Kyrinovič, J. Erdélyi, R. Paar, & A. Marendić (Eds.), *Contributions to International Conferences on Engineering Surveying, INGEO & SIG 2020*. Dubrovnik, Croatia: Springer line.

Medić, T., Kuhlmann, H., & Holst, C. (2020b). Designing and evaluating a user-oriented calibration field for the target-based self-calibration of panoramic terrestrial laser

scanners, (I), 1–22.

Medić, T., Kuhlmann, H., & Holst, C. (2020c). Empirical evaluation of terrestrial laser scanner calibration strategies : manufacturer-based , target-based and keypoint-based. In *Contributions to International Conferences on Engineering Surveying, INGEO & SIG 2020; Dubrovnik, Croatia 2020*.

Medić, T., Holst, C., & Kuhlmann, H. (2020d). Optimizing the target-based calibration procedure of terrestrial laser scanners. *AVN Allgemeine Vermessungs-Nachrichten*, *127*(1), 18–27.

Mettenleiter, M., Härtl, F., Kresser, S., & Fröhlich, C. (2015). *Laserscanning—Phasenbasierte Lasermesstechnik für die hochpräzise und schnelle dreidimensionale Umgebungserfassung; Die Bibliothek der Technik*. Süddeutscher Verlag onpact GmbH: Munich, Germany.

Mikhail, E. W. (1976). *Observations and Least Squares*. New York, Hagerstown, San Francisco,London: IEP Don-Donnelley.

Mukupa, W., Roberts, G. W., Hancock, C. M., & Al-Manasir, K. (2017). A review of the use of terrestrial laser scanning application for change detection and deformation monitoring of structures. *Survey Review*, *49*(353), 99–116. https://doi.org/10.1080/00396265.2015.1133039

Muralikrishnan, B., Sawyer, D., Blackburn, C., Phillips, S., Borchardt, B., & Estler, W. T. (2009). ASME B89. 4.19 performance evaluation tests and geometric misalignments in laser trackers. *Journal of Research of the National Institute of Standards and Technology*, *114*(1), 21. https://doi.org/10.6028/jres.114.003

Muralikrishnan, B., Blackburn, C., Sawyer, D., & Phillips, S. (2010). Measuring Scale Errors in a Laser Tracker's Horizontal Angle Encoder Through Simple Length Measurement and Two-Face System Tests. *Journal of Research of the National Institute of Standards and Technology*, *115*(5), 291–301.

Muralikrishnan, B., Shilling, M., Sawyer, D., Rachakonda, P., Lee, V., Phillips, S., et al. (2014). Laser scanner two-face errors on spherical targets. In *Proceedings of the Annual Meeting of the ASPE*.

Muralikrishnan, B., Shilling, M., Rachakonda, P., Ren, W., Lee, V., & Sawyer, D. (2015a). Toward the development of a documentary standard for derived-point to derived-point distance performance evaluation of spherical coordinate 3D imaging systems. *Journal of Manufacturing Systems*, *37*, 550–557. https://doi.org/10.1016/j.jmsy.2015.04.002

Muralikrishnan, B., Ferrucci, M., Sawyer, D., Gerner, G., Lee, V., Blackburn, C., et al. (2015b). Volumetric performance evaluation of a laser scanner based on geometric error model. *Precision Engineering*, *40*(July 2016), 139–150. https://doi.org/10.1016/j.precisioneng.2014.11.002

Muralikrishnan, B., Rachakonda, P., Shilling, M., Lee, V., Blackburn, C., Sawyer, D., et al. (2016). Report on the May 2016 ASTM E57.02 Instrument Runoff at NIST, Part 1 - Background Information and Key Findings, (May). https://doi.org/10.6028/NIST.IR.8152

Neitzel, F. (2006). Investigation of Axes Errors of Terrestrial Laser Scanners. In *5th International Symposium Turkish-German Joint Geodetic Days*. Berlin.

Neitzel, F., Gordon, B., & Wujanz, D. (2014). Verfahren zur standardisierten Überprüfung von terrestrischen Laserscannern (TLS). *DVW-Merkblatt*, *7–2014*. Retrieved from www.dvw.de

Neuner, H. (2019). Qualitätsbetrachtungen zu TLS-Daten. In *180. DVW-Seminar "Qualitätssicherung geodätischer Mess- und Auswerteverfahren 2019*. Stuttgart.

Neuner, H., Holst, C., & Kuhlmann, H. (2016). Overview on Current Modelling Strategies of Point Clouds for Deformation Analysis / Überblick aktueller Methoden zur Modellierung von Punktwolken für die Deformationsanalyse. *Allgemeine Vermessungs-Nachrichten (AVN)*, *123*(11–12), 328–339.

Niemeier, W. (1985). Anlage von Überwachungsnetzen. In H. Pelzer (Ed.), *Geodätische Netze in der Landes- und Ingenieurvermessung*. Stuttgart.: Konrad Wittwer Verlag.

Niemeier, W. (2008). *Ausgleichungsrechnung: Statistische Auswertemethoden*. Walter de

Gruyter.

Nuttens, T., Wulf, A. D. E., Bral, L., Wit, B. D. E., Carlier, L., Ryck, M. D. E., et al. (2010). High Resolution Terrestrial Laser Scanning for Tunnel Deformation Measurements High Resolution Terrestrial Laser Scanning for Tunnel Deformation Measurements, (April), 11–16.

Ogundare, J. O. (2015). *Precision Surveying: The Principles and Geomatics Practice*. *John Wiley & Sons, Inc*. https://doi.org/10.1002/ejoc.201200111

Parian, J. A., Gruen, A., & Image, P. (2005). Integrated Laser Scanner and Intensity Image Calibration and Accuracy Assessment. *ISPRS WG III3 III4 V3 Workshop Laser Scanning 2005*, *36*(3), 18–23. Retrieved from http://www.isprs.org/proceedings/XXXVI/3-W19/papers/018.pdf

Pfeifer, N., Dorninger, P., Haring, A., & Fan, H. (2007). Investigating terrestrial laser scanning intensity data: Quality and functional relations. *8th Conference on Optical 3-D Measurement Techniques*, 328–337.

Prieto, E., Pérez, M. M., Yandayan, T., Przybylska, J., Just, A., & Geckeler, R. (2018). *Guidelines on the Calibration of Angular Encoders*. Braunschweig, Germany.

Rachakonda, P., Muralikrishnan, B., Cournoyer, L., Cheok, G., Lee, V., Shilling, M., & Sawyer, D. (2017). Methods and considerations to determine sphere center from terrestrial laser scanner point cloud data. *Measurement Science and Technology*, *28*(10). https://doi.org/10.1088/1361-6501/aa8011

Rachakonda, P., Muralikrishnan, B., & Sawyer, D. (2018). Metrological Evaluation of Contrast Target Center Algorithm for Terrestrial Laser Scanners. *Measurement*, (134), 15–24. https://doi.org/10.1016/j.measurement.2018.08.039

Remondino, F. (2006). Detectors and descriptors for photogrammetric applications. *International Archives of the Photogrammetry, Remote Sensing and Spatial Information Sciences*, *36*(3), 49–54.

Reshetyuk, Y. (2007). Calibration of Terrestrial Laser Scanners. *Survey Review*, *302*(October 2006), 703–713. https://doi.org/10.1179/sre.2006.38.302.703

Reshetyuk, Y. (2009). *Self-calibration and direct georeferencing in terrestrial laser scanning*. KTH Stockholm. https://doi.org/978-91-85539-34-5

Reshetyuk, Y. (2010). A unified approach to self-calibration of terrestrial laser scanners. *ISPRS Journal of Photogrammetry and Remote Sensing*, *65*(5), 445–456. https://doi.org/10.1016/j.isprsjprs.2010.05.005

Rodehorst, V., & Koschan, A. (2006). Comparison and Evaluation of Feature Point Detectors. In *5th International Symposium Turkish-German Joint Geodetic Days*.

Saleh, H. A., & Chelouah, R. (2004). The design of the global navigation satellite system surveying networks using genetic algorithms. *Engineering Applications of Artificial Intelligence*, *17*(1), 111–122.

Salido-Monzú, D., & Wieser, A. (2019). An instrumental basis for multispectral LiDAR with spectrally-resolved distance measurements. *International Archives of the Photogrammetry, Remote Sensing and Spatial Information Sciences-ISPRS Archives*, *42*(2/W13), 1121–1126.

Schäfer, T. (2017). Berührungslose und flächenhafte Deformationsmessungen an Betonoberflächen unter besonderer Berücksichtigung der Interaktion zwischen Laserstrahl und Oberfläche. Technische Universität München.

Schmitt, G. (1982). Optimization of geodetic networks. *Reviews of Geophysics*, *20*(4), 877–884.

Schmitz, B., Holst, C., Medić, T., Lichti, D. D., & Kuhlmann, H. (2019). How to Efficiently Determine the Range Precision of 3D Terrestrial Laser Scanners. *Sensors*, *19(6)*, 1466. https://doi.org/10.3390/s19061466

Schmitz, B., Kuhlmann, H., & Holst, C. (2020a). Investigating the resolution capability of terrestrial laser scanners and its impact on the effective number of measurements. *ISPRS Journal of Photogrammetry and Remote Sensing*, *159*, 41–52.

Schmitz, B., Kuhlmann, H., & Holst, C. (2020b). Using the Resolution Capability and the Effective Number of Measurements to Select

the " Right " Terrestrial Laser Scanner. In K. A., P. Kyrinovič, J. Erdélyi, R. Paar, & A. Marendić (Eds.), *Contributions to International Conferences on Engineering Surveying, INGEO & SIG 2020*. Dubrovnik, Croatia: Springer line.

Schofield, W., & Breach, M. (2007). *Engineering Surveying* (6th ed.). Oxford: Elsevier.

Schulz, T. (2007). Calibration of a Terrestrial Laser Scanner for Engineering Geodesy. Technical University of Berlin. Thesis Doctoral of Science.

Schwieger, V. (2007). Sensitivity analysis as a general tool for model optimisation – examples for trajectory estimation. *Journal of Applied Geodesy*, *1*(1), 27–34. https://doi.org/10.1515/jag.2007.004

Sheehan, M., Harrison, A., & Newman, P. (2012). Self-calibration for a 3D laser. *The International Journal of Robotics Research*, *31*(5), 675–687.

Soudarissanane, S. (2016). *The geometry of terrestrial laser scanning; identification of errors, modeling and mitigation of scanning geometry*. TU Delft. https://doi.org/doi:10.4233/uuid:b7ae0bd3-23b8-4a8a-9b7d-5e494ebb54e5

Soudarissanane, S., & Lindenbergh, R. C. (2012). Optimizing Terrestrial Laser Scanning Measurement Set-Up. *ISPRS - International Archives of the Photogrammetry, Remote Sensing and Spatial Information Sciences*, *XXXVIII-5/*(MAY 2012), 127–132. https://doi.org/10.5194/isprsarchives-XXXVIII-5-W12-127-2011

Tan, K., & Cheng, X. (2016). Correction of incidence angle and distance effects on TLS intensity data based on reference targets. *Remote Sensing*, *8*(3), 15–18. https://doi.org/10.3390/rs8030251

Telling, J., Lyda, A., Hartzell, P., & Glennie, C. L. (2017). Review of Earth science research using terrestrial laser scanning. *Earth-Science Reviews*, *169*, 35–68.

Tiede, C. (2005). *Integration of optimization algorithms with sensitivity analysis, with application to volcanic regions*. Technische Universität Darmstadt. Retrieved from http://tuprints.ulb.tu-darmstadt.de/581/

Urban, S., & Weinmann, M. (2015). Finding a good feature detector-descriptor combination for the 2D keypoint-based registration of TLS point clouds. In *ISPRS Annals of the Photogrammetry, Remote Sensing and Spatial Information Sciences, ISPRS Geospatial Week 2015* (Vol. II-3/W5, pp. 121–128). La Grande Motte, France. https://doi.org/10.5194/isprsannals-II-3-W5-121-2015

Vosselman, G., & Maas, H. G. (2010). *Airborne and Terrestrial Laser Scanning*. Whittles Publishing. Retrieved from https://books.google.de/books?id=J0DNQQAACAAJ

Wagner, A., Wiedemann, W., Wasmeier, P., & Wunderlich, T. (2016). Improved concepts of using natural targets for geo-monitoring. *3rd Joint International Symposium on Deformation Monitoring (JISDM)*, (December), CD-ROM. Retrieved from http://www.fig.net/resources/proceedings/2016/2016_03_jisdm_pdf/nonreviewed/JISDM_2016_submission_2.pdf

Walsh, G. (2015). Leica ScanStation P-Series – Details that matter. Leica ScanStation - White Paper. Retrieved May 21, 2019, from http://blog.hexagongeosystems.com/wp-content/uploads/2015/12/Leica_ScanStation_P-Series_details_that_matter_white_paper_en-4.pdf

Wang, L., Muralikrishnan, B., Rachakonda, P., & Sawyer, D. (2017). Determining geometric error model parameters of a terrestrial laser scanner through two-face, length-consistency, and network methods. *Measurement Science and Technology*, *28(6)*.

Wang, Z., & Brenner, C. (2008). Point based registration of terrestrial laser data using intensity and geometry features. *International Archives of Photogrammetry, Remote Sensing and Spatial Information Sciences*, *37*(Part B5), 583–589.

Witte, B., & Schmidt, H. (2000). Vermessungskunde und Grundlagen der Statistik im Bauwesen. 4. neubearbeitete Auflage. *Stuttgart: K. Wittwer*.

Wujanz, D., Burger, M., Mettenleiter, M., & Neitzel, F. (2017). An intensity-based stochastic model for terrestrial laser scanners. *ISPRS Journal of Photogrammetry and Remote Sensing*, *125*, 146–155.

https://doi.org/10.1016/j.isprsjprs.2016.12.006

Wunderlich, T., Ohlmann-Lauber, J., Schäfer, T., Reidl, F., Wunderlich, T., Ohlmann-Lauber, J., et al. (2013). *Objective Specifications of Terrestrial Laserscanners–A Contribution of the Geodetic Laboratory at the Technische Universität München*. *Metrica.Gr* (Vol. 21). Retrieved from http://metrica.gr/files/downloads/ObjectiveSpecsOfLS-EN.pdf

Wunderlich, T., Niemeier, W., Wujanz, D., Holst, C., Neitzel, F., & Kuhlmann, H. (2016). Areal Deformation Analysis from TLS Point Clouds – The Challenge / Flächenhafte Deformationsanalyse aus TLS-Punktwolken – die Herausforderung. *Allgemeine Vermessungs-Nachrichten (AVN)*, *123*(11–12), 340–351.

Yi, C., Xing, H., Wu, Q., Zhang, Y., Wei, M., Wang, B. O., & Zhou, L. (2018). Automatic Detection of Cross-Shaped Targets for Laser Scan Registration. *IEEE Access*, *6*, 8483–8500.

Yu, Q., Liang, J., Xiao, J., Lu, H., & Zheng, Z. (2018). A Novel perspective invariant feature transform for RGB-D images. *Computer Vision and Image Understanding*, *167*(December), 109–120. https://doi.org/10.1016/j.cviu.2017.12.001

Z+F GmbH. (2016). Z+F Imager 5016 Preliminary Data Sheet.

Zámecnikova, M., & Neuner, H. (2017). Investigation of the distance dependence of the combined influence of the incidence angle and the surface roughness on the reflectorless distance measurement of a scanning total station. *Allgemeine Vermessungs-Nachrichten (AVN)*, *124*(11–12), 353–361.

Zámecnikova, M., Wieser, A., Woschitz, H., & Ressl, C. (2014). Influence of surface reflectivity on reflectorless electronic distance measurement and terrestrial laser scanning. *Journal of Applied Geodesy*, *8*(4), 311–325. https://doi.org/10.1515/jag-2014-0016

Zámecnikova, M., Neuner, H., Pegritz, S., & Sonnleitner, R. (2015). Investigation on the influence of the incidence angle on the reflectorless distance measurement of a terrestrial laser scanner. *Vermessung & Geoinformation*, (2+3), 208–218.

Zhao, X., Kargoll, B., Alkhatib, H., & Neumann, I. (2019). Influence of the simplified stochastic model of TLS measurements on geometry-based deformation analysis.

Zheng, J., Li, K., Liu, S., Ge, H., Zhang, Z., Gu, C., et al. (2018). Effect of shape imperfection on the buckling of large-scale thin-walled ellipsoidal head in steel nuclear containment. *Thin-Walled Structures*, *124*(December 2017), 514–522. https://doi.org/10.1016/j.tws.2018.01.001

Zogg, H.-M. (2008). Investigations of high precision terrestrial laser scanning with emphasis on the development of a robust close-range 3D-laser scanning system. ETH Zurich.